Title

Heparin-Mimicking Polymers for Improving Stability and Bioactivity of Basic Fibroblast Growth Factor

Permalink

https://escholarship.org/uc/item/9h2889gz

Author

Nguyen, Thi H.

Publication Date

2014

Peer reviewed|Thesis/dissertation

UNIVERSITY OF CALIFORNIA

Los Angeles

Heparin-Mimicking Polymers

for Improving Stability

and Bioactivity of Basic Fibroblast Growth Factor

A dissertation submitted in partial satisfaction of the

requirements for the degree Doctor of Philosophy in Chemistry

by

Thi H. Nguyen

2014

ABSTRACT OF THE DISSERTATION

Heparin-Mimicking Polymers

for Improving Stability

and Bioactivity of Basic Fibroblast Growth Factor

by

Thi H. Nguyen

Doctor of Philosophy in Chemistry

University of California, Los Angeles, 2014

Professor Heather D. Maynard, Chair

Proteins are an important class of therapeutics. The have many advantages over small-molecule drugs including high target specificity, low cytotoxicity and low immunogenicity. However, due to their inherent instability during storage, transport and delivery *in vitro* and *in vivo*, their therapeutic usefulness has not been maximized. One approach is to conjugate poly(ethylene glycol) to proteins to enhance pharmacokinetics *in vivo*, and there are eleven FDA approved therapeutic PEG conjugates. However, efforts to stabilize proteins against environmental stressors are still limited. In this dissertation, the development of biomimetic polymers, specifically heparin-mimicking polymers, to stabilize an important unstable therapeutic protein, basic fibroblast growth factor (bFGF), is described.

Chapter 1 reviews the biomedical applications of heparin-based hydrogels and heparin-mimicking polymers. Heparin is a naturally occurring polysaccharide that was first exploited for its antithrombotic activity. It was later realized that heparin-mediated biological functions were wide-ranging and included cell differentiation, angiogenesis, inflammation, host defense and viral infection mechanisms, lipid transport and clearance, and cell adhesion and interaction. Thus, researchers have shifted to investigate other properties of heparin-mimicking polymers besides its use as an anticoagulant. This chapter focuses on the development of heparin-based hydrogels and heparin-mimicking polymers for treatments of skin wounds specifically.

Chapter 2 describes the stabilization of bFGF by covalent conjugation of a heparin-mimicking polymer, a copolymer consisting of styrene sulfonate units and methyl methacrylate units bearing poly(ethylene glycol) side chains. bFGF plays a crucial role in diverse cellular functions from wound healing to bone regeneration. However, a major obstacle in the widespread application of bFGF is its inherent instability during storage and delivery. The bFGF conjugate of this polymer, bFGF-p(SS-*co*-PEGMA), retained bioactivity after synthesis and was stable to a variety of environmentally and therapeutically relevant stressors, such as heat, mild and harsh acidic conditions, storage, and proteolytic degradation, compared to native bFGF. After applied stress, the conjugate was also significantly more active than the control conjugate system where the styrene sulfonate units were omitted from the polymer structure. This research has important implications for the clinical use of bFGF and for stabilization of heparin-binding growth factors in general.

Chapter 3 describes a study of the preclinical value of the bFGF-p(SS-*co*-PEGMA) conjugate as a potential therapy for active wound healing. The cellular uptake and trafficking of the bFGF-heparin-mimcking polymer conjugate, bFGF-p(SS-*co*-PEGMA), was studied to better

understand the cellular fate of the conjugate. The long-term storage stability of the conjugate was examined at 4 °C and 23 °C to evaluate the usefulness of the conjugate as a widely available therapeutic to patients, including at-home patients and patients in the remote areas. In addition, we report for the first time the superagonist characteristic of the heparin-mimicking polymer conjugate when used in the presence of exogenous heparin.

Chapter 4 describes the development of a 2nd-generation and a 3rd-generation heparin-mimicking polymer. Since the 1st-generation heparin-mimicking polymer described in Chapters 2 and 3, p(SS-*co*-PEGMA), stabilizes bFGF but is unable to activate FGF receptors (FGFRs) as is heparin, we looked for other heparin-mimicking polymers that could do both. Activation of FGFRs by two bFGF molecules and a heparin molecule leads to the dimerization and phosphorylation of the receptors, and subsequently results in cell responses such as proliferation or migration. Thus, 2nd and 3rd-generation sulfonated polymers were prepared. The 2nd-generation polymer was found to be a strong activator of FGFRs but its conjugate to bFGF had reduced bioactivity. The 3rd-generation polymer was a block copolymer of the 1st- and the 2nd-generation polymers. Although it was not as strong an activator as the 2nd-generation polymer, its conjugate to bFGF exhibited enhanced mitogenic activity compared to other conjugates and native bFGF in heparan sulfate-deficient cells and in human umbilical vein endothelial cells (HUVECs). The 3rd-generation conjugate also stimulated HUVEC migration better than the native protein. Taken together, the 3rd-genration conjugate is promising for applications where promoting angiogenesis is desired, such as in tissue engineering.

The dissertation of Thi H. Nguyen is approved.

Joseph A. Loo, PhD

Daniel T. Kamei, PhD

Heather D. Maynard, Committee Chair

University of California, Los Angeles

2014

I dedicate this dissertation to my late father

who inspired me with his life, his love and his sacrifices.

He will be forever missed.

TABLE OF CONTENTS

LIST OF FIGURES

xi

LIST OF TABLES

LIST OF SCHEMES

LIST OF ABBREIVATIONS

AIBN	Azobisisobutyronitrile
ATRP	Atom Transfer Radical Polymerization
$CDCl_3$	Deuterated Chloroform
CTA	Chain Transfer Agent
D_2O	Deuterated Water
DCM	Dichloro Methane
DMF	*N, N´*-Dimethylformamide
DTT	Dithiothreitol
D-PBS	Dulbecco's Phosphate Buffered Saline
EDTA	Ethylenediaminetetraacetic Acid
ELISA	Enzyme-Linked Immunosorbent Assay
FT-IR	Fourier Transform-Infrared Spectroscopy
GPC	Gel Permeation Chromatography
HDF	Human Dermal Fibroblast
HS	Heparan Sulfate
HUVEC	Human Umbilical Vein Endothelial Cell
MeOH	Methanol
M_n	Number Average Molecular Weight
PB	Phosphate Buffer
PMMA	Poly(Methyl Methacrylate)
MW	Molecular Weight
MWCO	Molecular Weight Cut Off

NMR   Nuclear Magnetic Resonance

PDI   Polydispersity Index

PEG   Poly(ethylene glycol)

RAFT   Reversible Addition-Fragmentation Chain Transfer

SDS-PAGE   Sodium Dodecyl Sulfate-Polyacrylamide Gel Electrophoresis

SEM   Standard Error Of the Mean

STDEV   Standard Deviation

TFA   Trifluoroacetic Acid

THF   Tetrahydrofuran

ACKNOWLEDGEMENTS

This dissertation would have never been realized if it was not because of several people.

First, I would like to acknowledge my late father. My father was a scientist at heart. He liked to listen to me talking about my research, but he did not fully support my decision in continuing with graduate school. He said he did not want to see me stressed. I had never told him this, but if he was here with me now, I would tell him: it was a good kind of stress - the kind that one must experience once in her life time. My father influenced me tremendously as a person and as a scientist I am today. He taught me many things such as to be humble, thoughtful, and dedicated; some of which served me greatly in graduate school were to be inventive, to always question your own success, and to "make sure you can repeat repeat repeat your own results."

Second, I would like to thank my advisor, Professor Heather Maynard, for her mentorship. I thank her for allowing me to uncover the joy in research since I was a naïve undergraduate researcher in her lab. Because of her unwavering support and belief in me, even at times that I lost trust in myself, I found within the confidence to continue with my graduate career. Her guidance was invaluable to me.

I am grateful to have the opportunity to work with many talented past members of the Maynard Group: Dr. Karina Heredia, Dr. Chein-Wen Chang, Dr. Chris Kolodziej, Dr. Sung-Hye Kim, Dr. Greg Grover, Dr. Rocky Mancini, Dr. Sina Saxer, Dr. Darice Wong and Peter Lee. They were generous both with their friendship and advices.

I appreciate the company of all of the current members of the Maynard Group and my best friend Amy Ferreira in the Tolbert Group; they are great colleagues as well as great friends.

I thank the following people for the collaborative effort in my dissertation: Dr. Yang Liu (Chapter 1), Dr. Sung-Hye Kim, Caitlin Decker, Dr. Darice Wong, Dr. Joseph Loo (Chapter 2), Dr. Yang Liu, Dr. Lloyd Miller (Chapter 3), and Peter Lee, AJ McGahran, Dr. Yang Liu, Samantha Paluck (Chapter 4).

Lastly, I would like to acknowledge my dear family. I thank my husband for his undoubted love, patient, and most of all his untiring optimism. I could not imagine a better partner to have spent this journey with. I thank my dear mother and sister for their endless moral support. Having their understanding and forgiveness even before I could make any mistake was surely comforting throughout my graduate career.

§ Chapter 2 is reproduced from "Nguyen, T. H.; Kim, S. H.; Decker, C. G.; Wong, D. Y.; Loo, J. A.; Maynard, H. D., "A Heparin-Mimicking Polymer Conjugate Stabilizes Basic Fibroblast Growth Factor (bFGF)," *Nature Chem.*, **2013**, 5, 221-227."

VITA

MS in Organic Chemistry   June 2011
   University of California, Los Angeles

BS in Chemistry   June 2009
   University of California, Los Angeles

AA in Chemistry   June 2007
   Los Angeles Pierce College, Woodland Hills, CA

Research Experience

Intern – International NSF Research Experience for Undergraduates   June – Sep 2008
   University of Buenos Aires, Buenos Aires, Argentina

Undergraduate Student Researcher – Advisor: Heather Maynard, PhD   Sep 2007 – June 2009
   University of California, Los Angeles

Intern – Research Experience for Undergraduates (BRITE)   June – Aug 2007
   University of California, Riverside

Awards

Thomas L. and Ruth F. Jacobs Award, UCLA   June 2014
   For outstanding research achievements in organic chemistry

Excellence in Graduate Polymer Research, UCLA & ACS   Nov 2013
   Selected by ACS committee to present at the national ACS meeting

Dissertation Year Fellowship, UCLA   June 2013
   Finances highly meritorious graduate students in their last year

The Majeti-Alapati Fellowship, UCLA   Nov 2012
   For outstanding research in organic chemistry

The Geissman Award, UCLA   June 2009
   For excellence in organic chemistry

Organic-Biochemistry Award, Los Angeles Pierce College   June 2007
   For outstanding performance in organic chemistry

PUBLICATIONS

(1) **Nguyen, T. H**.; Kim, S. H.; Decker, C. G.; Wong, D. Y.; Loo, J. A.; Maynard, H. D., "A Heparin-Mimicking Polymer Conjugate Stabilizes Basic Fibroblast Growth Factor (bFGF)," *Nature Chem.*, **2013**, 5, 221-227.

> * Paper highlighted on the front webpage of *Nature Chemistry* and mentioned on the cover of that issue. Paper also highlighted by: C&E News, FierceBiotechResearch, Metro US, ScienceDaily, Medical Xpress, Examiner, News-Metal.net, Domain-b, RedOrbit, Vyages.com, ScienceCodex, Isaúde, Science Newsline, EurekAlert!, WoundCareJobs, Phyics News, International Hopsital, Press-News.org, Grays Medicine, UC Newsroom, UC Health, UCLA News Room, UCLA Physical Sciences, UCLA Department of Chemistry and Biochemistry, Natures Science-Business eXchange.

(2) Griffin, D. R.; Schlosser, J. L.; Lam, S. F.; **Nguyen, T. H.**; Maynard, H. D.; Kasko, A. M., "Synthesis of Photodegradable Macromers for Conjugation and Release of Bioactive Molecules," *Biomacromolecules*, **2013**, 14, 1199-1207.

(3) Grover, G. N.; Lam, J.; **Nguyen, T. H.**; Segura, T.; Maynard, H. D., "Biocompatible Hydrogels by Oxime Click Chemistry," *Biomacromolecules,* **2012**,13, 3013-3017. * Paper was one of the "Most Read Articles of 2012"

(4) Kim, S. H.; **Nguyen, T. H.**; Maynard, H. D., "Polymeric Drug Conjugates by Controlled Radical Polymerization," in Comprehensive Biomaterials, Edited by P. Ducheyne, K. Healy, D. Hutmacher, J. Kirkpatrick, Elsevier, **2011**, vol 4, part 423, pp 377-388.

(5) Gunasekaran, K.; **Nguyen, T. H.**; Maynard, H. D.; Davis, T. P.; Bulmus, V., "Conjugation of siRNA with Comb-Type PEG Enhances Serum Stability and Gene Silencing Efficiency," *Macromol. Rapid Commun.,* **2011**, 32, 654-659.

(6) Chang, C. W.; **Nguyen, T. H.**; Maynard, H. D., "Thermoprecipitation of Glutathione *S*-Transferase by Glutathione-Poly(*N*-isopropylacrylamide) Prepared by RAFT Polymerization," *Macromol. Rapid Commun.*, **2010**, 31, 1691-1695.

    * Paper chosen as "Best of Macromolecular Journals of 2011"

(7) Heredia, K. L.; **Nguyen, T. H.**; Chang, C. -W.; Bulmus, V.; Davis, T. P.; Maynard, H. D., "Reversible siRNA-Polymer Conjugates by RAFT Polymerization," *Chem. Commun.*, **2008**, 28, 3245-3247.

PATENT

Maynard, H. D. & **Nguyen, T. H.** "bFGF-Polymer Conjugates Stable to Environmental Stressors," US Patent Application PCT/US2012/066905.

PRESENTATIONS

(1) "Heparin-Mimicking Polymer Conjugate Stabilizes Basic Fibroblast Growth Factor," Oral presentation at 247th ACS National Meeting & Exposition, Excellence in Graduate Polymer Research Symposium, Dallas, TX, March 2014.

(2) "Heparin-Mimicking Polymer Stabilizes bFGF," Poster presentation at Symposium for Celebration of the 100th Birthday of Saul Winstein, California NanoSystems Institute (CNSI), UCLA, CA, October 2012.

(3) "Thermoprecipitation of Glutathione *S*-Transferase by Glutathione-Poly(*N*-

isopropylacrylamide) Prepared by RAFT Polymerization," Poster presentation at 241st ACS National Meeting & Exposition, Anaheim, CA, March 2011.

(4) "Metallomesogenic Carboxylates with Tri-block Architecture," Poster presentation at University of Florida & Morehouse College HHMI Celebration of Undergraduate Creativity in the Arts & Sciences, Gainesville, FL, January 2009.

(5) "Characterization of Bare and Surface-modified Gold Nanoparticles," Oral presentation at Southern California Conference for Undergraduate Research, California State University, Los Angeles, CA, November 2007.

Chapter 1

Heparin-based Hydrogels and Heparin Mimicking Polymers

for Wound Healing

1.1. Introduction

Heparin is a linear polysaccharide that interacts with and regulates the activities of a wide range of proteins. It consists of 1, 4 linked disaccharide repeating units of uronic acid and glucosamine with varying degrees of sulfation and *N*-acetylation, with an average molecular weight of about 15 kDa (Figure 1.1).[1] Although most heparin molecules are microheterogeneous in their structures due to the variability of epimerization and sulfation during the process of biosynthesis, the prevalence of sulfate and carboxylate groups endows heparin with a high negative charge density.[2] Indeed, heparin has the highest electronegative charge of any known biological molecule (approximately 75 per molecule). Heparin mediates its interaction with proteins mainly through electrostatic interactions although hydrophobic effects, hydrogen bonding and the promotion of secondary structure in the proteins binding to heparin also play a role.[3] Proteins that bind to heparin include growth factors such as basic fibroblast growth factor (bFGF), vascular endothelial growth factor (VEGF), platelet-derived growth factor (PDGF), epidermal growth factor (EGF), antithrombin III, as well as hepatocyte growth factor (HGF) and transforming growth factor (TGF).[4,5] The heparin-binding motifs on these proteins have been defined by molecular modeling and crystallography studies.[6] In general, these interactions stabilize the proteins and/or regulate their affinity for cell receptors.[7] For example, heparin facilitates binding of bFGF to its receptor and increases its bioactivity.[8] However, exogenous heparin can also inhibit binding to cell surface receptors, depending on its concentration.[9]
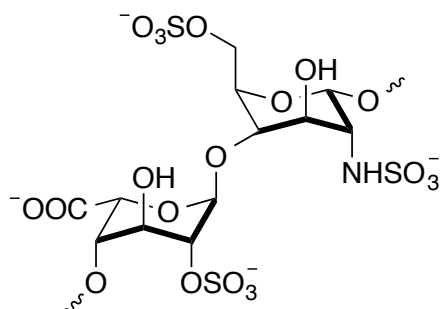
Figure 1.1. Chemical structure of heparin (major unit is shown).

Based on the biological functions of heparin, heparin-based materials are increasingly studied for the encapsulation and controlled release of growth factors to promote angiogenesis and tissue regeneration important in wound healing. Additionally, scaffolds modified with heparin have been explored for spatial delivery of growth factors to promote cell attachment and proliferation. Heparin is often physically encapsulated or covalently conjugated to polymeric hydrogels. Hydrogel materials provide highly hydrated, three-dimensional environments suitable for molecular and cellular biological interactions; their mechanical properties are readily tunable. A range of well-established chemistries have been developed to functionalize hydrogels with favorable properties such as responsiveness to externally applied triggers.[10,11] Alternatively, synthetic mimetic of heparin are developed to provide more selective synthetic control of the structure, since heparin itself is highly heterogeneous in structure, difficult to modify and susceptible to desulfation.[9,12] It has been demonstrated that sulfated and sulfonated polymers can mimic heparin and binding with heparin-binding growth factors.[13] These heparin-mimicking polymers are superior to heparin in purity, which may reduce the risks associated with batch-to-batch variation of heparin; they should also be resistant to heparinase *in vivo* which could result in long-acting activity.[9] Furthermore, the synthetic mimetic approach could allow better control

of binding affinity and potential for developing sequences that can potentiate the bioactivity of heparin-binding proteins or selectively bind one protein over another.

In this review, we focus on hydrogel materials that incorporate heparin as crosslinkers and/or polymer networks and their application for wound healing application. The use of heparin-mimicking polymers as heparin alternative in biomedical applications will also be discussed. The application of these materials in other biomedical applications such as tissue regeneration have been reviewed in other articles.[9,10]

1.2. Heparin-based hydrogels

Heparin-based hydrogels via covalent or non-covalent strategies have been employed as scaffolds or controlled release platforms for the delivery of a wide range of growth factors for wound healing. Furthermore, heparin-based hydrogels have been fabricated into a three-dimensional scaffolds suitable for cell delivery or transplantation. The rheological and drug release properties of these hydrogels can be tuned by heparin functionality and hydrogel composition (polymer concentration and molar ratio of crosslinkers). These are discussed below.

1.2.1. Non-covalently crosslinked heparin hydrogels

1.2.1.1. Heparin-binding peptide/protein as crosslinkers

Non-covalent crosslinking avoids the addition of toxic crosslinking reagents in gel formation, which might potentially inactivate the encapsulated therapeutic agents. Among the various non-covalent crosslinking mechanisms, heparin–protein/peptide interaction has been widely used in which assembly and biological properties of the hydrogel are designed to mimic the biological environment. Several heparin interacting proteins (HIPs) and heparin-binding peptides (HBPs), such as those derived from antithrombin III and human platelet factor 4, have been exploited for the non-covalent assembly of hydrogel networks. Based on the fact that dimeric growth factors, including VEGF and HGF, can bind to heparin, they have also been employed as multifunctional crosslinkers in the formation of hydrogels.[14] A schematic illustration of these non-covalently assembly was shown in Figure 1.2.
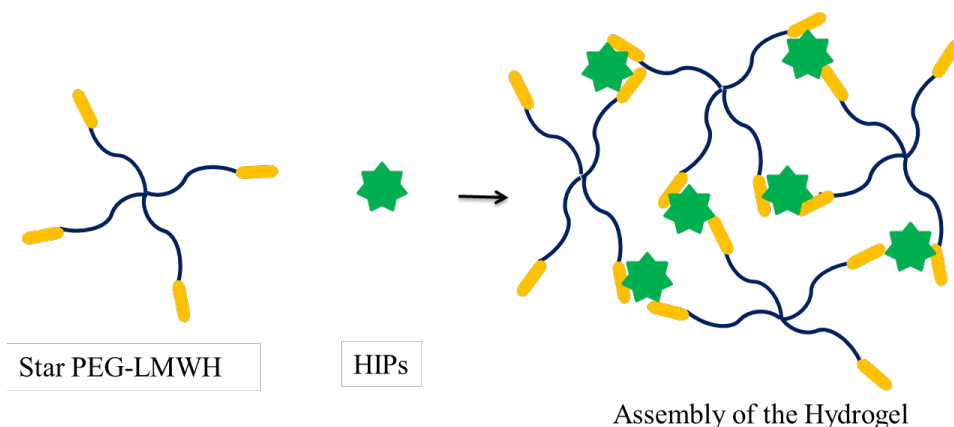
Figure 1.2. A schematic of non-covalently assembled hydrogel formed by the crosslinking of low molecular weight heparin (LMWH)-derivatized star PEG by heparin interacting proteins (HIPs).

Interactions between heparin and HBPs have been shown to be a useful strategy for the assembly of hydrogels. For example, the Hubbell group incorporated heparin-binding peptides into fibrin matrices during coagulation which served to immobilize heparin electrostatically to the matrix.[15] Such materials were then used to encapsulate and deliver bFGF.[16] Similarly, heparin has been incorporated both covalently and non-covalently into fibrin gels, prepared from fibrinogen and thrombin, for delivery of heparin-binding growth factors. Although in these cases heparin did not participate in the formation of hydrogels, it served to sequester the growth factors and altered the release kinetics.[17,18]

Bio-hybrid hydrogels consisting of heparin and synthetic polymers have been studied to provide increased control over mechanical and chemical properties. Hydrogels could be prepared by using HBPs or multiarm PEG functionalized with HBPs to form the non-covalent interaction with heparin.[19-22] The early studies built upon this approach by using star PEG

6

copolymer modified with either low molecular weight heparin (LMWH) or HBP derived from the heparin-binding region of antithrombin III. In the later studies, optimized sequences were explored. For example, a heparin-binding, coiled-coil peptide PF4$_{ZIP}$ derived from human platelet factor 4, was applied to assemble hydrogel non-covalently and can deliver bFGF in a controlled-release manner.[23-25] PF4$_{ZIP}$ was demonstrated to have higher binding affinity with heparin compared to that of antithrombin III sequences. The assembly, rheological properties, and degradation profiles of non-covalently associated hydrogel networks produced via these strategies could be tuned by the binding affinity and heparin association rate of the HBPs. In order to identify the key properties of a heparin-binding motif required for the non-covalent peptide-mediated assembly of hydrogels, researchers have designed a library of star PEG-peptide conjugates and screened the structure/function relationship and determined that both basic residues and heparin induced α-helix formation are important for the assembly process.[26] Particularly, star PEGs modified with peptide sequences of poly RA and KA formed stable hydrogels with heparin, where R and K are basic residues (arginine and lysine) and A is alanine which tend to form α-helical structures.[26] In addition to the synthetic polymer materials comprising PEG, an extracellular matrix (ECM)-derived polysaccharide such as hyaluronic acid (HA) have also been introduced to heparin hydrogels due to their role in tissue regeneration and biocompatibility. For instance, hydrogels could be produced via the interaction of LMWH-modified HA and HIP-modified star PEG copolymer.[22] This system was able to direct the differentiation of stem cells and mediate adipogenesis *in vitro*.

1.2.1.2. Therapeutically relevant proteins as crosslinkers

Growth factors have been used directly as crosslinkers for the assembly of non-covalent hydrogels. An important advantage of hydrogel networks produced by this strategy is the selective receptor-mediated gel degradation and drug release. For example, Kiick's group reported the assembly of hydrogels via the non-covalent interaction of LMWH-functionalized star PEG polymers and a therapeutically relevant, heparin-binding protein VEGF. A viscoelastic hydrogel could be formed *in situ* upon addition of VEGF solution to PEG-LMWH solution. The degradation of the crosslinks occurred in the presence of VEGF receptors with concurrent release of VEGF. The released protein induced proliferation in VEGF-responsive cell lines.[14,27] Hydrogels of this type offers a novel mechanism for targeted delivery of therapeutic relevant heparin-binding proteins.

1.2.2. Covalently crosslinked heparin hydrogels

Covalent interactions provide an alternative method for crosslinking. The degree of cross-linking can be precisely controlled which in turn determines important physicochemical characteristics of the gel including rheology, mesh size, hydration, degradation and drug release.

1.2.2.1. Michael-type addition for crosslinking

Compared with other covalent cross-linking methods using radiation, ultraviolet light or high temperatures, which may damage the protein drugs, Michael-type addition reactions typically occur in physiologically-relevant conditions (eg. aqueous medium, room temperature and moderate pH).[28,29] For example, a heparin-based hydrogel system was prepared by modifying the carboxyl groups of heparin to have pendant thiol groups and then reacting with PEG diacrylate via Michael addition to form thioether linkages, as shown in Figure 1.3. Thiol

functionalization of heparin carboxylic groups was controlled from 10% to 60% of the total available carboxylic groups so that the binding affinity of heparin with heparin-binding proteins was retained after modification.[30,31] Thiol-modified heparin could also be combined with ECM-derived polymers (e.g. thiol-modified HA or chondroitin sulfate (CS)) to form an injectable hydrogel with PEG-diacrylate.[32] Such hydrogels containing bFGF were proangiogenic *in vivo*.[33,34] It was believed that the immobilized heparin in these systems chemically mimicked naturally occurring heparan sulfate proteoglcyans on the cell surface, which are the major bFGF-binding molecules *in vivo*.[34] Similarly, heparin was functionalized with maleimide groups and crosslinked into hydrogels via reaction with thiol-derivatized PEG of various molecular weights and polymer structures.[35,36] Rational design of the chemical identity of the thiol permits tunable sensitivity of gel degradation. For instance, PEG esterified with phenylthiol derivatives, specifically 4-mercaptophenylpropionic acid or 2,2-dimethyl-3-(4-mercaptophenyl)propionic acid, resulted in reduction-sensitive bonds to glutathione (GSH), a reducing agent found naturally in intracellular compartments.[37]
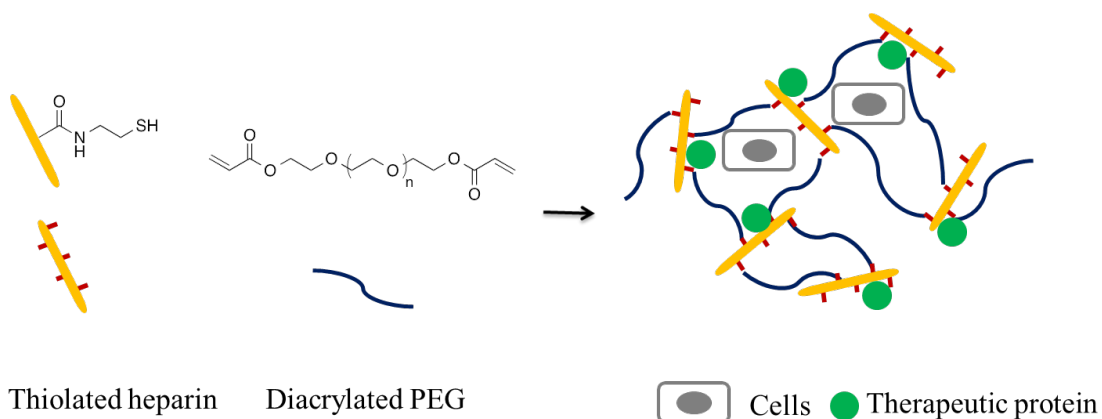
Figure 1.3. A schematic representation of assembled hydrogel formed by Michael-type addition for crosslinking and encapsulation of proteins/cells.

1.2.2.2. Amide coupling for crosslinking

1-Ethyl-3-(3-dimethylaminopropyl)carbodiimide/*N*-hydroxysulfosuccinimide (EDC/NHS) has been widely used to covalently immobilize heparin on amine end-functionalized materials including collagen matric, albumin and poly(L-lactide-co-glycolide) (PLGA)-based materials.[38,39] Similarly, this reaction has been utilized to form hydrogels. As shown in Figure 1.4, the Werner group developed a bio-hybrid hydrogel by crosslinking amino end-functionalized star PEG with NHS-activated carboxylic acid groups of heparin.[39,40] NHS activated heparin could be additionally functionalized through covalent attachment of Arg-Gly-Asp (RGD) peptides for cell adhesion.[40] It has been shown that bFGF, VEGF and other therapeutic growth factors could be bound and released by these star PEG-based heparin hydrogels. Furthermore, human umbilical vein endothelial cells (HUVECs) could be successfully cultured on these hydrogels, which made them the ideal candidates for multifunctional delivery systems for wound healing.[41-43] Likewise, poloxamer block copolymers consisting of ethylene oxide (EO) and propylene oxide (PO) blocks have been introduced to form thermosensitive hydrogels. Mono amine-terminated poloxamer was crosslinked with NHS activated heparin.[44] EDC/NHS chemistry is also widely employed in heparin-containing materials for coupling with peptides or antibodies. The physiochemical and biological properties of these gels could be tuned by controlling the functionality of heparin, the identity of the crosslinker, the concentration of the polymers and the molar ratio between the reactive groups.

NHS activated heparin **Amino end-functionalized starPEG**
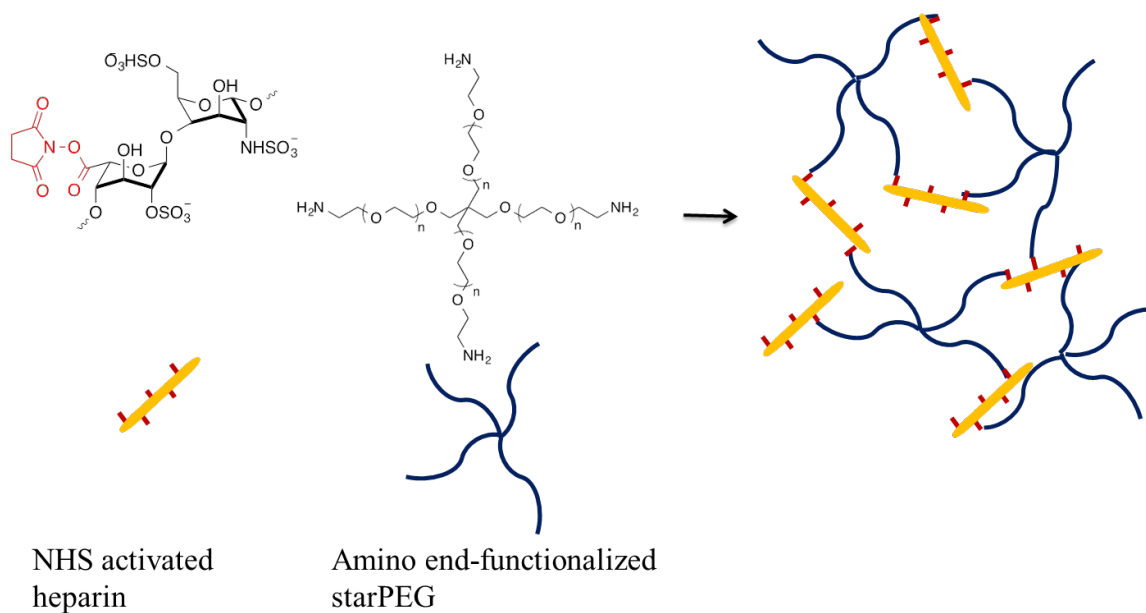
Figure 1.4. A schematic representation of assembled hydrogel formed by amide coupling.

1.2.3. Bio-responsive heparin hydrogels

Recent reports on hydrogels highlight those "smart" biomaterials that can change properties upon exposure to selective chemical or biological triggers, including changes in pH, temperature receptor, antibody and enzyme. A wide variety of labile bonds have been explored to regulate hydrogel degradation and drug release in response to environmental stimuli. As described above, reduction-sensitive hydrogels can be readily produced by Michael-type reactions. Although the reduction of disulfide bonds by GSH has long been employed for bio-responsive materials, biomedical applications of this approach are largely limited to intracellular or cancer drug delivery, where GSH is overproduced (up to 10-fold greater levels of GSH in intracellular compartments or tumors than that in extracellular environment and normal tissues).[9,45]

11

A commonly employed mechanism to design bio-responsive hydrogels is to incorporate peptides, which could be cleaved by a specific enzyme, into the hydrogel networks. For example, a thrombin-responsive peptide, NH_2-Gly-Gly-(D)Phe-Pip-Arg-Ser-Trp-Gly-Cys-Gly-$CONH_2$, was conjugated to maleimide terminated star PEG molecules through the cysteine residue. Then the gel was prepared by reacting activated carboxylic acid groups of heparin with the N-termini of PEG-peptide conjugate. Thrombin could cleave the peptide of the linker unit between the arginine and serine residues in the hybrid star PEG-heparin hydrogel. As a result, heparin was released, which inactivated thrombin to induce anticoagulation.[46] Likewise, peptide motifs that are degraded by matrix metalloproteinases (MMPs) were incorporated into heparin-based hydrogels.[47,48] The enzyme-cleavable peptide sequences were conjugated to functionalized polymers with thiols from the cysteine residues via Michael-type addition. Then a hydrogel was formed by coupling the carboxylate groups of heparin to the N-terminal amine of the PEG–peptide conjugates via EDC/NHS chemistry. A schematic representation of this approach was shown in Figure 1.5. The incorporation of MMP-sensitive peptides into hydrogel networks accelerated migration of encapsulated cells and therefore could promote tissue remodeling and regeneration.[47-49]

Activated heparin   Functionalized starPEG
with enzyme-cleavable
peptide sequences

Enzyme

Enzyme-cleavable peptide
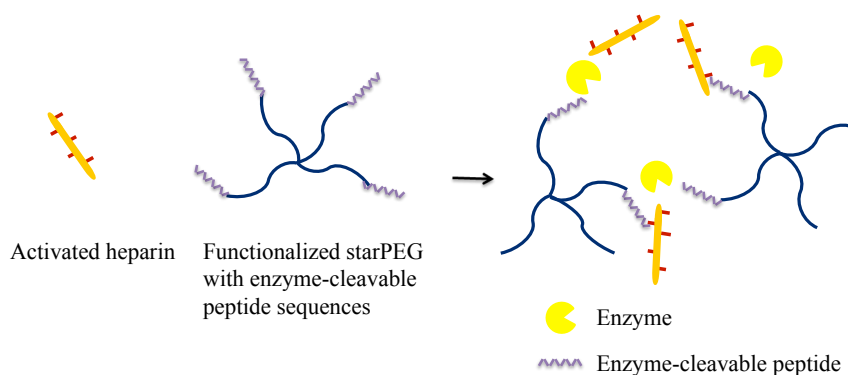
Figure 1.5. A schematic representation of bio-responsive hydrogel with enzyme-cleavable peptide sequences.

1.2.4. Heparin-containing hydrogels for wound healing

Wound healing is a highly regulated process that involves hemostasis, inflammation, angiogenesis, ECM formation and remodeling.[50] Heparin-containing hydrogels could serve as a "passive healing" dressing which presents adequate physical properties to create a favorable environment for the healing process. More importantly, incorporation of growth factors and/or cells into the hydrogels could represent an attractive new generation of therapeutic agents for "active healing" strategy. Protein drugs such as growth factors undergo proteolytic degradation, rapid diffusion, consequently loose bioactivity under physiological conditions; therefore, a hydrogel scaffold is not only beneficial but necessary to sustain the protein bioactivity in many instances.[51] For example, a hydrogel cross-linked by thiol-modified heparin and PEG-diacrylate was used to deliver a pro-angiogenic agent osteoprotegerin, which stimulated angiogenesis *in vivo*.[52] Hydrogel films composed of co-crosslinked thiolated CS and heparin were utilized for controlled-release delivery of bFGF to full-thickness wounds in genetically diabetic (db/db) mice and showed acceleration of wound healing, as well as improved dermis formation and vascularization.[34] Heparin-conjugated fibrin loaded with growth factor-rich plasma promoted wound closure as well as dermal and epidermal regeneration in a murine wound model.[53] However, there is concern that incorporating a sufficiently large quantity of heparin into the hydrogel matrix may lead to unfavorable side effects such as hemorrhage when heparin-containing materials are degraded *in vivo*.[33] Thus, heparin is usually used in a small amount to functionalize more inert hydrogel networks such as PEG and chitosan.[54,55] The addition of heparin within the gel scaffolds was proven to be crucial for sustain the release kinetics and maintain the activity of the growth factors.

1.3. Heparin-mimicking polymers

Historically, heparin-mimicking polymers were developed to identify potential antithrombotic alternatives to heparin. Since the realization of its importance and necessity as an anticoagulant a century ago, heparin has been exploited heavily in the clinic, yet the only sources of heparin are exclusively animal tissues. This, raises the concern of the possible risk of virus contamination from the isolating sources and immunological response,[56,57] variable patient-dependent dose-response,[58] and cytothrombopenia[59] and inspired researchers to study synthetic heparin mimics. Since heparin-mediated biological functions are wide-ranging and include cell differentiation, angiogenesis, inflammation, host defense and viral infection mechanisms, lipid transport and clearance, and cell adhesion and interaction, researchers have shifted to investigate other properties of heparin-mimicking polymers.[60] This part of the review will be focus on the development of classes of heparin-mimicking polymers as therapeutic replacement to treat various conditions such as thrombocytopenia, delayed angiogenesis, impaired tissue regeneration, all of which are important in wound healing.

1.3.1. Carboxymethyl Benzylamide Sulfonate Dextrans (CMDBS)

The first semi-synthetic heparin-mimicking polymers reported were functionalized dextrans, carboxymethyl benzylamide sulfonate dextrans (CMDBS), named after the substituents added (Figure 1.6).[61] Dextran is a complex branched glucan that was already widely used in the clinical as plasma volume expander. Mauzac and Jozefonvics reported the synthesis of soluble CMDBS polymers, which comprised of three reaction steps.[62] First, the hydroxyl groups on D-glucosyl units of dextran were carboxymethylated (CM). The carboxylic groups were then subjected partially to benzylamidation (B). Lastly, some of the phenyl rings were sulfonated (S)

in the presence of diluted chlorosulfonic acid. It was reported that to achieve higher degree of modification, each step could be repeated multiple times before the next.
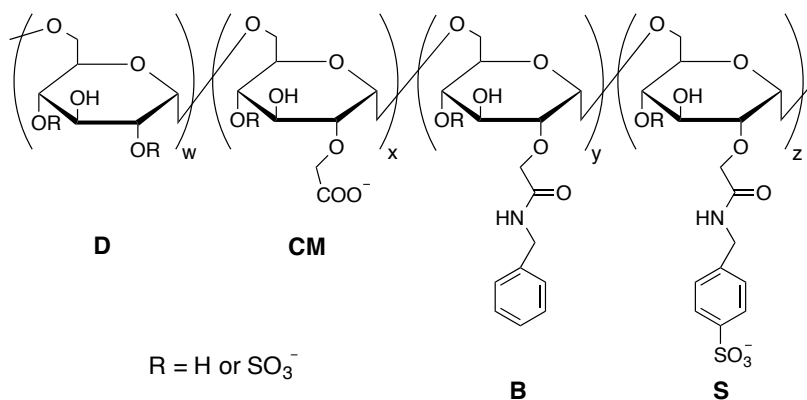
Figure 1.6. Chemical structure of carboxymethyl benzylamide sulfonate dextrans (CMDBS).

A number of dextran derivatives with different substituent compositions were reported with varying degrees of anticoagulation potency.[62] The anticoagulant activity of CMDBS polymers depended on the respective ratio of the functional groups. The CM group substitution needed to be greater than 40% to exhibit activity. At constant CM content of 47.5%, antithrombic activity increases exponentially with increasing S content of up to 15%. The CMDBS polymers exhibited low antithrombic activity compared to heparin, the activity increased with increasing molecular weight and plateaued at 40 kDa.[63]
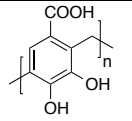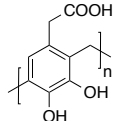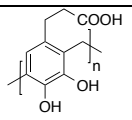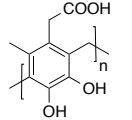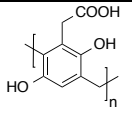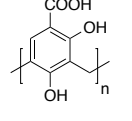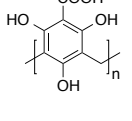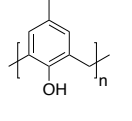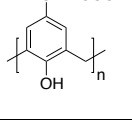
The CMDBS family also attracted much attention for its potential as biomimetic material for therapeutic replacement. Within almost two decades since its first account, many findings were reported on the diverse biological properties of CMDBS family including antithrombotic activities, anti-inflammatory activity, antibacterial and antiviral activities, regenerating activity,

modulation of vascular cell proliferation, and antiproliferative and antitumoral activity.[64] The capability of the functionalized dextrans to mimic the role of heparin in skin,[65,66] bone,[67-72] colon,[73] cornea,[74] and muscle[75-79] has gained the most attention, and the materials were provided the name ReGeneraTing Agent (RGTA) for their ability to help regenerate these tissues. The movement of the research began in 1989 when Tardieu and colleagues discovered a member of the CMDBS family with 82% CM, 6% B and 5% S potentiated the mitogenic activity of acidic fibroblast growth factor (aFGF) in chinese hamster fibroblast cells similar to heparin at 20 times higher concentration.[80] Varying the degree of substitution and the respective ratios of the functional groups resulted in polymers with unique abilities. In term of growth factor protection, CMDBS polymer with 82% CM, 23% B and 13% S was shown to protect bFGF better than aFGF.[81] In another example, Meddahi et al used RGTA11 polymer comprising of 110% CM, 2.5% B, 36.5% S to promote rat extensor digitorum longus (EDL) muscle regeneration post crushing via single systemic administration.[77] The compound also promoted endothelialization of vascular prostheses in combination with bFGF *in vitro*.[82,83] RGTA OTR4120 is another member of the RGTA family. Papy-Garcia and coworkers reported the synthesis and characterization of RGTA OTR4120 in 2005.[84] Basically, the compound was prepared by carboxymethylation and subsequent *O*-sulfonation of T40 dextran. The compound is marketed in France under the name CACIPLIQ20® to treat chronic wounds. More interestingly, unlike heparin, these polymers exhibited very little anticoagulant activity making them suitable candidates for regenerative medicine. The *in vivo* studies of the RGTA compounds for the treatment of skin wounds are reviewed in Section 1.3.5.

1.3.2. Polyaromatic anionic compounds

Regan and colleagues reported a series of nonsulfated, polyaromatic compounds that were synthesized from acid catalyzed polymerization of various anionic group-substituted phenols with formaldehyde ammonium salt (Table 1.1).[85] Among those, poly(4-hydroxyphenoxyacetic acid) termed RG-13577 was first identified as the most worthy candidate of its class for the ability to revert the bFGF-mediated transformed phenotype of tumorigenic cells.[86,87] The Vlodavsky group reported that RG-13577 mimicked heparin in many aspects including: inhibiting proliferation of vascular smooth muscle cells (SMCs) induced by thrombin, bFGF, and serum, efficiently releasing surface-bound bFGF, and inhibiting heparanase activity.[87,88] However, unlike heparin (MW = 5 k – 30 kDa), RG-13577 has a narrow molecular weight distribution (MW = 5 kDa) and a defined linear backbone structure making it a simple but effective model to elucidate the interactions with complex biomacromolecules. Desirably, the compound exhibited only 1% of the anticoagulant of heparin.[85]

Table 1.1. Structures and biological activities of polyaromatic anionic heparin-mimicking compounds. Adapted from Reference 80 with permission.

Compound	Antiproliferative activity of VSMC stimulated with			Release of ECM-bound bFGF	Heparanase inhibitory activity
	Thrombin 10^{-7} M	bFGF 2 ng/ml	Serum 10%		
RG-13525	++	++	+++	+	++
RG-13527	+++	++	+++	+++	+++
RG-13528	++	++	+	+++	++
RG-14444	+	+	+	+	+++
RG-13576	+++	++	++	+	+++
RG-13530	+++	++	+	+	++
RG-13519	+++	++	+	+++	++
RG-13524	+	++	+	+	+
RG-13577	+++	+++	+++	++	+++

Heparin and HS proteoglycan are key factors in growth factor-induced vascular endothelial cell proliferation, which is key in diseases such as cancer.[89,90] Increasing interest has been focused on developing chemical structures that can turn off the angiogenic-promoting activity of heparin/HS in many diseases. Miao and co-workers found that polyaromatic compounds inhibited binding of heparin to bFGF and of bFGF to its receptor FGFR1.[91] High concentrations of RG-13577 also abrogated the dimerization effects heparin had on bFGF molecules and FGFRs. In the presence of bFGF, RG-13577 completely inhibited tyrosine phosphorylation of FGFR1 in HS-knocked out cells but only partially in untreated cells suggesting that the compound competed directly with HS for binding to bFGF. Furthermore, RG-13577 was shown to inhibit proliferation in both HS-expressing and HS-deficient cells in the presence of heparin. Microvessel formation was reversibly completely inhibited in the presence of 10-25 μg/ml of RG-13577. It is worth noting that the compound was shown to enhance the stimulatory effect that heparin had on bFGF binding to FGFR1 and bFGF-induced cell proliferation when added at low concentrations. Even though RG-13577 has received attention for its inhibitory activity in angiogenesis arteriosclerosis and glomerulosclerosis,[92-96] these findings suggested that RG-13577 could be further investigated as candidate for regenerative therapy.

1.3.3. Sulfated Glycopolymers

Synthetic heparin-mimicking glycopolymers are polymers that have hydrocarbon backbone and pendant sulfated mono- or disaccharide units. Even though LMWH (average MW 6 kDa) and synthetic ultralow-molecular-weight heparin (average MW 1.5 kDa) have developed to overcome problems associated with unfractionated heparin such as heparin-induced thrombocytopenia (a development of low platelet count), their syntheses are still extremely

cumbersome.[59,97] Polymerization methods allowing for the assembly of key minimal units to form multivalent heparin-mimicking glycopolymer are more straightforward.

The Chaikof group reported the synthesis of sulfated 2-acrylamidoethyl *beta*-lactosides for the preparation of lactose heptasulfate-based glycopolymer via cyanoxyl-mediated free radical polymerization.[98,99] The sulfated glycopolymers were much less effective than heparin in term of the anticoagulant activity.[98] They were shown to have prolonged coagulation time compared to nonsulfated glycopolymers. The copolymer between lactose heptasulfate-based acrylamides and acrylamides (Figure 1.7a) was later demonstrated as a chaperon for bFGF in protecting the protein from trypsin, acid and heat-induced degradation.[99] The sulfated heteroglycopolymer was able to replace heparin in facilitating binding of bFGF to FGFRs, as well as dimerization of bFGF and FGFR, which are key events leading to cell proliferation in HS-deficient cell line.
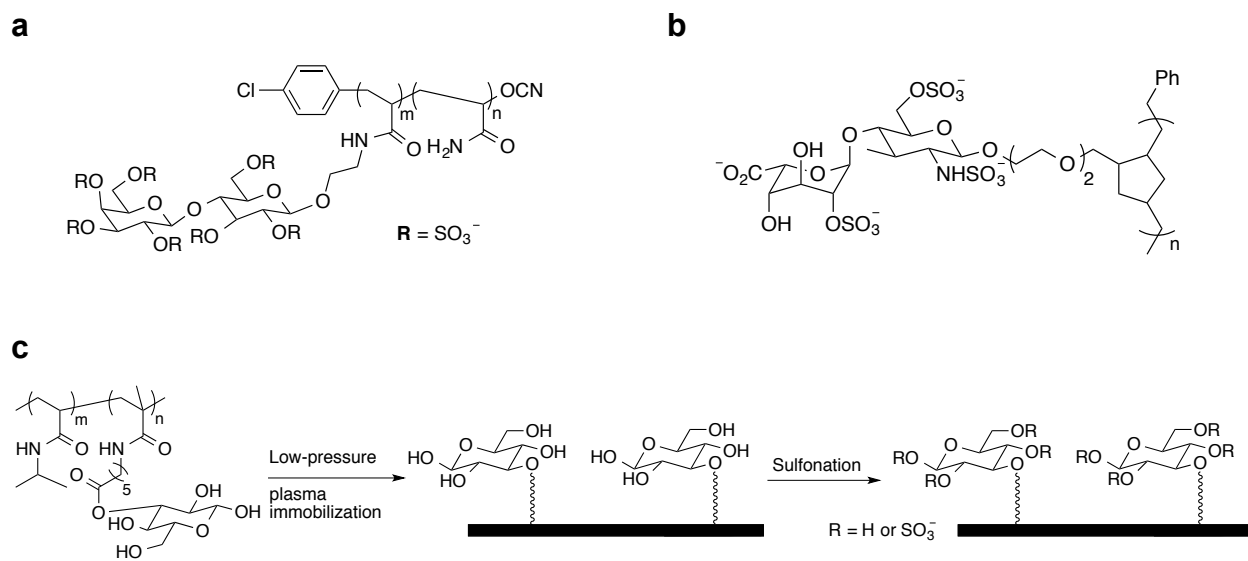
Figure 1.7. Chemical structures of heparin-mimicking glycopolymers. a) Copolymer of lactose heptasulfate-based acrylamides and acrylamides. b) Glycopolymer of trisulfated disaccharide-based norbornene prepaered via ROMP. c) Copolymer of *D*-glucofuranose-based methacrylamide and *N*-isopropylacrylamide on thin film.

Oezyuerek and co-workers reported the preparation of glycol-block copolymer surfaces with a combined thermoresponsive and heparin-like functionalities to mimic the ECM characteristics of growth factor binding and cell adhesion ligands.[100,101] The block-copolymer between D-glucofuranose-based methacrylamide and *N*-isopropylacrylamide monomers were prepared via reversible addition-fragmentation chain transfer (RAFT) polymerization and then covalently attached onto a fluorocarbon substrate via low-pressure plasma immobilization. Upon sulfonation of the hydroxyl groups, dual functionalized films were obtained (see Figure 1.7c). The sulfated glycol-block copolymer surfaces exhibited lower critical solution temperature of 33.7 °C and were shown to support adhesion and proliferation of HUVECs in the presence of bFGF, better than nonsulfated surfaces.[101] It was hypothesized that heparin-mimicking

glycopolymer brushes specifically bound to bFGF, thus they supported prolonged proliferation of HUVECs. At 37 °C, the sulfated glycol-block copolymer surfaces were shown to immobilize more bFGF than at room-temperature. The authors attributed this observation to the increase in hydrophobic interactions of the protein to the collapsed glycol-block copolymer brushes. The described technology was aimed at controlling binding and release of growth factors and cell adhesion that could potentially add value to tissue engineering and wound healing applications including implants.

The Hsieh-Wilson group reported the synthesis of glycopolymers via ring-opening metathesis polymerization (ROMP); the side chains were the tetrasulfated disaccharides identified in the ultralow-molecular-weight heparin.[102] The utilization of norbornene-based tetrasulfated disaccharide monomers allowed for homogeneous sulfation of the resulting glycopolymers. The glycopolymers were shown to have potent anticoagulant activity similar to low molecular weight heparin. In a subsequent report, the same group reported the synthesis of norbornene-based trisulfated HS disaccharide epitopes that were identified to be necessary to bind to most chemokines.[103] Glycopolymers with these pendant groups (Figure 1.7b) were synthesized via ROMP and shown to bind to and inhibit activity of RANTES (regulated on activation, normal T cell expressed and secreted, also known as CCL5), a pro-inflammatory chemokine, with similar efficiency to heparin. Importantly, these heparin-mimicking glycopolymers did not exhibit anticoagulant activity; therefore, they have potential therapeutic value in treatment of atherosclerosis, cancer and autoimmune disorders, without the bleeding complications of heparin.

1.3.4. Polysulfonated compounds

Polysulfonated polymers are fully synthetic polymers that make up another class of heparin-mimicking polymers. Heparin is a well-known co-factor in growth factor-induced angiogenesis in HS-deficient cell lines.[90,104] In contrast, free heparin can act as an anti-angiogenic factor in HS-expressed cell lines supposedly by binding to the growth factors such as bFGF, preventing bFGF from binding to FGFRs, and abrogating the vital formation of HS/bFGF/FGFR complex in endothelial cells.[105,106] Likens and co-workers studied the salt form of poly(2-acrylamido-2-methyl-1-propanesulfonic acid) (pAMPS), poly(anetholesulfonic acid) (pAS), poly(4-styrenesulfonic acid) (pSS), and poly(vinylsulfonic acid) (pVS) for their anti-angiogenic properties.[107] PAMPS, pAS and pSS were found to have potent anti-proliferative activity in fetal bovine aortic endothelial GM7373 cells; therefore, they were believed to have promising therapeutic value in treating angiogenesis-promoted cancers. PSS was also demonstrated to promote myogenic differentiation of muscle progenitor cells, which is important in tissue engineering.[108]

a

b
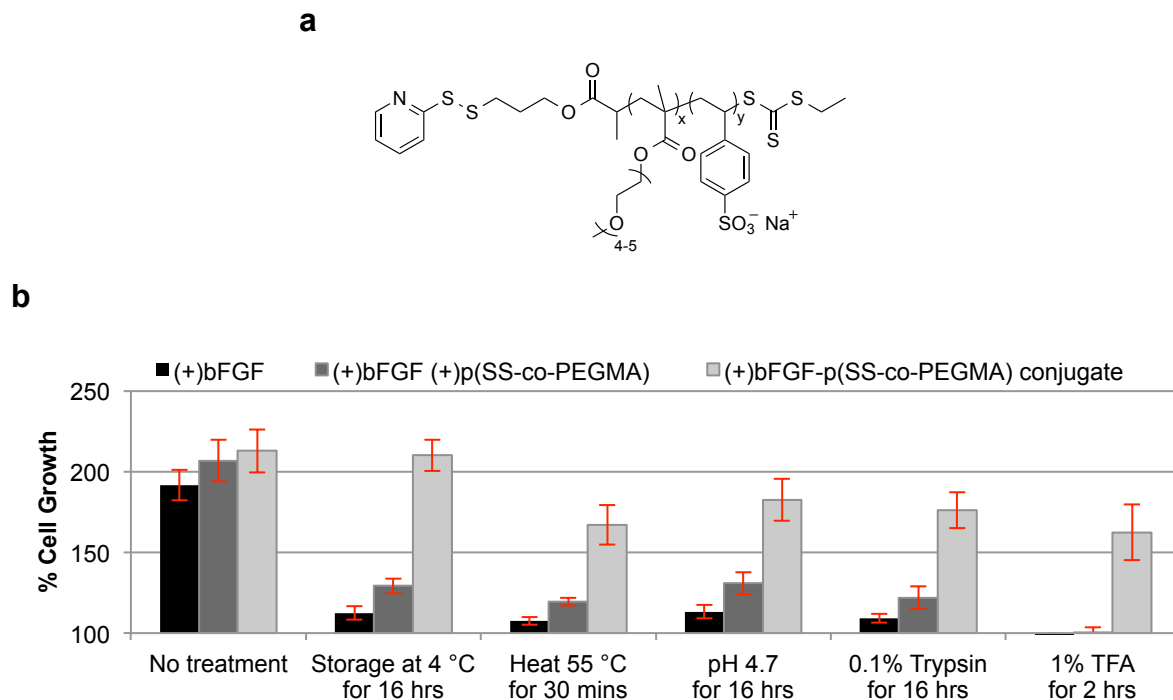
Figure 1.8. Polysulfonated heparin-mimicking polymer, p(SS-*co*-PEGMA) and the stability profile of its conjugate to bFGF. a) Chemical structure of the polymer. b) Stability of the bFGF-p(SS-*co*-PEGMA) conjugate against various stressors, tested on human dermal fibroblast cells for stimulated cell proliferation. The data was published in Nature Chemistry Journal[109] and the permission to reprint has been obtained.

We reported the synthesis of poly(sodium 4-styrenesulfonate-co-poly(ethylene glycol) methyl ether methacrylate) (p(SS-*co*-PEGMA)) via RAFT polymerization and showed that the polymer can bind to bFGF at the heparin-binding domain.[110,111] The structure of the polymer is shown in Figure 1.8a. We also reported a highly stable protein-heparin-mimicking polymer conjugate, bFGF-p(SS-*co*-PEGMA).[112] Heparin is a natural stabilizer for many heparin-binding proteins including bFGF, an extremely unstable protein.[7] bFGF-p(SS-*co*-PEGMA) was demonstrated to be stable to a variety of environmentally and therapeutically relevant stressors

such as: heat, mild and harsh acidic conditions, storage and proteolytic degradation (see Figure 1.8b). The conjugate also induced proliferation of human dermal fibroblast cells, a critical cell line in wound healing, as effectively as native protein and the data is presented in Chapter 2 of this thesis. The results indicate that the technology could be applied to stabilize important heparin-binding growth factors that involve in the wound healing process and efforts to preclinical verification are described in Chapter 3 of this thesis. Further iterations to increase the efficacy of bFGF are described in Chapter 4.

1.3.5. Heparin-mimicking polymers in wound healing

The reviewed classes of heparin-mimicking polymers show great potential in wound healing therapy. However, the field is still young and there are a few reports in *in vivo* studies showcasing the potential of these polymers as wound healing agents.

Meddahi and coworkers studied two CMDBS polymers with the compositions 83% CM, 23% B, 13 % S and 110% CM, 2.6% B 36.5% S (RGTA11), and showed that besides their ability to protect the FGFs from heat, pH and proteolytic degradation *in vitro*,[77,81] these polymers could stimulate deep wound healing better than the saline control in term of rate and new skin integrity.[65,66] The wounds (6 mm diameter) via biopsy punch were created on the back of rats; collagen plaster that had been soaked in saline solution with or without RGTA11 polymer was dressed on each wound subsequently. The rats were sacrificed at day 2, 3, and 6 post wounding for histology to evaluate the extent and quality of wound healing. It was observed that the groups treated with RGTA11 polymer (less than 1 μg/wound) show faster epidermis migration, thicker and more organized collagen deposition, as well as denser vessel formation compared to the control group. The authors proposed that the roles of the RGTA11 polymer in

binding/trapping the growth factors presented in the wound and protecting them from the up-regulated proteases in the wound were responsible for the stimulated wound closing observed.

RGTA OTR4120 was shown to enhance VEGF-induced HUVEC proliferation and migration *in vitro* and VEGF-induced angiogenesis *in vivo*.[113] The positive dermal effects of RGTA OTR4120 have been demonstrated in various animal models including: necrotic skin ulcers in mice,[114] second degree burn wounds in rats,[115] surgical excision wounds in rats,[116,117] dermal ischemia ulcers in rats,[118] and diabetes-impaired wounds in rats.[119] These studies have been recently reviewed elsewhere.[120]

1.4. Conclusions

The use of heparin in hydrogels and heparin-mimicking polymers has demonstrated significant implications in wound healing application. Numerous hydrogel-based systems have been fabricated for controlled delivery of growth factors and sequestration of cells for cell-mediated therapy. The benefits of incorporating heparin in these hydrogels include functionalization of the hydrogel, encapsulation of heparin-binding proteins and promoting cell adhesion. Recent advances in heparin-mimicking polymers offer opportunities for development of more structurally defined molecules. Such approaches would be of significant value in enhancing therapeutic efficacy and reducing side effects by fine-tuning the heparin binding motif and other molecular characteristics. The development of a broader range of heparin- and heparin-mimicking-based materials would further expand impact of these materials in the treatment of various dermal wounds and other diseases.

1.5. References

1) Sasisekharan, R.; Venkataraman, G. *Curr. Opin. Chem. Biol.* **2000**, *4*, 626.

2) Rosenberg, R. D.; Lam, L. *Proc. Nat. Aca. Sci.* **1979**, *76*, 1218.

3) Capila, I.; Linhardt, R. J. *Angew. Chem. Int. Ed. Engl.* **2002**, *41*, 391.

4) Klagsbrun, M. *Curr. Opin. Cell Biol.* **1990**, *2*, 857.

5) Hileman, R. E.; Fromm, J. R.; Weiler, J. M.; Linhardt, R. J. *Bioessays* **1998**, *20*, 156.

6) Cardin, A. D.; Weintraub, H. J. R. *Arteriosclerosis* **1989**, *9*, 21.

7) Gospodarowicz, D.; Cheng, J. *J. Cell. Physiol.* **1986**, *128*, 475.

8) Ornitz, D. M.; Yayon, A.; Flanagan, J. G.; Svahn, C. M.; Levi, E.; Leder, P. *Mol. Cell. Biol.* **1992**, *12*, 240.

9) Liang, Y.; Kiick, K. L. *Acta Biomater.* **2014**, *10*, 1588.

10) Ulijn, R. V.; Bibi, N.; Jayawarna, V.; Thornton, P. D.; Todd, S. J.; Mart, R. J.; Smith, A. M.; Gough, J. E. *Mater. Today* **2007**, *10*, 40.

11) Corkhill, P. H.; Hamilton, C. J.; Tighe, B. J. *Biomaterials* **1989**, *10*, 3.

12) Nguyen, T. H.; Kim, S.-H.; Decker, C. G.; Wong, D. Y.; Loo, J. A.; Maynard, H. D. *Nature Chem.* **2013**, *5*, 221.

13) Guan, R.; Sun, X.-L.; Hou, S.; Wu, P.; Chaikof, E. L. *Bioconj. Chem.* **2004**, *15*, 145.

14) Yamaguchi, N.; Zhang, L.; Chae, B.-S.; Palla, C. S.; Furst, E. M.; Kiick, K. L. *J. Am. Chem. Soc.* **2007**, *129*, 3040.

15) Sakiyama, S. E.; Schense, J. C.; Hubbell, J. A. *FASEB J.* **1999**, *13*, 2214.

16) Sakiyama-Elbert, S. E.; Hubbell, J. A. *J. Control. Release* **2000**, *65*, 389.

17) Oju, J.; Soo Hyun, R.; Ji Hyung, C.; Kim, B.-S. *J. Control. Release* **2005**, *105*, 249.

18) Yang, H. S.; Bhang, S. H.; Hwang, J. W.; Kim, D. I.; Kim, B. S. *Tissue Eng. Pt. A* **2010**, *16*, 2113.

19) Jeong, K. J.; Panitch, A. *Biomacromolecules* **2009**, *10*, 1090.

20) Seal, B. L.; Panitch, A. *Macromolecules* **2006**, *39*, 2268.

21) Kiick, K. L. *Soft Matter* **2008**, *4*, 29.

22) Tan, H.; Zhou, Q.; Qi, H.; Zhu, D.; Ma, X.; Xiong, D. *Macromol. Biosci.* **2012**, *12*, 621.

23) Zhang, L.; Furst, E. M.; Kiick, K. L. *J. Control. Release* **2006**, *114*, 130.

24) Yamaguchi, N.; Kiick, K. L. *Biomacromolecules* **2005**, *6*, 1921.

25) Yamaguchi, N.; Chae, B.-S.; Zhang, L.; Kiick, K. L.; Furst, E. M. *Biomacromolecules* **2005**, *6*, 1931.

26) Wieduwild, R.; Tsurkan, M.; Chwalek, K.; Murawala, P.; Nowak, M.; Freudenberg, U.; Neinhuis, C.; Werner, C.; Zhang, Y. *J. Am. Chem. Soc.* **2013**, *135*, 2919.

27) Kim, S. H.; Kiick, K. L. *Macromol. Rapid Commun.* **2010**, *31*, 1231.

28) Peppas, N. A.; Keys, K. B.; Torres-Lugo, M.; Lowman, A. M. *J. Control. Release* **1999**, *62*, 81.

29) Elbert, D. L.; Pratt, A. B.; Lutolf, M. P.; Halstenberg, S.; Hubbell, J. A. *J. Control. Release* **2001**, *76*, 11.

30) Tae, G.; Kim, Y.-J.; Choi, W.-I.; Kim, M.; Stayton, P. S.; Hoffman, A. S. *Biomacromolecules* **2007**, *8*, 1979.

31) Choi, W. I.; Kim, M.; Tae, G.; Kim, Y. H. *Biomacromolecules* **2008**, *9*, 1698.

32) Elia, R.; Fuegy, P. W.; VanDelden, A.; Firpo, M. A.; Prestwich, G. D.; Peattie, R. A. *Biomaterials* **2010**, *31*, 4630.

33) Cai, S.; Liu, Y.; Zheng Shu, X.; Prestwich, G. D. *Biomaterials* **2005**, *26*, 6054.

34) Liu, Y.; Cai, S.; Shu, X. Z.; Shelby, J.; Prestwich, G. D. *Wound Repair Regen.* **2007**, *15*, 245.

35) Nie, T.; Baldwin, A.; Yamaguchi, N.; Kiick, K. L. *J. Control. Release* **2007**, *122*, 287.

36) Robinson, K. G.; Nie, T.; Baldwin, A. D.; Yang, E. C.; Kiick, K. L.; Akins, R. E. *J. Biomed. Mater. Res. Part A* **2012**, *100A*, 1356.

37) Baldwin, A. D.; Kiick, K. L. *Polym. Chem.* **2013**, *4*, 133.

38) Jeon, O.; Kang, S.-W.; Lim, H.-W.; Hyung Chung, J.; Kim, B.-S. *Biomaterials* **2006**, *27*, 1598.

39) Wissink, M. J. B.; Beernink, R.; Poot, A. A.; Engbers, G. H. M.; Beugeling, T.; van Aken, W. G.; Feijen, J. *J. Control. Release* **2000**, *64*, 103.

40) Freudenberg, U.; Hermann, A.; Welzel, P. B.; Stirl, K.; Schwarz, S. C.; Grimmer, M.; Zieris, A.; Panyanuwat, W.; Zschoche, S.; Meinhold, D.; Storch, A.; Werner, C. *Biomaterials* **2009**, *30*, 5049.

41) Zieris, A.; Prokoph, S.; Levental, K. R.; Welzel, P. B.; Grimmer, M.; Freudenberg, U.; Werner, C. *Biomaterials* **2010**, *31*, 7985.

42) Zieris, A.; Chwalek, K.; Prokoph, S.; Levental, K. R.; Welzel, P. B.; Freudenberg, U.; Werner, C. *J. Control. Release* **2011**, *156*, 28.

43) Baumann, L.; Prokoph, S.; Gabriel, C.; Freudenberg, U.; Werner, C.; Beck-Sickinger, A. G. *J. Control. Release* **2012**, *162*, 68.

44) Zhao, Y. Z.; Lv, H. F.; Lu, C. T.; Chen, L. J.; Lin, M.; Zhang, M.; Jiang, X.; Shen, X. T.; Jin, R. R.; Cai, J.; Tian, X. Q.; Wong, H. L. *Plos One* **2013**, *8*, e73178.

45) Wu, G.; Fang, Y.-Z.; Yang, S.; Lupton, J. R.; Turner, N. D. *J. Nutr.* **2004**, *134*, 489.

46) Maitz, M. F.; Freudenberg, U.; Tsurkan, M. V.; Fischer, M.; Beyrich, T.; Werner, C. *Nature Commun.* **2013**, *4*.

47) Nilasaroya, A.; Martens, P. J.; Whitelock, J. M. *Biomaterials* **2012**, *33*, 5534.

48) Tsurkan, M. V.; Chwalek, K.; Levental, K. R.; Freudenberg, U.; Werner, C. *Macromol. Rapid Commun.* **2010**, *31*, 1529.

49) Anderson, S. B.; Lin, C.-C.; Kuntzler, D. V.; Anseth, K. S. *Biomaterials* **2011**, *32*, 3564.

50) Guo, S.; Dipietro, L. A. *J. Dent. Res.* **2010**, *89*, 219.

51) Edelman, E. R.; Mathiowitz, E.; Langer, R.; Klagsbrun, M. *Biomaterials* **1991**, *12*, 619.

52) McGonigle, J. S.; Tae, G.; Stayton, P. S.; Hoffman, A. S.; Scatena, M. *J. Biomater. Sci. Polym. Ed.* **2008**, *19*, 1021.

53) Yang, H. S.; Shin, J.; Bhang, S. H.; Shin, J.-Y.; Park, J.; Im, G.-I.; Kim, C.-S.; Kim, B.-S. *Exp. Mol. Med.* **2011**, *43*, 622.

54) Andreopoulos, F. M.; Persaud, I. *Biomaterials* **2006**, *27*, 2468.

55) Ishihara, M.; Fujita, M.; Obara, K.; Hattori, H.; Nakamura, S.; Nambu, M.; Kiyosawa, T.; Kanatani, Y.; Takase, B.; Kikuchi, M.; Maehara, T. *Curr. Drug Deliv.* **2006**, *3*, 351.

56) Blossom, D. B.; Kallen, A. J.; Patel, P. R.; Elward, A.; Robinson, L.; Gao, G.; Langer, R.; Perkins, K. M.; Jaeger, J. L.; Kurkjian, K. M.; Jones, M.; Schillie, S. F.; Shehab, N.; Ketterer, D.; Venkataraman, G.; Kishimoto, T. K.; Shriver, Z.; McMahon, A. W.; Austen, K. F.; Kozlowski, S.; Srinivasan, A.; Turabelidze, G.; Gould, C. V.; Arduino, M. J.; Sasisekharan, R. *New Engl. J. Med.* **2008**, *359*, 2674.

57) Guerrini, M.; Beccati, D.; Shriver, Z.; Naggi, A.; Viswanathan, K.; Bisio, A.; Capila, I.; Lansing, J. C.; Guglieri, S.; Fraser, B.; Al-Hakim, A.; Gunay, N. S.; Zhang, Z. Q.; Robinson,

L.; Buhse, L.; Nasr, M.; Woodcock, J.; Langer, R.; Venkataraman, G.; Linhardt, R. J.; Casu, B.; Torri, G.; Sasisekharan, R. *Nature Biotechnol.* **2008**, *26*, 669.

58) Hirsh, J.; Dalen, J. E.; Anderson, D. R.; Poller, L.; Bussey, H.; Ansell, J.; Deykin, D.; Brandt, J. T. *Chest* **1998**, *114*, 445S.

59) Warkentin, T. E.; Levine, M. N.; Hirsh, J.; Horsewood, P.; Roberts, R. S.; Gent, M.; Kelton, J. G. *New Engl. J. Med.* **1995**, *332*, 1330.

60) Capila, I.; Linhardt, R. J. *Angew. Chem. Int. Edit.* **2002**, *41*, 391.

61) Mauzac, M.; Aubert, N.; Jozefonvicz, J. *Biomaterials* **1982**, *3*, 221.

62) Mauzac, M.; Jozefonvicz, J. *Biomaterials* **1984**, *5*, 301.

63) Crepon, B.; Maillet, F.; Kazatchkine, M. D.; Jozefonvicz, J. *Biomaterials* **1987**, *8*, 248.

64) Logeart-Avramoglou, D.; Jozefonvicz, J. *J. Biomed. Mater. Res.* **1999**, *48*, 578.

65) Meddahi, A.; Blanquaert, F.; Saffar, J. L.; Colombier, M. L.; Caruelle, J. P.; Josefonvicz, J.; Barritault, D. *Path. Res. Prac.* **1994**, *190*, 923.

66) Meddahi, A.; Caruelle, J. P.; Gold, L.; Rosso, Y.; Barritault, D. *Diabetes Metab.* **1996**, *22*, 274.

67) Albo, D.; Long, C.; Jhala, N.; Atkinson, B.; Granick, M. S.; Wang, T.; Meddahi, A.; Barritault, D.; Solomon, M. P. *J Craniofac. Surg.* **1996**, *7*, 19.

68) Blanquaert, F.; Saffar, J. L.; Colombier, M. L.; Carpentier, G.; Barritault, D.; Caruelle, J. P. *Bone* **1995**, *17*, 499.

69) Lafont, J.; Colombier, M. L.; Barritault, D.; Saffar, J. L. *J. Dent. Res.* **1998**, *77*, 1248.

70) Blanquaert, F.; Barritault, D.; Caruelle, J. P. *J. Biomed. Mater. Res.* **1999**, *44*, 63.

71) Lafont, J.; Baroukh, B.; Berdal, A.; Colombier, M. L.; Barritault, D.; Caruelle, J. P.; Saffar, J. L. *Growth Factors* **1998**, *16*, 23.

72) Lafont, J.; Blanquaert, F.; Colombier, M. L.; Barritault, D.; Carueelle, J. P.; Saffar, J. L. *Calcif. Tissue Int.* **2004**, *75*, 517.

73) Meddahi, A.; Benoit, J.; Ayoub, N.; Sezeur, A.; Barritault, D. *J. Biomed. Mater. Res.* **1996**, *31*, 293.

74) Fredjreygrobellet, D.; Hristova, D. L.; Ettaiche, M.; Meddahi, A.; Jozefonwicz, J.; Barritault, D. *Ophthalmic. Res.* **1994**, *26*, 325.

75) Meddahi, A.; Blanquaert, F.; Saffar, J. L.; Colombier, M. L.; Caruelle, J. P.; Josefonvicz, J.; Barritault, D. *Path. Res. Prac.* **1994**, *190*, 923.

76) Desgranges, P.; Barbaud, C.; Caruelle, J. P.; Barritault, D.; Gautron, J. *FASEB* **1999**, *13*, 761.

77) Meddahi, A.; Bree, F.; Papy-Garcia, D.; Gautron, J.; Barritault, D.; Caruelle, J. P. *J. Biomed. Mater. Res.* **2002**, *62*, 525.

78) Papy-Garcia, D.; Barbosa, I.; Duchesnay, A.; Saadi, S.; Caruelle, J. P.; Barritault, D.; Martelly, I. *J. Biomed. Mater. Res.* **2002**, *62*, 46.

79) Rouet, V.; Meddahi-Pelle, A.; Miao, H. Q.; Vlodavsky, I.; Caruelle, J. P.; Barritault, D. *J Biomed. Mater. Res. A* **2006**, *78A*, 792.

80) Tardieu, M.; Slaoui, F.; Josefonvicz, J.; Courty, J.; Gamby, C.; Barritault, D. *J. Biomater. Sci. Poly. Ed.* **1989**, *1*, 63

81) Tardieu, M.; Gamby, C.; Avramoglou, T.; Jozefonvicz, J.; Barritault, D. *J. Cell. Physiol.* **1992**, *150*, 194.

82) Desgranges, F.; Barritault, D.; Caruelle, J. P.; Tardieu, M. *Int. J. Artif. Organs* **1997**, *20*, 589.

83) Desgranges, P.; Caruelle, J. P.; Carpentier, G.; Barritault, D.; Tardieu, M. *J. Biomed. Mater. Res.* **2001**, *58*, 1.

84) Papy-Garcia, D.; Barbier-Chassefiere, V.; Rouet, V.; Kerros, M. E.; Klochendler, C.; Tournaire, M. C.; Barritault, D.; Caruelle, J. P.; Petit, E. *Macromolecules* **2005**, *38*, 4647.

85) Benezra, M.; Vlodavsky, I.; Yayon, A.; Bar-Shavit, R.; Regan, J.; Chang, M.; Ben-Sasson, S. *Cancer Res.* **1992**, *52*, 5656.

86) Regan, J. R.; Bruno, J. G.; Chang, M. N.; Sabatino, R.; Dalisa, R.; Bensasson, S. A.; Eilat, D. *J. Bioact. Compatible Polym.* **1993**, *8*, 317.

87) Benezra, M.; Ishai-Michaeli, R.; Ben-Sasson, S. A.; Vlodavsky, I. *J. Cell. Physiol.* **2002**, *192*, 276.

88) Benezra, M.; Bensasson, S. A.; Regan, J.; Chang, M.; Barshavit, R.; Vlodavsky, I. *Arterioscler. Thromb.* **1994**, *14*, 1992.

89) Cariou, R.; Harousseau, J. L.; Tobelem, G. *Cell. Biol. Int. Rep.* **1988**, *12*, 1037.

90) Folkman, J.; Shing, Y. *Adv. Exp. Med. Biol.* **1992**, *313*, 355.

91) Miao, H. Q.; Ornitz, D. M.; Aingorn, E.; BenSasson, S. A.; Vlodavsky, I. *J. Clin. Invest.* **1997**, *99*, 1565.

92) Katz, A.; Vlodavsky, I.; Davies, M.; Miao, H. Q.; BenSasson, S. A.; Darmon, D.; Hurwitz, H.; Borgel, H.; Benezra, M. *J. Am. Soc. Nephrol.* **1997**, *8*, 1688.

93) Schmidt, A.; Vlodavsky, I.; Volker, W.; Buddecke, E. *Atherosclerosis* **1999**, *147*, 387.

94) Benezra, M.; Vogel, T.; Ben-Sasson, S. A.; Panet, A.; Sehayek, E.; Al-Haideiri, M.; Decklbaum, R. J.; Vlodavsky, I. *J. Cell. Biochem.* **2001**, *81*, 114.

95) Neuger, L.; Ruge, T.; Makoveichuk, E.; Vlodavsky, I.; Olivecrona, G. *Atherosclerosis* **2001**, *157*, 13.

96) Irony-Tur-Sinai, M.; Vlodavsky, I.; Ben-Sasson, S. A.; Pinto, F.; Sicsic, C.; Brenner, T. *J Neurol. Sci.* **2003**, *206*, 49.

97) Junqueira, D. R. G.; Perini, E.; Penholati, R. R. M.; Carvalho, M. G. *Cochrane. Db. Syst. Rev.* **2012**.

98) Sun, X. L.; Grande, D.; Baskaran, S.; Hanson, S. R.; Chaikof, E. L. *Biomacromolecules* **2002**, *3*, 1065.

99) Guan, R.; Sun, X. L.; Hou, S. J.; Wu, P. Y.; Chaikof, E. L. *Bioconjugate Chem.* **2004**, *15*, 145.

100) Ozyurek, Z.; Komber, H.; Gramm, S.; Schmaljohann, D.; Muller, A. H. E.; Voit, B. *Macromol. Chem. Physic.* **2007**, *208*, 1035.

101) Oezyuerek, Z.; Franke, K.; Nitschke, M.; Schulze, R.; Simon, F.; Eichhorn, K. J.; Pompe, T.; Werner, C.; Voit, B. *Biomaterials* **2009**, *30*, 1026.

102) Oh, Y. I.; Sheng, G. J.; Chang, S. K.; Hsieh-Wilson, L. C. *Angew. Chem. Int. Edit.* **2013**, *52*, 11796.

103) Sheng, G. J.; Oh, Y. I.; Chang, S. K.; Hsieh-Wilson, L. C. *J. Am. Chem. Soc.* **2013**, *135*, 10898.

104) Yayon, A.; Klagsbrun, M.; Esko, J. D.; Leder, P.; Ornitz, D. M. *Cell* **1991**, *64*, 841.

105) Ferrao, A. V.; Mason, R. M. *Biochim. Biophys. Acta.* **1993**, *1180*, 225.

106) Ishihara, M.; Tyrrell, D. J.; Stauber, G. B.; Brown, S.; Cousens, L. S.; Stack, R. J. *J. Biol. Chem.* **1993**, *268*, 4675.

107) Liekens, S.; Leali, D.; Neyts, J.; Esnouf, R.; Rusnati, M.; Dell'Era, P.; Maudgal, P. C.; De Clercq, E.; Presta, M. *Mol. Pharmacol.* **1999**, *56*, 204.

108) Sangaj, N.; Kyriakakis, P.; Yang, D.; Chang, C. W.; Arya, G.; Varghese, S. *Biomacromolecules* **2010**, *11*, 3294.

109) Nguyen, T. H.; Kim, S. H.; Decker, C. G.; Wong, D. Y.; Loo, J. A.; Maynard, H. D. *Nature Chem.* **2013**, 5, 221.

110) Christman, K. L.; Vazquez-Dorbatt, V.; Schopf, E.; Kolodziej, C. M.; Li, R. C.; Broyer, R. M.; Chen, Y.; Maynard, H. D. *J. Am. Chem. Soc.* **2008**, *130*, 16585.

111) Kolodziej, C. M.; Kim, S. H.; Broyer, R. M.; Saxer, S. S.; Decker, C. G.; Maynard, H. D. *J. Am. Chem. Soc.* **2012**, *134*, 247.

112) Nguyen, T. H.; Kim, S. H.; Decker, C. G.; Wong, D. Y.; Loo, J. A.; Maynard, H. D. *Nature Chem.* **2013**, *5*, 221.

113) Rouet, V.; Hamma-Kourbali, Y.; Petit, E.; Panagopoulou, P.; Katsoris, P.; Barritault, D.; Caruelle, J. P.; Courty, J. *J. Biol. Chem.* **2005**, *280*, 32792.

114) Barbier-Chassefiere, V.; Garcia-Filipe, S.; Yue, X. L.; Kerros, M. E.; Petit, E.; Kern, P.; Saffar, J. L.; Papy-Garcia, D.; Caruelle, J. P.; Barritault, D. *J. Biomed. Mater. Res. A* **2009**, *90A*, 641.

115) Garcia-Filipe, S.; Barbier-Chassefiere, V.; Alexakis, C.; Huetl, E.; Ledoux, D.; Kerros, M. E.; Petit, E.; Barritault, D.; Caruelle, J. P.; Kern, P. *J. Biomed. Mater. Res. A* **2007**, *80A*, 75.

116) Tong, M.; Tuk, B.; Hekking, I. M.; Vermeij, M.; Barritault, D.; van Neck, J. W. *Wound Repair Regen.* **2009**, *17*, 840.

117) Tong, M.; Zbinden, M. M.; Hekking, I. J. M.; Vermeij, M.; Barritault, D.; van Neck, J. W. *Wound Repair Regen.* **2008**, *16*, 294.

118) Tong, M.; Tuk, B.; Hekking, I. M.; Pleumeekers, M. M.; Boldewijn, M. B.; Hovius, S. E. R.; van Neck, J. W. *Wound Repair Regen.* **2011**, *19*, 505.

119) Tong, M.; Tuk, B.; Shang, P.; Hekking, I. M.; Fijneman, E. M. G.; Guijt, M.; Hovius, S. E. R.; van Neck, J. W. *Diabetes* **2012**, *61*, 2633.

120)van Neck, J.; Tuk, B.; Barritault, D.; Tong, M. In *Tissue regeneration - from basic biology to clinical application*; Davies, J., Ed.; InTech: 2012.

Chapter 2

A Heparin-Mimicking Polymer Conjugate Stabilizes

Basic Fibroblast Growth Factor (bFGF)[§]

2.1. Introduction

Covalent conjugation of synthetic polymers, in particular PEG, has been widely explored as a means to improve the half-lives of proteins in vivo, and to lower the immunogenicities and antigenicities of proteins.[1,2] Consequently, a number of PEGylated proteins have been approved by the US Food and Drug Administration for treatment of a variety of diseases.[3] However, therapeutic proteins often suffer from instability during storage and use, and PEG does not necessarily stabilize proteins to external stressors. Yet, there are only a few reports on conjugating polymers to promote protein stabilization: Keefe et al. demonstrated that covalently binding poly(carboxybetaine) to α-chymotrypsin improved stability and at the same time retained the enzyme's native binding affinity.[4] We showed that polystyrene with pendent trehalose disaccharides resulted in lysozyme conjugates stable to high temperatures and repeated lyophilization.[5] Herein, we demonstrate for the first time stabilization of a protein that is a member of a large class of therapeutically useful biologics, namely the heparin-binding proteins, with a polymer specifically designed to interact with the heparin-binding domain of the growth factor.

A considerable number of proteins interact with the polysaccharide heparin and make up the class of heparin-binding proteins, including proteases, growth factors, chemokines, lipid-binding proteins, pathogens, and adhesion proteins.[6] Their key biological functions are wide ranging and include blood coagulantion, cell differentiation, angiogenesis, inflammation, host defense and viral infection mechanisms, lipid transport and clearance, and cell adhesion and interaction. Since the introduction of heparin in the early 1900s as an anticoagulant agent, it is now known that the role of heparin in the body is far reaching. Molecular modeling and crystallography studies have defined the heparin-binding motifs on numerous proteins,[7] and

researchers have found that their interactions with heparin were not only critical for bioactivity, but in many cases also for stabilization. In this report, we describe that an important heparin-binding protein, basic fibroblast growth factor (bFGF), is stabilized by conjugation of a synthetic heparin-mimicking polymer.

bFGF is a therapeutic target widely investigated because of its crucial role in diverse cellular functions including: embryonic development,[8] angiogenesis,[9] tissue regeneration,[10] bone regeneration,[11] development and maintenance of the nervous system,[12] stem cell self-renewal,[13] and wound healing.[14] bFGF is a potent stimulator of proliferation, differentiation and migration of multiple cell types.[15,16] Therefore, bFGF is promising for a wide variety of applications in regenerative medicine and others. However, due to the protein's extreme instability in storage and delivery,[17,18] its therapeutic effectiveness is not yet widely realized.[19]

Since heparin is the natural stabilizer of bFGF,[18,20] many researchers employ heparin in controlled release systems of this growth factor.[21] However, heparin itself is difficult to modify, is susceptible to desulfation, suffers from batch-to-batch variation and impurities, and has significant activity in other, non-target biological pathways. In addition, it has been reported to inhibit normal growth of certain cell types including human umbilical vein endothelial cells and human dermal fibroblasts, which could possibly counteract the desirable effects of bFGF.[22,23] It is known that sulfated and sulfonated polymers can mimic heparin.[24,25] Here, we report that covalent conjugation of a heparin-mimicking polymer, poly(sodium 4-styrenesulfonate-*co*-poly(ethylene glycol) methyl ether methacrylate) (p(SS-*co*-PEGMA)),[26,27] to bFGF significantly enhances protein stability. Thus far, only PEG has been covalently conjugated to bFGF;[28-32] but these conjugates either have significantly reduced protein activity, require addition of heparin to

40

stabilize the conjugate, or require large protein concentrations. To our knowledge, this is the

first example of a stabilized bFGF conjugate.

2.2. Experimental

2.2.1. Materials

Chemicals and reagents were purchased from Fisher or Sigma-Aldrich unless indicated otherwise. bFGF and ELISA Development DuoSet® kits were purchased from R&D Systems. Heparin was purchased from PromoCell. Rabbit anti-fibroblast growth factor basic antibody and goat anti-rabbit IgG-HRP conjugate for Western blot were purchased from CALBIOCHEM and Bio-Rad, respectively. Normal HDF cells were purchased from PromoCell. BaF3 cells that express FGFR1 (FR1C-11) were kindly provided by Prof. David Ornitz (Washington University, Saint Louis). Media and supplements for cell culture were either purchased from PromoCell, Lonza or Invitrogen. PD173074 (N-[2-[[4-(diethylamino)butyl]amino]- 6- (3, 5- dimethoxyphenyl)pyrido[2, 3-d]pyrimidin-7-yl]- N'-(1, 1- dimethylethyl)- urea) was purchased from Cayman Chemical. LIVE/DEAD® viability/cytotoxicity assay kit and CellTiter-Blue® cell viability assay were obtained from Invitrogen and Promega, respectively. HiTrap™ Heparin HP 1 ml was purchased from GE Healthcare. PMMA standards for GPC calibration were purchased from Polymer Laboratories. PEG 4 kDa was purchased from Polymer Laboratories. Merck 60 (230-400 mesh) silica gel was used for column chromatography. DCM was distilled over CaH_2 prior to use. AIBN was recrystallized twice from ethanol and dried prior to use. Copper bromide (CuBr) was purified by stirring in glacial acetic acid for 12 hours, filtering and rinsing with ethanol and diethyl ether, and drying under vacuum. Prior to use, 4-styrene sulfonic acid, sodium salt hydrate monomer was pre-treated with Na^+-activated DOWEX 50WX8 200-400 mesh resin to produce the sodium salt. 3-(Pyridin-2-yldisulfanyl)propyl-2-(ethylthiocarbonothioylthio) propanoate[33] and 2-(pyridin-2-yldisulfanyl)ethanol[34] were synthesized as previously described.

2.2.2. Analytical Techniques

^{1}H and ^{13}C NMR spectroscopy were performed on an Avance DRX 400 or 500 MHz spectroscopy instruments. Infrared spectroscopy was performed on a PerkinElmer FT-IR equipped with an ATR accessory. UV-Vis spectrophotometry analyses were performed on a Biomate 5 Thermo Spectronic spectrometer. GPC was conducted on a Shimadzu HPLC system equipped with a refractive index detector RID-10A, one Polymer Laboratories PLgel guard column, and two Polymer Laboratories PLgel 5 μm mixed D columns. DMF containing 0.10 M LiBr at 40 °C was used as the eluent and near-monodisperse poly(methyl methacrylate) standards were used for calibration at 0.6 ml/min. Chromatograms were processed using the EZStart 7.2 chromatography software. Gel electrophoresis was performed using NuPAGE® 4-12% Bis-tris gels with 2-(*N*-morpholino)ethanesulfonic acid sodium dodecyl sulfate (MES SDS) buffer as running buffer (Invitrogen, Grand Island) or Any kD™ Mini-PROTEAN® TGX™ precast gels with Tris-glycine as running buffer (Bio-rad, Hercules). ELISA assay results were read on the ELX800 Universal Microplate Reader (Bio-Tek Instrument Inc., Winooski) with λ = 450 nm and 630 nm for signal and background, respectively. Western blot was developed on a FluorChem® FC2 System version 3.2 (Cell Biosciences, Santa Clara). Fluorescent signals from CellTiter-Blue® assay were read using a SpectraMax M5 microplate reader (Molecular Devices, Sunnyvale). Fluorescent images of the cells from LIVE/DEAD® viability/cytotoxicity assays were acquired on an Axiovert 200 microscope equipped with an AxioCam MRm camera and FluoArc mercury lamp (Carl Zeiss, Thornwood). NIH ImageJ software was used to assist cell counting. Mass spectrometry analysis of the conjugates was done on the electrospray ionization-gas-phase electrophoretic mobility molecular analyzer (ESI-GEMMA) instrument (TSI Inc.,

Shoreview), which consists of an ESI unit 3480 with a neutralizing chamber, a nano differential mobility analyzer (DMA) model 3085, and a condensation particle counter (CPC) type 3025A.

2.2.3. Methods

Synthesis and characterization of PDS-p(SS-co-PEGMA). RAFT polymerization was employed to copolymerize sodium 4- styrenesulfonate (SS) and poly(ethylene glycol) methyl ether methacrylate (PEGMA). 3-(Pyridin-2-yldisulfanyl)propyl-2-(ethylthiocarbonothioylthio) propanoate was used as the CTA. The polymerization was performed with an initial feed ratio of [SS]:[PEGMA]:[CTA]:[AIBN] = 105:30:1:0.5 using standard Schlenk techniques. The CTA (30 mg, 0.08 mmol), SS (1.65 g, 8.00 mmol), PEGMA (0.65 ml, 2.29 mmol), and AIBN (6.26 mg, 0.038 mmol) were dissolved in 5 ml of Milli-Q water and 5 ml of DMF in a Schlenk tube. The system was sealed and subjected to four freeze-pump-thaw cycles before immersion in a 70 °C oil bath. Aliquots were removed at predetermined time points and diluted in D_2O or DMF for ^1H NMR or GPC analysis, respectively. Conversions were calculated from the ^1H NMR spectra using the sum of the integral values of the vinylic protons of SS monomer and PEGMA monomer at 5.9 ppm and 6.2 ppm, respectively, and the sum of integral values of the regions where the monomer protons and the growing polymer protons overlap (7.8-6.3 ppm for SS and 4.0-3.2 ppm for PEGMA). The polymerization was stopped at 83% conversion. The polymer was purified by dialysis first with 1:1 v/v Milli-Q water:MeOH to remove residual monomer followed by dialysis with Milli-Q water (MWCO 8000) and lyophilized to remove solvent. δ ^1H NMR 500 MHz (D_2O): 8.6 (1H, end group C**H**N), 8.2 (1H, end group NCCHC**H**), 8.1 (1H, end group NCC**H**CH), 8.0-6.0 ($Na^+SO_3^-C_6$**H$_4$** side chains), 4.4-2.8 (PEGMA side chains), 2.8-0.0 (polymer backbone). IR (cm^{-1}): 3448, 2924, 1718, 1647, 1453, 1410, 1181, 1122, 1035, 1008, 947, 832, 773, 671. The M_n = 26.1 kDa by NMR, 24.5 kDa by GPC, PDI = 1.16 by GPC. To

remove the trithiocarbonate end group, the resulting polymer (42.7 mg, 1.6 x 10^{-3} mmol) was combined with AIBN (13.48 mg, 0.08 mmol) in 10 ml of 1:1:1 v/v/v DMF:dioxane:MeOH in a Schlenk tube. The system was degassed by three freeze-pump-thaw cycles and stirred for 4.5 hours at 70 °C. The resulting PDS-p(SS-*co*-PEGMA) was purified by dialysis in 1:1 v/v Milli-Q water:MeOH followed by Milli-Q water (MWCO 8000) and lyophilized to remove solvent. UV-vis spectrophotometry was used to monitor the disappearance of the trithiocarbonate group (λ = 309 nm). After radical exchange, M_n = 26.0 kDa by GPC, PDI = 1.18 by GPC.

Quantification of pyridyl disulfide (PDS) end group retention. To quantify the amount of PDS end group retention, PDS-p(SS-*co*-PEGMA) (1.43 mg, 2.74 x 10^{-5} mmol) was dissolved in 1 ml of 0.1 M PB pH 8.0. The volume was split into two halves. In one vial, 4.2 μl of 100 μg/μl of DTT in 0.1 M PB was added. The sample was diluted to 1 ml and allowed to incubate at 23 °C for 2 hours.   In the second vial, the volume was brought to 1 ml with 0.1 M PB pH 8.0 without DTT to use as the control group. Absorbance of the by-product, pyridine-2-thione, at λ = 343 nm (ε = 8080 M^{-1} cm^{-1} in water) was assessed via UV-vis spectrophotometry. Percentage of PDS end group retention was calculated using the formula:

$$\%PDS = \frac{[PDS]}{[PDS-p(SS-co-PEGMA)]} = \frac{Abs_{343}/\varepsilon}{[PDS-p(SS-co-PEGMA)]}$$

where Abs_{343} was the difference in absorbance between the sample (with DTT) and the control (without DTT) at λ = 343 nm. The experiment was repeated three times. The molecular weight of the polymer reported by NMR was used to determine the polymer concentration.

Synthesis of 2-(pyridin-2-yldisulfanyl)ethyl 2-bromo-2-methylpropanoate. 2-(Pyridin-2-yldisulfanyl)ethanol (698 mg, 3.73 mmol) was dissolved in 15 mL dichloromethane.

Triethylamine (1.04 mL, 7.46 mmol) was added drop-wise. The solution was cooled to 0 °C in an ice-bath and 2-bromoisobutyrylbromide (484 μL, 3.92 mmol) was added drop-wise. The mixture was stirred over 16 hours and allowed to warm to room temperature. The crude solution was washed twice with de-ionized water, once with saturated $NaHCO_3$ solution, once with brine, and once more with de-ionized water. The crude product was purified by silica column chromatography (1:1 v/v hexane:ethyl acetate, $R_f = 0.7$), and lyophilized to give a clear yellow oil (327 mg, 47% yield). δ ^{1}H NMR (500 MHz, $CDCl_3$): 8.41-8.37 (1H, dq, $J = 4.55$, 0.90 Hz, **CH**N), 7.66-7.62 (1H, dt, $J = 8.07$, 0.94, **CH**CHCN), 7.60-7.55 (1H, td, $J = 7.68$, 1.82, CH**CH**CN), 7.05-7.01 (1H, ddd, $J = 7.30$, 4.83, 1.10 Hz, CH**CH**CHN), 4.38-.32 (2H, t, $J = 6.45$ Hz, SS**CH$_2$**), 3.06-2.99 (2H, t, $J = 6.45$ Hz, **CH$_2$**O), 1.90-1.82 (6H, s, **CH$_3$**CBr). δ ^{13}C NMR (500 MHz, $CDCl_3$): 171.15, 159.42, 149.48, 137.01, 120.80, 119.65, 63.38, 55.45, 36.87, 30.59. FT-IR (cm^{-1}): 3045, 2974, 2923, 1732, 1573, 1561, 1446, 1417, 1388, 1370, 1268, 1154, 1106, 1083, 1043, 1010, 985, 860, 835, 804, 758, 733, 716. MALDI-TOF MS (expected, observed) (Da) : [M_{H+}] = (335.97, 335.96), [M_{Na+}] = (357.95, 357.97).

Synthesis and characterization of PDS-pPEGMA. ATRP was employed to synthesize PDS-pPEGMA. In a Schlenk tube, PEGMA (856 mg, 2.85 mmol), 2-(pyridin-2-yldisulfanyl)ethyl 2-bromo-2-methylpropanoate (30 mg, 0.09 mmol), and 2 ml of MeOH were combined, sealed, and subjected to five freeze-pump-thaw cycles. In a two-neck round bottom flask, CuBr (51.2 mg, 0.36 mmol) and 2, 2'-bipyridine (111 mg, 0.71 mmol) were combined and subjected to 4 vacuum-Ar refill cycles. An amount of 2 ml of degassed MeOH was added to the two-neck round bottom flask, and 0.5 ml of the mixture was transferred to the Schlenk tube via syringe to start the polymerization. After 6 hours, air was bubbled through the reaction to stop the polymerization. The polymer was purified by dialysis against MeOH with 10 mM EDTA

first to remove Cu^{II}, then against MilliQ-water (MWCO 3500). δ ^{1}H NMR 500 MHz (D$_2$O): 8.4 (1H, end group NC**H**), 7.7-7.6 (2H, end group NCC**H**C**H**), 7.0 (1H, end group NCHC**H**), 4.2-2.9 (PEGMA side chains), 3.0 (2H, end group SSC**H$_2$**), 2.8 (2H, last C**H$_2$** in the polymer backbone), 2.7-0.0 (polymer backbone). IR (cm^{-1}): 3527, 2873, 1726, 1451, 1350, 1245, 1099, 1029, 945, 852, 747. The M$_n$ = 23.0 kDa by NMR, 11.1 kDa by GPC and PDI = 1.13 by GPC.

Synthesis of bFGF-p(SS-co-PEGMA) conjugate. bFGF (25 μg, 1.6 x 10^{-3} μmol) was diluted into 900 μl of D-PBS + 1mM EDTA, and loaded onto a hand-packed 1ml-heparin Sepharose column$^{®}$. PDS-p(SS-*co*-PEGMA) (3.6 mg, 0.14 μmol) was dissolved in 900 μl of D-PBS + 1mM EDTA, and loaded onto the column; the flow-through volume was collected for analysis. The column was allowed to incubate at 4 °C for 16 hours. The unconjugated polymer, and weakly bound bFGF were washed off the column with 2 x 6 ml of D-PBS and 1 x 3 ml of 0.5 M NaCl D-PBS, respectively. The conjugate was eluted off the column using 2 x 6 ml of 2 M NaCl D-PBS. All of the fractions, except for the 2 M NaCl fraction, were then desalted, concentrated using a CentriPrep$^{®}$ centrifugal membrane MWCO 3000 with D-PBS, and stored at -80 °C. To purify the conjugate, the 2M NaCl fractions were subjected to dialysis against D-PBS using MWCO 26,000 tubing for 12 hours at 4 °C, then washed for 10 cycles using a CentriPrep® centrifugal membrane MWCO 30,000 with D-PBS at 12.0 rcf for 8 minutes/cycle. The collected conjugate was then characterized by Western blot. ELISA was carried out three times and averaged to determine the concentration of bFGF in the conjugate prior to cell studies.

Quantification analysis of bFGF conjugate. The fractions collected from on-column conjugation were subjected to ELISA. The experiment was performed using the recommended protocol from the manufacturer. In summary, a 96-well plate was first coated with the capture antibody solution and incubated for 16 hours at 23 °C. Then, the plate was blocked for 2 hours

with 1% BSA in D-PBS. The bFGF standards (supplied with the ELISA kit) and the samples in triplicate were allowed to incubate for 2 hours at 23 °C. Subsequently, detection antibody-biotin conjugate solution was probed for 2 hours before streptavidin-horseradish peroxidase solution was added for 20 minutes. The colorimetric signals were developed by incubating the working plate with 1-Step™ Ultra TMB solution (Pierce Biotechnology, Rockford) for 6 minutes. The assay was stopped by addition of 50 μl of 1 M H_2SO_4/well. The absorbance signals were recorded at $\lambda = 450$ nm, and the background at $\lambda = 630$ nm was subtracted. The concentration of bFGF in each sample was determined via extrapolation from the linear standard curve consisting of 0, 12.5, 25, 50, 100, 200, 400, and 800 pg/ml bFGF.

Gel electrophoresis. The collected fractions from conjugation were subjected to SDS-PAGE analysis. Samples were assessed under non-reducing conditions using NuPAGE® 4-12% Bis-tris gels and MES SDS running buffer. The gel was run at 150 V, 200 mA for 40 minutes, fixed in gel fixing solution for 30 minutes, and then stained with iodine stain.

Western blot analysis. First, samples were assessed via SDS-PAGE or Native PAGE. For SDS-PAGE, the samples were first incubated with or without 54 mg/ml of DTT for 3-5 minutes at 85 °C assessed similarly as described above. For Native PAGE, the samples were first prepared in the same manner, then assessed using Any kD™ Mini-PROTEAN® TGX™ precast gels with Tris-glycine as running buffer. The gels were run at 200 V for 30 minutes. After PAGE, the gels were transferred to nitrocellulose membranes (Whatman® Protran BA 95 Nitrocellulose) at 100 V for 2 hours. The membranes were immediately blocked with 5% fat-free dry milk containing 1% BSA (blocking solution) for 24 hours at 23 °C before incubation with rabbit anti-fibroblast growth factor basic antibody (1:20 dilution in blocking solution) at 4 °C for 16 hours. The membrane was washed by shaking in a Tris-buffered saline Tween-20 (TBST)

solution for 3 of 10-minute cycles. Subsequently, the membrane was incubated with goat anti-rabbit IgG-HRP conjugate (1:1000 dilution in blocking solution) for 30 minutes at 23 °C. After 3 x 10 minutes of washing in TBST, the membrane was developed for 5 minutes using SuperSignal® West Pico Chemiluminescent Substrate (Thermo Scientific, Waltham) and exposed for 1-15 minutes on a FluorChem® FC2 system.

Electrospray ionization-gas-phase electrophoretic mobility molecular analysis (ESI-GEMMA). Samples of proteins, polymers or conjugates were typically prepared in 5 or 20 mM ammonium acetate at a concentration range of 0.2 to 5.0 µg/ml. The ESI-GEMMA instrument (TSI Inc., Shoreview, MN USA) consists of an electrospray aerosol generator 3480 with a neutralizer chamber, a nano differential mobility analyzer (DMA) model 3085, and a condensation particle counter (CPC) type 3025A. The inlet flow rate and voltages were set to 70 nl/min, and 2-3 kV, respectively. The DMA sheath flow was set to 20 L/min, and the voltage was scanned from -10 to -10 000 V for 135 seconds to detect the electrophoretic mobility diameter (EMD) range of 2-56 nm. Particle counts per EMD were recorded by Aerosol Instrument Manager Software (TSI Inc.). An average of 5-10 spectra per sample was obtained. Curve smoothing was accomplished using the moving average over 7 points in Excel. The EMD of the protein/conjugate was found from the maximum of the peak of interest. Molecular weights were calculated using the formula $MW = V*d*N_a$, where d (in g/cm^3) is the effective density modeled to a sphere, N_a is Avogadro's number, and $V = (EMD)^3*\pi/6$. Lysozyme was used as the standard.

The ESI-GEMMA spectrum of bFGF (MW=16 kDa) showed a major peak at 4.45 nm corresponding to 16,116 Da when the average effective density for proteins (0.58 g/cm^3) was used in the calculation.[35] Effective densities of polymers and analytes in general vary depending

on their composition and shape.[35,36]   They were determined experimentally for p(SS-*co*-PEGMA) and pPEGMA to be 0.90 g/cm^3 and 0.69 g/cm^3, respectively (see Figure 2.1f, Figure 2.3e). The effective densities of bFGF-p(SS-*co*-PEGMA) and bFGF-pPEGMA, assuming one protein linked to one polymer molecule, were 0.78 g/cm^3 and 0.64 g/cm^3, respectively. Employing these values, the experimental MWs of the bFGF-p(SS-*co*-PEGMA) and bFGF-pPEGMA conjugates were 39 kDa and 30 kDa.

Cell culture. HDF primary cells were purchased from PromoCell and cultured in PromoCell fibroblast growth medium containing 2% fetal calf serum, 1 ng/ml bFGF, 5 μg/ml insulin, supplemented with 100 unit/ml penicillin and 100 μg/ml streptomycin at 37 °C, 5% CO_2. HDF cells were passaged every four days or after reaching 80% confluency. HDF cells were used up to passage 12. BaF3 cells were kindly provided by Dr. David Ornitz and cultured as recommended.   Specifically, the cells were grown in RPMI1640 medium containing 10% newborn bovine calf serum, 2 mM L-glutamine, 0.5 ng/ml of recombinant mouse IL-3, 600 μg/ml of G418, 50 nM of 2-mercaptoethanol, supplemented with 100 unit/ml penicillin and 100 μg/ml streptomycin at 37 °C, 5% CO_2. The medium was changed every two days.

Cytotoxicity study. HDF cells were trypsinized and resuspended in fibroblast growth medium lacking bFGF. The cells were plated at a concentration of 5,000 cells/well in a 48-well plate and allowed to adhere over 16 hours at 37 °C, 5% CO_2. Then, the medium in the wells was replaced with 200 μl of the working medium containing various amount of polymer or heparin. After an incubation of 24 hours at 37 °C, 5% CO_2, cell viability was assessed using LIVE/DEAD® viability/cytotoxicity assay. Briefly, the cells were washed twice with pre-warmed D-PBS, then incubated with 200 μl of 1 μM calcein AM and 4 μM ethidium homodimer-1 in D-PBS for 20 minutes at 37 °C, 5% CO_2. The fluorescent images of each well under a green

channel and red channel were captured on an Axiovert 200 microscope equipped with an AxioCam MRm camera and FluoArc mercury lamp. The numbers of live and dead cells were counted manually using NIH ImageJ software, and percent live cells was calculated by dividing the number of live cells by the total number of live and dead cells. Each experimental group was repeated four times, and the whole experiment was repeated four times.

Bioactivity study. HDF cells were trypsinized and resuspended in UltraCULTURE™ serum-free medium supplemented with 2 mM L-Glutamine, 100 unit/ml penicillin and 100 μg/ml streptomycin. The cells were plated at a concentration of 2,000 cells/well in a 96-well plate and allowed to adhere for 16 hours at 37 °C, 5% CO_2. At the end of the 16-hour incubation, 100 μL of medium containing bFGF or the tested compounds were replaced in each well. After an incubation of 72 hours at 37 °C, 5% CO_2, CellTiter-Blue® assay was carried out to evaluate cell proliferation. All experimental groups were normalized to the control group, which received only blank medium. Each group was done with six replicates.

Stability study of bFGF-p(SS-co-PEGMA) and controls under stressors. An amount of 15 μl of each experimental group in D-PBS was made up to contain 0.5 ng/μl of bFGF or either of the conjugates (bFGF-p(SS-*co*-PEGMA) and bFGF-pPEGMA). The control experimental groups were prepared to contain 0.5 ng/μl of bFGF with either 0.75 ng/μl of heparin, 0.5 μg/μl of heparin, 0.75 ng/μl of p(SS-*co*-PEGMA), or 0.75 ng/μl of pPEGMA. The blank group contained 15 μl of D-PBS. The 15 μl/experimental group was divided into 4 vials of 3 μl/vial for four separate treatments. In one set of the 3 μl-vials, 27 μl of D-PBS was added to each vial and the samples were stored at 4 °C for 16 hours. In another set of 3 μl-vials, 27 μl of pH 4.7 PBS was added to each vial and the samples were stored at 4 °C for 16 hours. In the third set of 3 μl-vials, 27 μl of 0.1% Trypsin was added to each vial and the samples were stored at 4 °C for 16 hours.

51

The fourth set of 3 μl-vials were stored at 4 °C for 16 hours before 27 μl of 1% TFA was added and treated for 2 hours at 4 °C. The samples under heat treatment were prepared fresh in the same manner towards the end of the 16 hour-treatment of the other samples. The samples were placed in a dry bath at 55 °C for 30 minutes. The concentrations of native bFGF and bFGF in the conjugates under treatment were 0.05 ng/μL. The concentrations of heparin under treatment were 0.075 ng/μl or 0.05 μg/μl, while the concentrations of the unconjugated polymers were 0.075 ng/μl. To stop all treatments, the samples were diluted to 1.5 ml of the UltraCULTURE^{TM} serum-free medium to bring final concentrations to 1 ng/ml of bFGF/bFGF-p(SS-*co*-PEGMA)/bFGF-pPEGMA, 1.5 ng/ml or 1 μg/ml of heparin, 1.5 ng/ml of p(SS-*co*-PEGMA)/pPEGMA. The untreated samples were prepared fresh to the indicated final concentrations in the working medium without serial dilutions. Then, the medium samples were used in the cell proliferation assay as described above. After incubation for 72 hours at 37 °C, 5% CO_2, the CellTiter-Blue® assay was carried out to evaluate the extent of cell growth. All experimental groups were normalized to the blank control of that treatment set, which had only treated buffer in medium. Each sample had six replicates, and the whole experiment was repeated eight times including one blinded study, except (+)bFGF (+)1.5 ng/ml pPEGMA and (+)bFGF-pPEGMA which were repeated four times, and the "pH 4.7 for 16 hrs" treatment set of other groups which was repeated seven times. A two-way ANOVA and Student's t-test were performed for statistical analysis.

Inhibition assay. HDF cells were plated at a concentration of 2,000 cells/well in a 96-well plate in the UltraCULTURE^{TM} serum-free medium and allowed to adhere over 16 hours at 37 °C, 5% CO_2. The experimental groups were prepared fresh to contain 1 ng/ml of bFGF, or 1 ng/ml of bFGF with 1 μg/ml of heparin, or 1 ng/ml of bFGF-p(SS-*co*-PEGMA); all with an

52

addition of 125 nM of the inhibitor PD173074. The control groups were the exact replicates with an exception of the addition of the inhibitor. The medium in the 96-well plate was replaced with 100 μl of each sample/well. After an incubation of 72 hours at 37 °C, 5% CO_2, CellTiter-Blue® assay was carried out to evaluate the extent of cell proliferation. All the groups were normalized to the blank, which only had the medium without the inhibitor. Each group was done with six replicates, and the whole experiment was repeated three times.

Proliferation assay of BaF3 cells. BaF3 cells were collected and washed three times with cultured medium lacking IL-3. The cells were plated at the density of 20,000 cells/well/50 μL in a 96-well plate in the working medium. The samples were prepared in the working medium to contain 2 ng/ml of bFGF or bFGF-p(SS-*co*-pPEGMA), 2 ng/ml of bFGF with either 3 ng/ml of heparin, 2 μg/ml of heparin, 3 ng/ml of p(SS-*co*-pPEGMA), or 2 μg/ml of p(SS-*co*-pPEGMA). Subsequently, 50 μL of each sample was added into each corresponding well. After an incubation for 42 hours at 37 °C, 5% CO_2, CellTiter-Blue® assay was carried out to evaluate the extent of cell growth. All of the groups were normalized to the control group, which had only medium. Each group was performed with six replicates.

Statistical analysis. The data was presented as the average and the STDEV or SEM where SEM = STDEV/$(n-1)^{1/2}$ and n = the number of independent repeats. A two-way ANOVA was performed with sample groups and treatments as the two factors and found that the p values were 1×10^{-46} and 4×10^{-47}. Individual comparisons were made with Student's t-test. All tests were two-tailed, unpaired and $p < 0.05$ was considered significant.

2.3. Results

2.3.1. Synthesis of polymers and analysis of cytotoxicity

p(SS-*co*-PEGMA) was selected because we previously demonstrated that the polymer bound to bFGF in cell culture media, likely through interaction with the heparin-binding domain.[26,27] bFGF has two free cysteines; thus, the polymer was prepared with a pyridyl disulfide (PDS) end group that reacts with thiols. Reversible addition-fragmentation chain transfer polymerization has been widely employed for preparation of protein-polymer conjugates.[37-39] RAFT polymerization of SS and PEGMA monomers in the presence of a PDS-functionalized trithiocarbonate CTA produced the desired polymer (Figure 2.1a). Since the trithiocarbonate moiety can exhibit cytotoxicity at high polymer concentrations,[40] this group was removed by radical exchange with AIBN. The resulting copolymer PDS-p(SS-*co*-PEGMA) had a M_n of 26.1 kDa by NMR and a PDI of 1.16 (Figure 2.1). The analogous control polymer, PDS-pPEGMA, was prepared via ATRP in the presence of an PDS-functionalized initiator, CuBr and 2, 2'-bipyridine (Figure 2.2 and 2.3). It had a M_n of 23.0 kDa by NMR and a PDI of 1.13.

a

AIBN, 1:1 DMF:H₂O
70 °C

AIBN
1:1:1 DMF:Dioxane: MeOH
70 °C

PDS-p(SS-*co*-PEGMA)

b

c

d

56
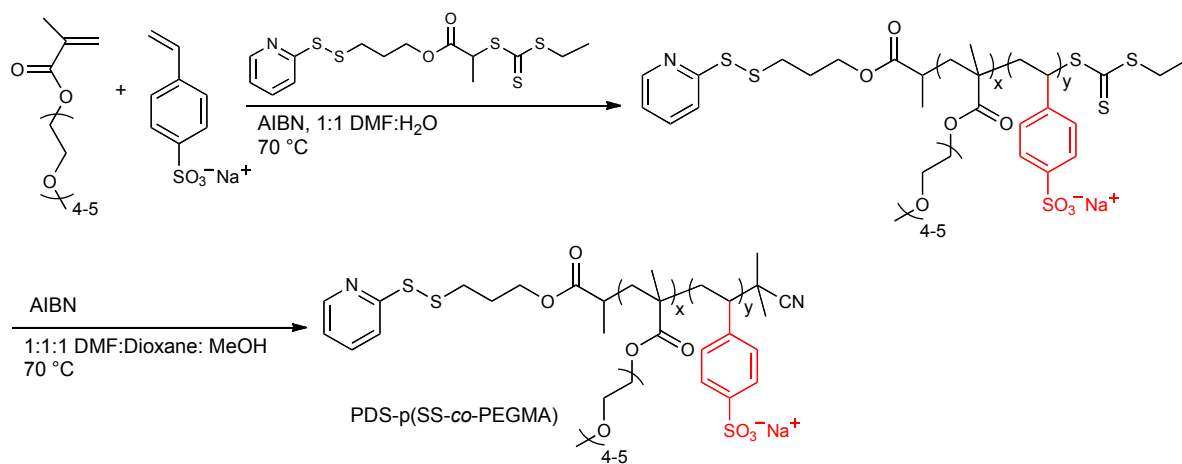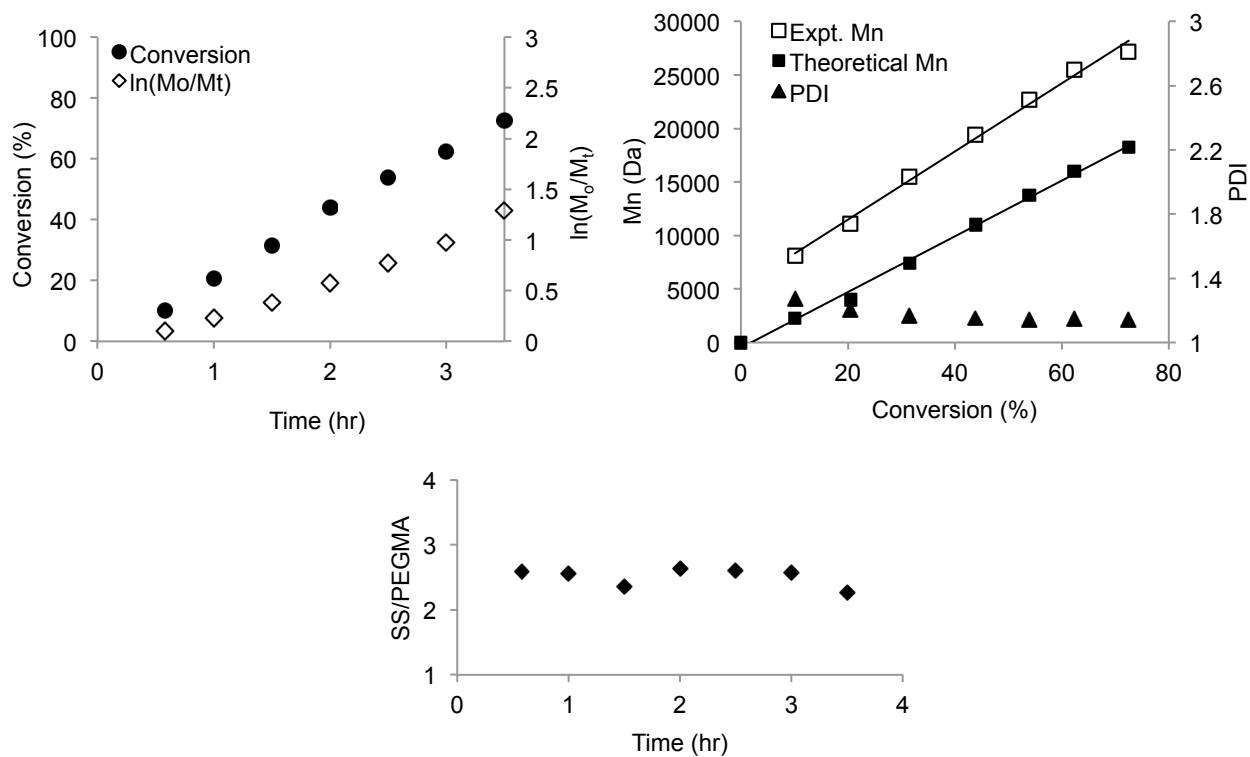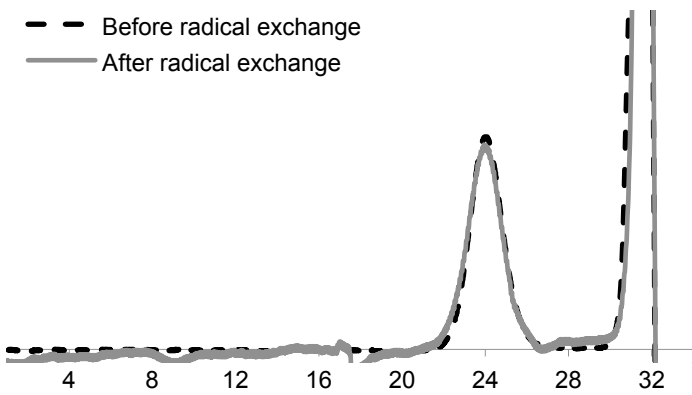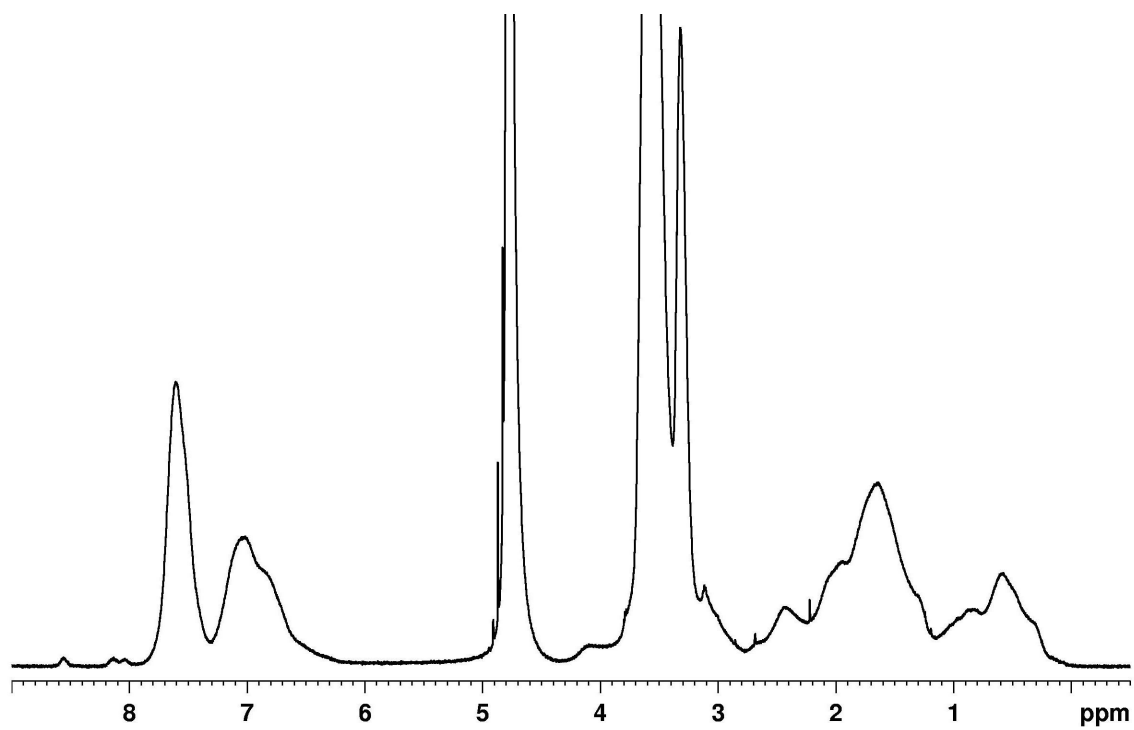
e
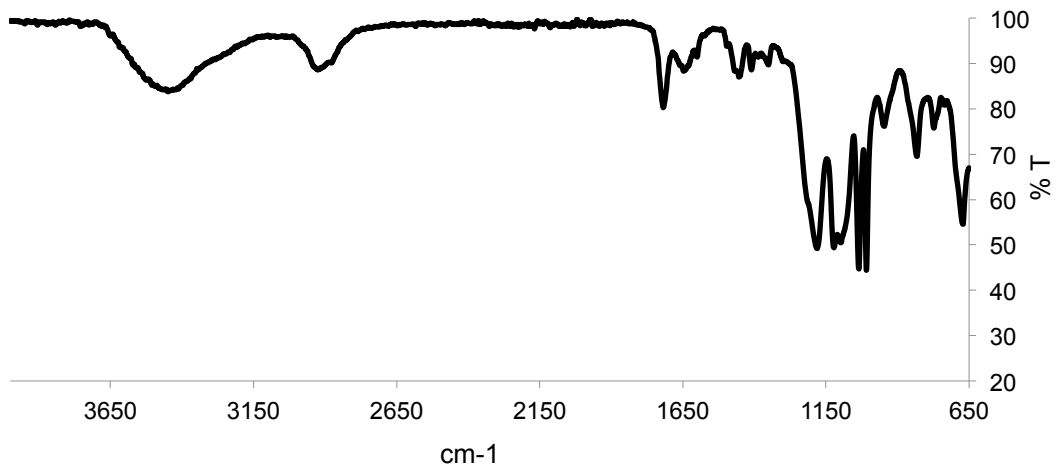
f
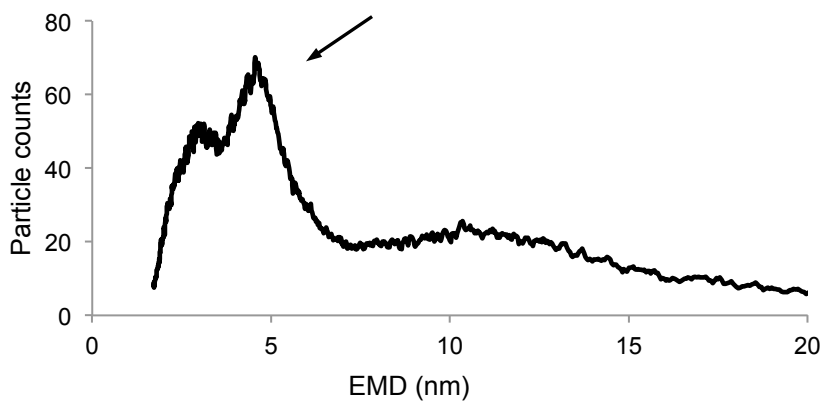
g
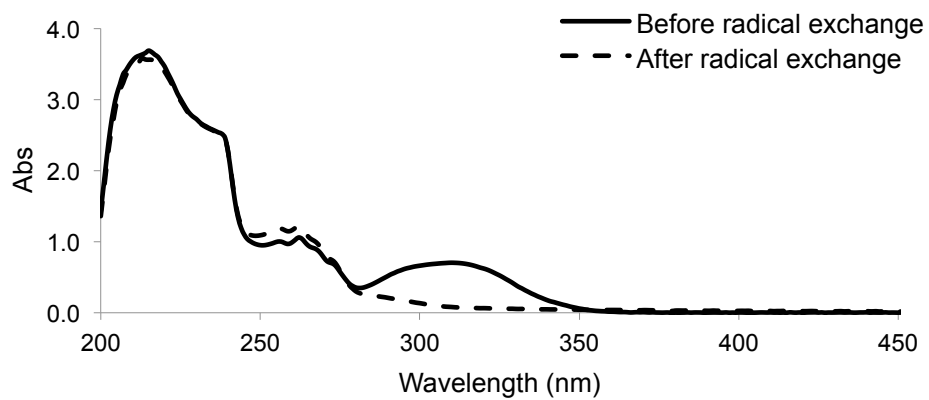
h

	Abs at 343 nm	% PDS retention
Trial #1	0.215	70
Trial #2	0.201	65
Trial #3	0.219	71
Ave ± Stdev		**68 ± 3**

Figure 2.1. Synthesis and characterization of PDS-p(SS-*co*-PEGMA). a) Synthesis scheme. b) Kinetic studies of the RAFT polymerization at 70 °C: kinetic trace and conversions determined from ^{1}H NMR spectroscopy (left), MWs and PDIs determined by GPC (right), ratios of incorporating monomers determined from ^{1}H NMR (bottom). c) GPC traces of the polymer before and after radical exchange in DMF 0.1 M LiBr. d) ^{1}H NMR spectrum of the polymer in D$_2$O. e) FT-IR spectrum of the polymer. f) ESI-GEMMA spectrum of the polymer taken in 20 mM ammonium acetate (EMD = 4.51 nm, d = 0.90 g/cm^3 calculated using formula: d = MW/(N$_a$*EMD^3*π/6)). g) UV-Vis spectra of the polymer before and after radical exchange with AIBN. h) Results of quantitative analysis of the PDS end group retention after radical exchange and purification.

a
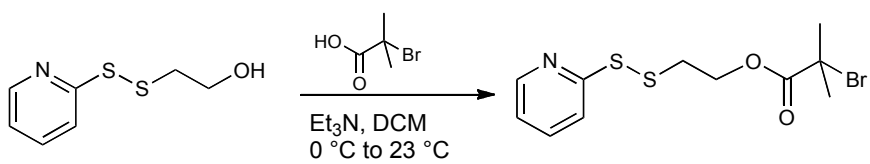
b
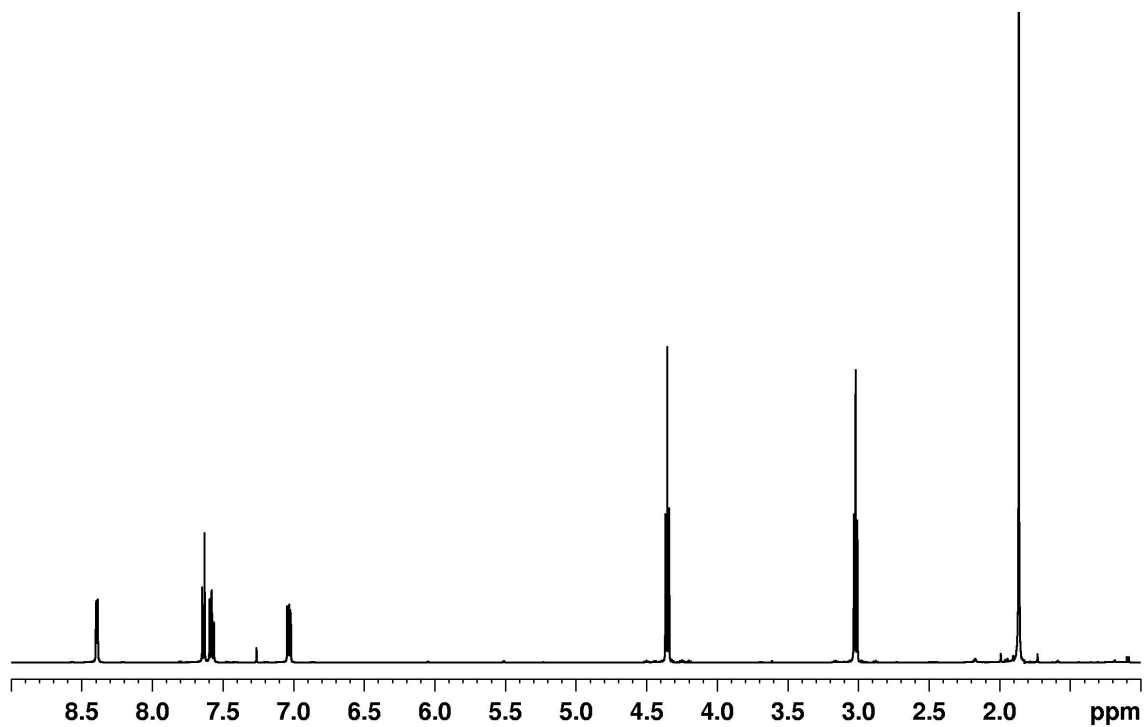
c
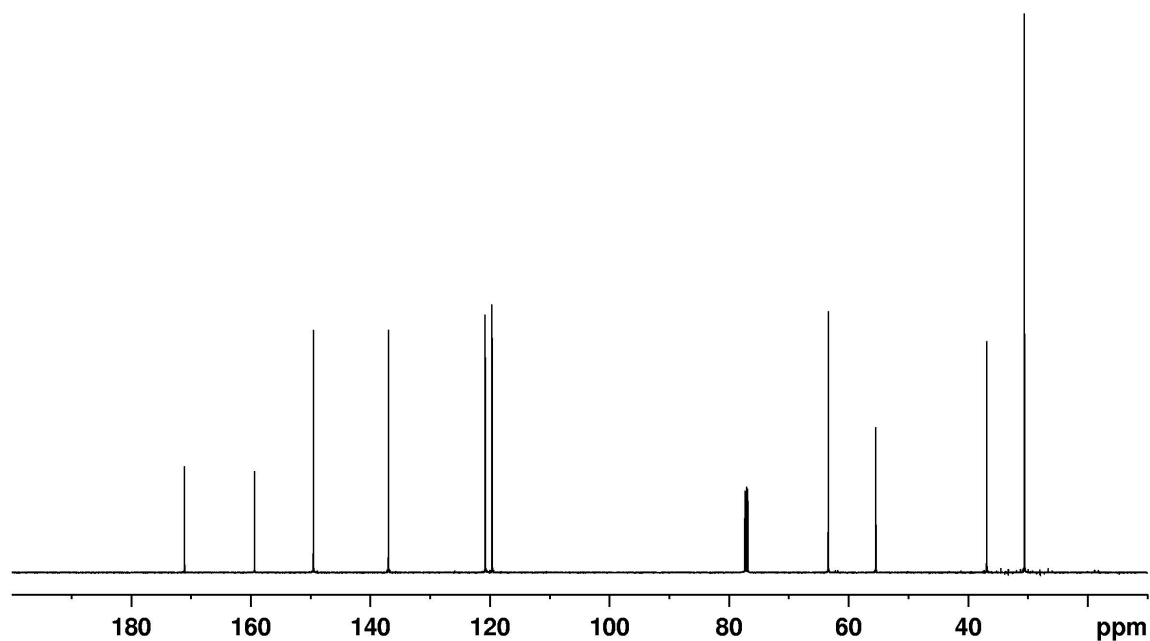
d
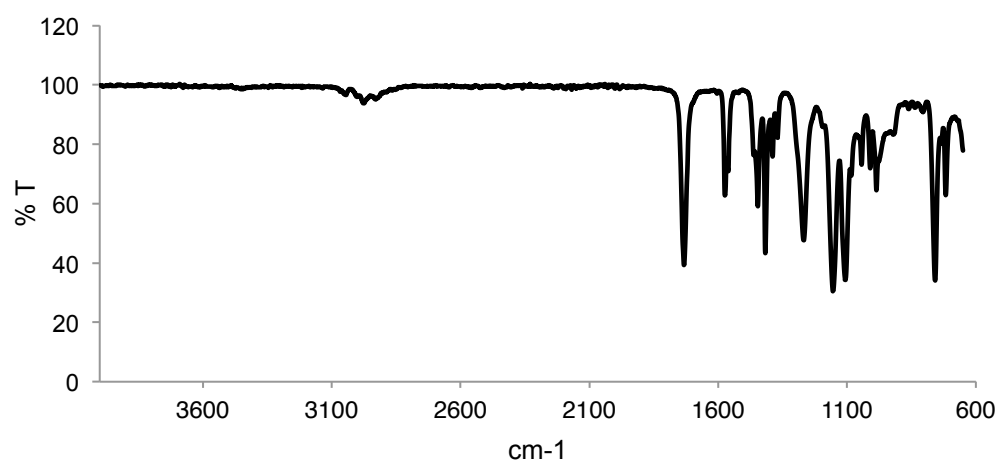
Figure 2.2. Synthesis and characterization of 2-(pyridin-2-yldisulfanyl)ethyl 2-bromo-2-methylpropanoate. a) Synthesis scheme. b) ^{1}H NMR spectrum in CDCl$_3$. c) ^{13}C NMR spectrum in CDCl$_3$. d) FT-IR spectrum of compound.

a

b

c

d

e
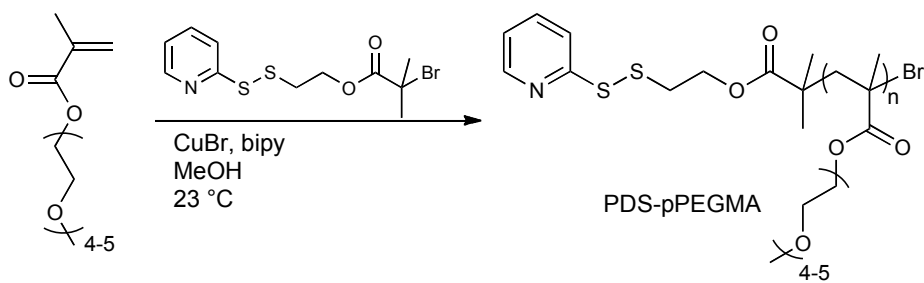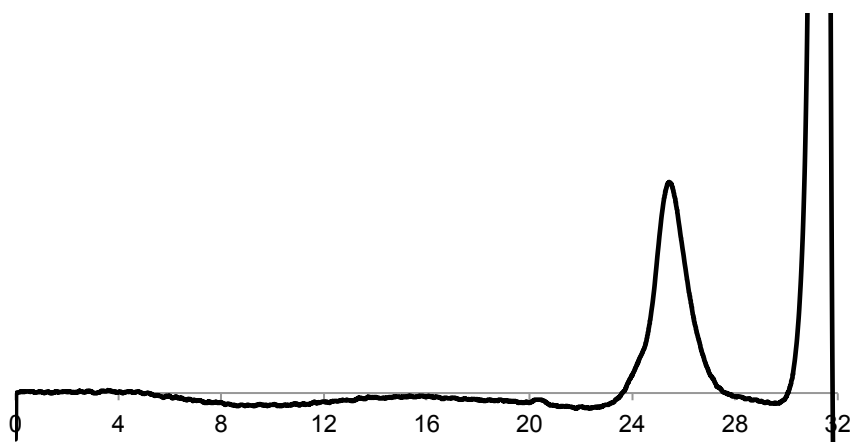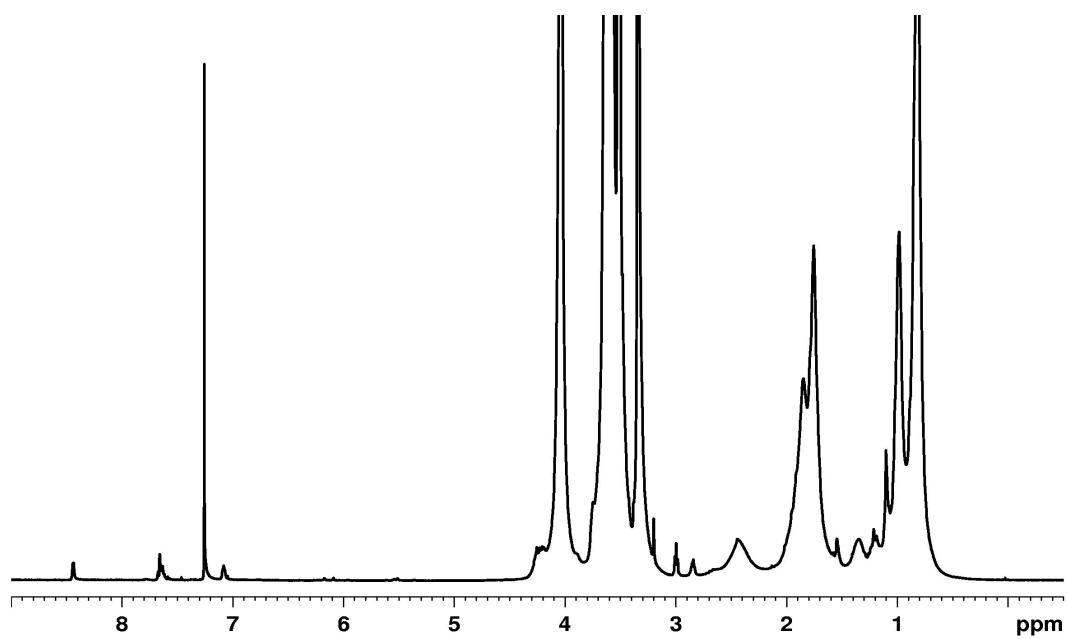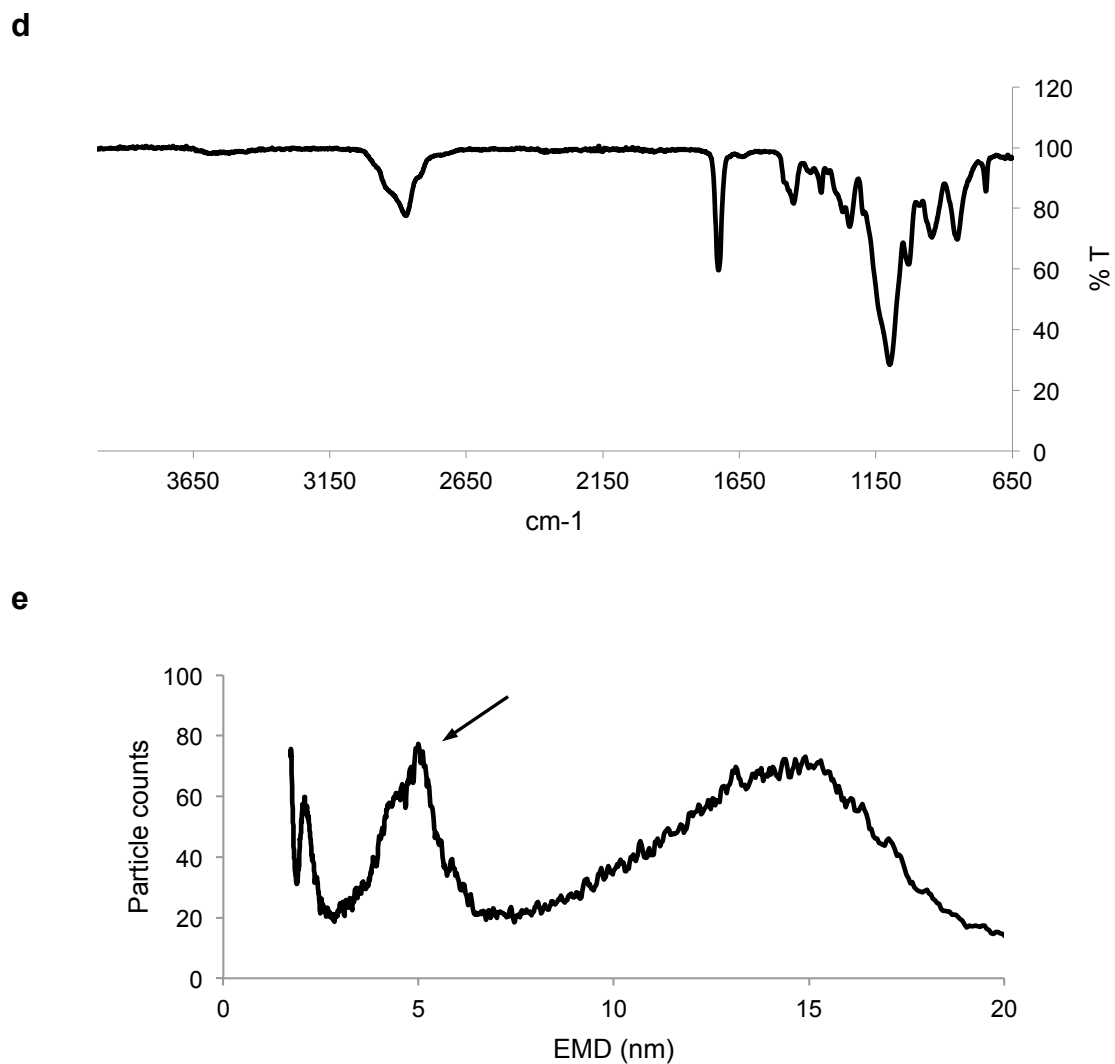
Figure 2.3. Synthesis and characterization of PDS-pPEGMA. a) Synthesis scheme. b) GPC trace of the polymer in DMF 0.1 M LiBr. c) ^{1}H NMR spectrum of the polymer in CDCl$_3$. d) FT-IR spectrum of the polymer. e) ESI-GEMMA spectrum of the polymer in 20 mM ammonium acetate (arrow, EMD = 4.73 nm, d = 0.69 g/cm^3 calculated using formula: d = MW/(N$_a$*EMD^3*π/6)).
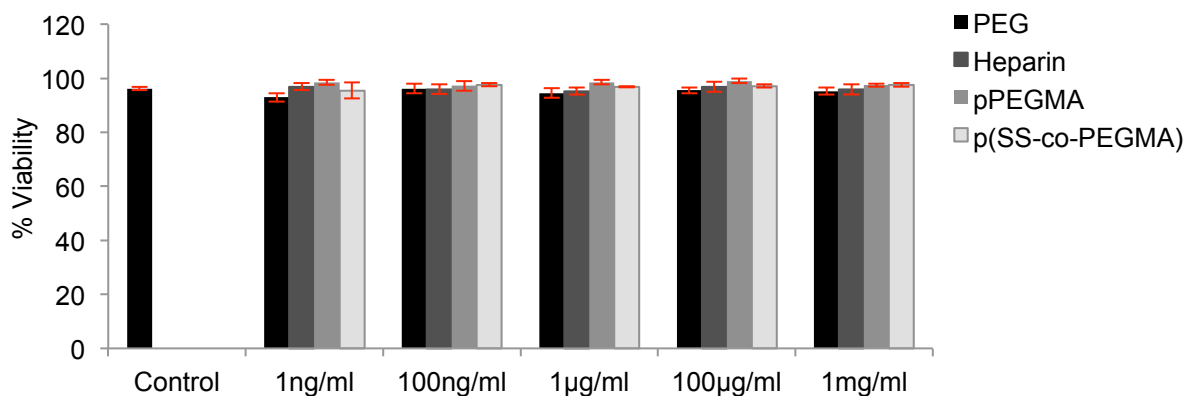
Figure 2.4. Cytotoxicity study of the polymers. Cytotoxicity study of the heparin-mimicking polymer compared to controls: 5,000 HDF cells/well in a 48-well plate were incubated with various concentrations of each polymer for 24 hours at 37 °C, 5% CO_2. Each well was washed twice with D-PBS and subsequently incubated with 1 μM calcein AM and 4 μM ethidium homodimer-1 for 20 minutes at 37 °C, 5% CO_2. The percentage of live cells was calculated by dividing the number of live cells by the total number of live and dead cells. The experiment was repeated four times. Error bars represent SEM.

Next, the cytotoxicity of the p(SS-*co*-PEGMA) without the PDS end group was evaluated and compared to nontoxic PEG, control polymer pPEGMA and heparin. PEG 4-kDa was chosen as the control because it has a comparable number of repeating units to p(SS-*co*-PEGMA) (DP = 91 and 98, respectively). The cytotoxicity study was performed with normal HDF cells. HDF cells play an important role in the wound healing process of skin, and the proliferation of these cells is largely stimulated by bFGF.[15] HDF cells were exposed to either p(SS-*co*-PEGMA), pPEGMA, PEG, or heparin at increasing concentrations from 1 ng/ml to 1 mg/ml for 24 hours in the absence of bFGF before assessment with the LIVE/DEAD® viability assay. The percent cell

viability was the same in the presence of all of the polymers at all concentrations tested, and the same as no polymer added (Figure 2.4). This demonstrated that the heparin-mimicking polymer p(SS-*co*-PEGMA) is non-cytotoxic to HDF cells to at least 1 mg/ml.

2.3.2. Preparation of conjugates

An on-column conjugation technique was utilized to synthesize bFGF-p(SS-*co*-PEGMA) and bFGF-pPEGMA.[41] Briefly, the conjugations were conducted by adding the corresponding polymer solution to heparin sepharose-bound bFGF, prior to eluting with increasing salt in D-PBS. In this way, the excess polymer was completely removed (Figure 2.7); the typical yield of the isolated conjugate was 50% (Table 2.1). Western blotting of SDS-PAGE showed diffuse bands at higher MW typical of protein-polymer conjugates (Figure 2.5b left, lane 2 and Figure 2.6b). Native PAGE showed a smear corresponding to the heparin-mimicking polymer conjugate due to the change in its overall surface charge (Figure 2.5b right, lane 2). Furthermore, the bands corresponding to the conjugates disappeared while the signals corresponding to the unconjugated bFGF were more intense under reducing conditions, as expected for conjugates prepared via disulfide bonds.
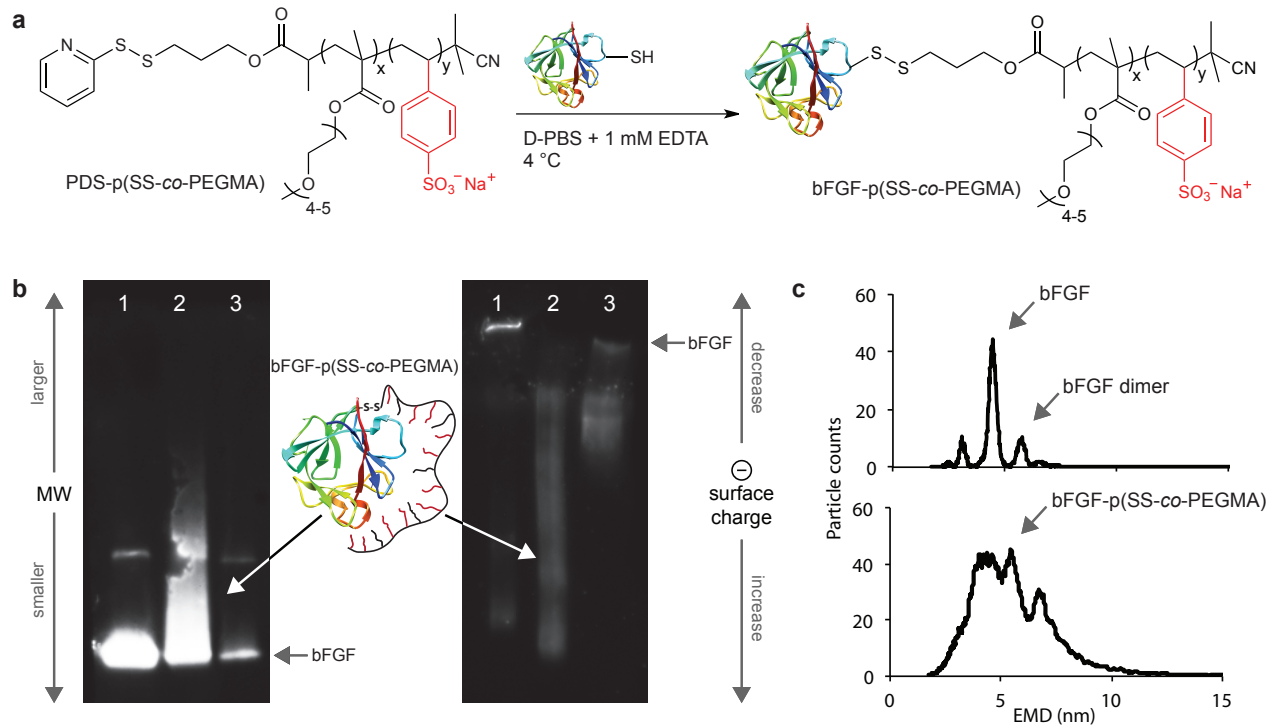
Figure 2.5. Conjugation of the polymers to bFGF and characterization. a) Synthesis scheme of bFGF-p(SS-*co*-PEGMA). b) Western blots of bFGF-p(SS-*co*-PEGMA) from SDS-PAGE (left) and Native PAGE (right), lane 1: bFGF-p(SS-*co*-PEGMA) with 54 mg/ml DTT, lane 2: bFGF-p(SS-*co*-PEGMA) without DTT (diffuse bands = conjugates), lane 3: bFGF without DTT. c) ESI-GEMMA spectra of bFGF (top, EMD = 5.43 nm, d = 0.58 g/cm^3, MW$_{calculated}$ = MW$_{theoretical}$ = 16 kDa), bFGF-p(SS-*co*-PEGMA) (bottom, EMD = 5.43 nm, d = 0.78 g/cm^3, MW$_{calculated}$ = 39 kDa, MW$_{theoretical}$ = 42 kDa) in 20 mM ammonium acetate.
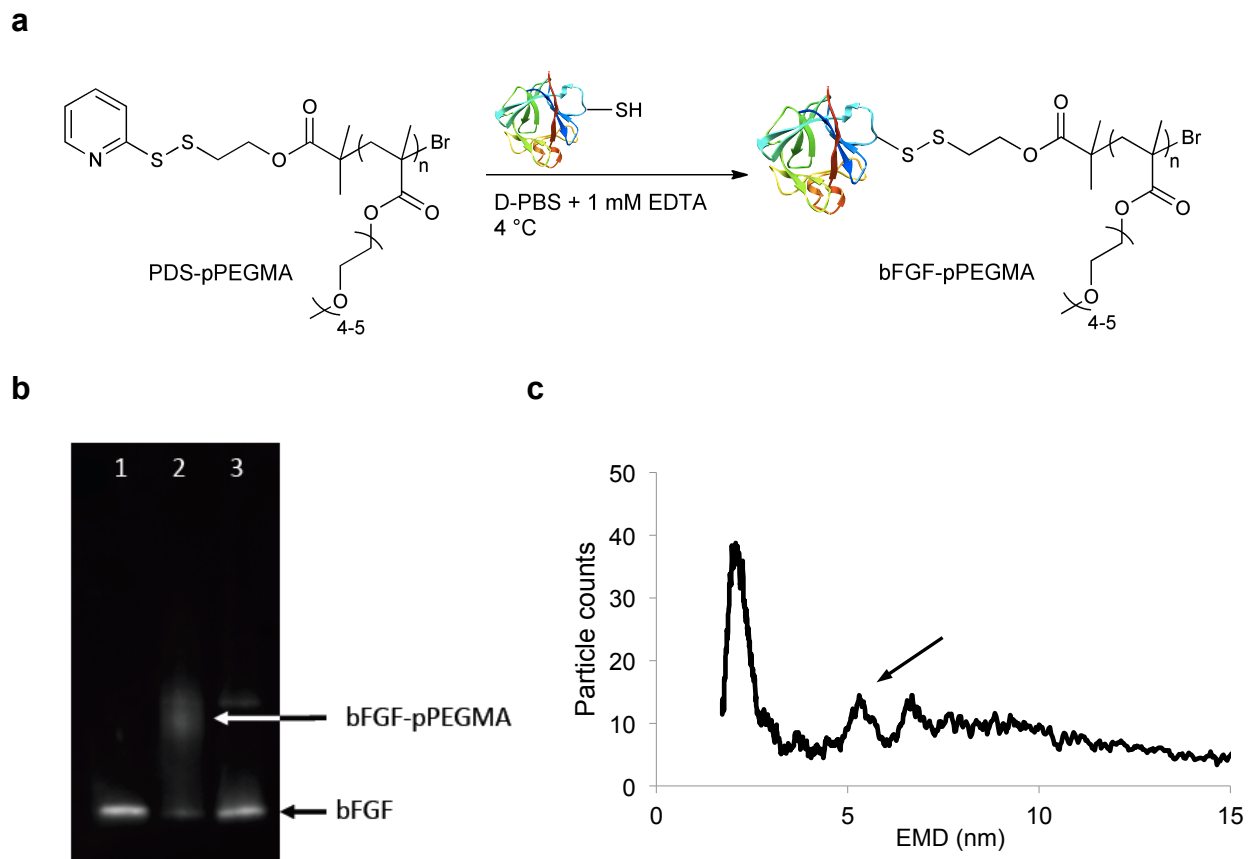
Figure 2.6. Synthesis and characterization of bFGF-pPEGMA conjugate. a) Synthesis scheme. b) Western blot of bFGF-pPEGMA, lane 1: bFGF-pPEGMA with 54 mg/ml of DTT, lane 2: bFGF-pPEGMA without DTT, lane 3: bFGF without DTT. c) ESI-GEMMA spectrum of bFGF-pPEGMA (arrow, EMD = 5.3 nm, d = 0.64 g/cm^3, MW$_{calculated}$ = 30 kDa, MW$_{theoretical}$ = 39 kDa) in 20 mM ammonium acetate.
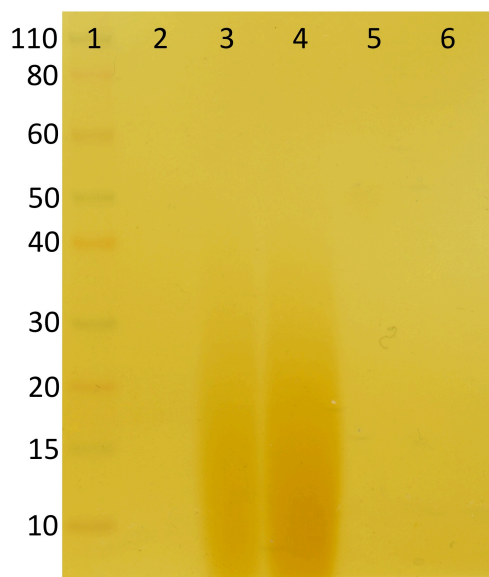
Figure 2.7. SDS-PAGE of collected fractions from on-column conjugation of bFGF to PDS-p(SS-*co*-PEGMA), stained with iodine stain. Lane 1: protein standards, lane 2: bFGF (not detected due to low sensitivity of iodine stain in detecting small amount of protein), lane 3: p(SS-*co*-PEGMA), lane 4: 0 M NaCl fraction (diffuse band = excess unconjugated polymer), lane 5: 0.5 M NaCl fraction (unconjugated polymer not detected), lane 6: 2 M NaCl fraction (unconjugated polymer not detected)

Table 2.1. Analysis of the efficiency of the on-column conjugation of bFGF to PDS-p(SS-*co*-PEGMA). Quantification of bFGF in the collected fractions was performed using ELISA; the concentrations were extracted from the standard curve (below). The percent of bFGF in the 2 M NaCl fraction was calculated by the dividing the amount of bFGF in the 2 M NaCl fraction by the total amount of bFGF collected in all fractions. Percent yield was calculated by dividing the total bFGF collected in the 2 M fraction to the original amount of bFGF used for conjugation.

	Conc. (µg/ml)	Total V collected (ml)	Total m collected (µg)	% bFGF in 2 M NaCl fraction	% yield
Flow through fraction	6.00E-05	0.055	3.30E-06		
Wash 0 M NaCl fraction	7.19E-03	0.050	3.60E-04		
Wash 0.5 M NaCl fraction	0.21	0.055	1.17E-02		
Elution 2 M NaCl fraction	27.98	0.057	1.59	**99.3**	**49.5**
bFGF used for conjugation	16.11	0.200	3.22		

Standard Curve

$y = 0.0021x + 0.0394$
$R^2 = 0.99493$

Abs vs. bFGF (pg/ml)
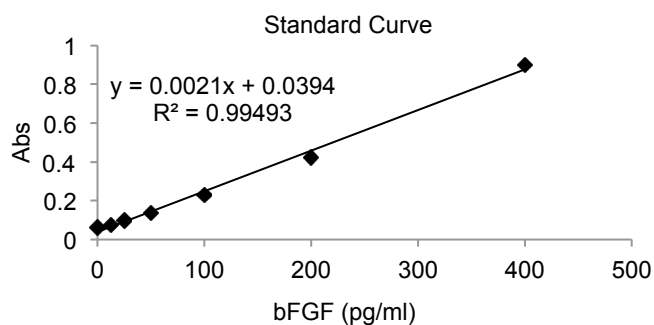
Analyses of the conjugates via matrix-assisted laser desorption/ionization (MALDI) and electrospray ionization mass spectrometry (ESI-MS) were unsuccessful due to difficulties with ionization and the sample heterogeneity. Therefore, electrospray ionization-gas-phase electrophoretic mobility molecular analysis (ESI-GEMMA) of the conjugates was employed. ESI-GEMMA separates macromolecules based on their electrophoretic mobility in air that is directly related to their electrophoretic mobility diameters (EMD); we have shown previously

that the technique can be applied to polymer conjugates.[42,43] The ESI-GEMMA spectrum of bFGF (MW=16 kDa) showed a major peak at 4.45 nm corresponding to 16,116 Da (Figure 2.5c, top). Utilizing the signals for the bFGF-p(SS-*co*-PEGMA) and bFGF-pPEGMA (Figure 2.5c bottom, Figure 2.6c), the calculated MWs were 39 kDa and 30 kDa, respectively, when assuming one polymer was attached to the protein (see ref. 38 for details of how the molecular weights were calculated). This agreed reasonably well with the theoretical MWs of 42 kDa and 39 kDa, respectively. The small discrepancy in the MWs was attributed to the polydispersity of the conjugated polymers. The results were significantly different if instead the calculation assumed two polymers were attached to one protein (for example for bFGF-p(SS-*co*-PEGMA), the calculated MW of this conjugate was 41 kDa compared to the theoretical MW of 68 kDa). The results strongly support that one polymer was conjugated to bFGF for both conjugates.

2.3.3. Stability Studies

HDF cells were used as the in vitro model to evaluate the bioactivity of the bFGF-heparin-mimicking polymer conjugate before and after exposure to various stresses. With careful storage at -80 °C before use for all samples, an addition of 1 ng/ml of bFGF-p(SS-*co*-PEGMA) conjugate stimulated cell growth to 213 ± 13%, which was not statistically different than when 1 ng/ml of bFGF (192 ± 9%), bFGF (+)1 µg/ml of heparin (205 ± 10%), bFGF (+)1.5 ng/ml of heparin (197 ± 4%), bFGF (+)1.5 ng/ml of pPEGMA (179 ± 14%), 1 ng/ml of bFGF-pPEGMA (190 ± 6%), or bFGF (+)1.5 ng/ml of p(SS-*co*-PEGMA) (207 ± 5%) were applied (Figure 2.8). Thus, all amples had similar activity prior to application of stress.
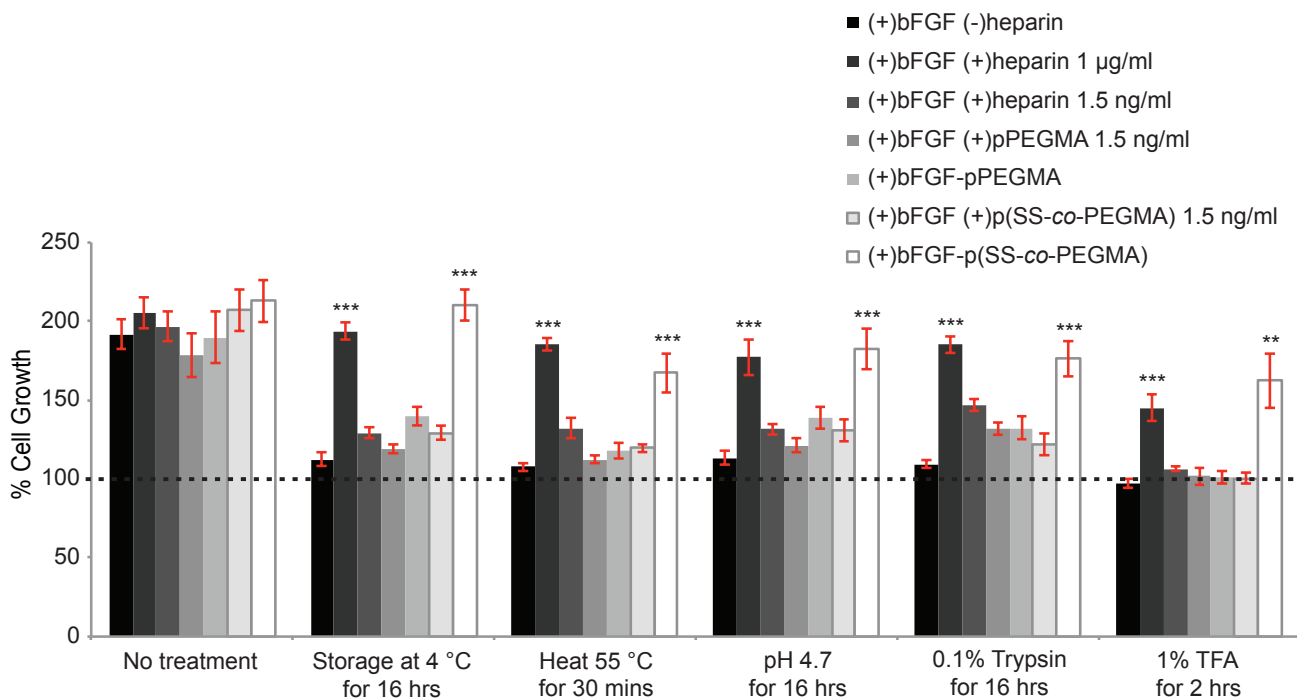
Figure 2.8. Stability study of bFGF-heparin-mimicking polymer conjugate, bFGF-p(SS-*co*-PEGMA), compared to control groups. The concentrations of bFGF and bFGF conjugates under treatment and later in the medium were 0.05 ng/μL and 1 ng/ml, respectively. Incubation of HDF cells with the samples was carried out for 72 hours. CellTiter®-Blue assay was performed to quantify the extent of cell growth. Data was normalized to the blank group (no bFGF added) in that same treatment set. Each sample had six repeats, and the whole experiment was repeated eight times including one blinded study, except (+)bFGF (+)1.5 ng/ml pPEGMA and (+)bFGF-pPEGMA which were repeated four times, and the "pH 4.7 for 16 hrs" treatment set of other groups which was repeated seven times. Error bars are SEM. Statistical analysis was done using two-way ANOVA and Student's t-test. ** Denotes $p < 0.01$ and *** Denotes $p < 0.001$ for (+)bFGF-p(SS-*co*-PEGMA) group or positive control group (+)bFGF (+)heparin 1 μg/mL compared to the negative control group (+)bFGF (-)heparin for each stressor. ········ Denotes no induced proliferation by bFGF.

Stressors were chosen to investigate the stability of the bFGF-p(SS-*co*-PEGMA) conjugate in comparison to other groups. The chosen treatments represent environmental stresses that the growth factor (or any heparin-binding protein) could be exposed to such as storage in the unfrozen form and exposure to heat during delivery, transport, or use (represented by "Storage at 4 °C for 16 hrs" and "Heat at 55 °C for 30 mins" in Figure 2.8). Incubation of the protein in pH 4.7 buffer for 16 hours is relevant because mildly acidic conditions are present during wound healing.[44] Furthermore, the stability of the bFGF-heparin-mimicking polymer conjugate was challenged against proteolytic degradation and extreme acidic conditions by incubating with 0.1% w/v trypsin for 16 hours and 1% TFA for 2 hours, respectively. The starting concentrations of bFGF and bFGF in the conjugates were equivalent and the concentrations of the unconjugated polymers and heparin were the same at approximately stoichiometric ratios to bFGF. The positive control group contained 700 fold molar excess of heparin to bFGF. The negative control was native bFGF alone.
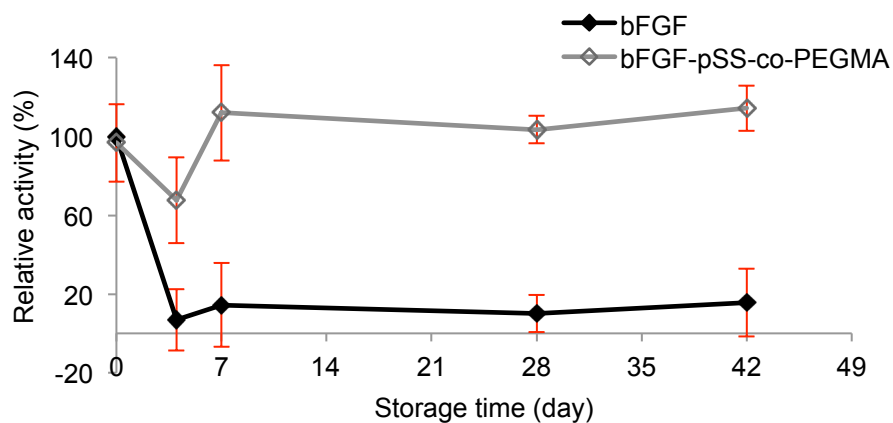
Figure 2.9. Long-term stability study of bFGF-heparin-mimicking polymer conjugate, bFGF-p(SS-*co*-PEGMA), against storage at 4 °C. Preparation of the treated samples is the same as detailed in the Methods section of the paper, except that storage was 4 days, 1 week, 4 weeks,

and 6 weeks. The concentrations of bFGF and bFGF conjugate under storage were 0.05 ng/µL. The final concentrations of bFGF and bFGF conjugate in the medium were 1 ng/ml. Incubation of 2,000-4,000 cells/well in 96-well plate with each of the samples was carried out for 72 hours. CellTiter®-Blue assay was performed to quantify the extent of cell growth. Data showed the percent activity of each group relative to fresh bFGF. Each sample was done with six replicates. Error bars are standard deviations.

In all cases, the bioactivity of bFGF-p(SS-*co*-PEGMA) was significantly higher than all the other groups including bFGF-pPEGMA, and the same as the positive control (Fig. 2.8). Upon exposure to storage and mildly acidic conditions, the bioactivity of bFGF-p(SS-*co*-PEGMA) ($210 \pm 10\%$ and $183 \pm 13\%$, respectively) was statistically the same as before treatment ($213 \pm 13\%$). The bFGF-heparin-mimicking polymer conjugate also showed no loss of bioactivity for at least 6 weeks when stored at 4 °C (Figure 2.9). The percent cell growth of bFGF-p(SS-*co*-PEGMA) under heat, trypsin and 1% TFA treatments were $167 \pm 12\%$, $176 \pm 11\%$, and $162 \pm 17\%$ respectively. In each case, the bFGF-heparin-mimicking polymer conjugate was statistically the same as the positive control, bFGF with a 700 molar excess of heparin. The bFGF-pPEGMA conjugate did exhibit some stability under storage, mildly acidic and trypsin treatments ($p < 0.01$). However, the bFGF-p(SS-*co*-PEGMA) conjugate had a significantly better stability profile than the bFGF-pPEGMA conjugate for all treatments ($p < 0.001$ for storage, $p < 0.05$ for others). This result demonstrates the importance of a heparin-mimicking polymer for the observed protective effect.

2.3.4. Inhibition study

To confirm that the bFGF-heparin-mimicking polymer conjugate promoted cell growth by the same signal transduction pathway as native bFGF, a potent inhibitor for FGF receptor 1 (FGFR1) was included in the medium. PD173074 competes with adenosine-5'-triphosphate (ATP) for binding to FGFR1, a key step for FGFR phosphorylation, and shuts down the signal transduction pathways associated with cell proliferation.[45,46] HDF cells express primarily FGFR1,[47] and PD173074 has been well demonstrated to deactivate FGFR1 phosphorylation at low concentrations.[46] Figure 2.10 shows the screening study for optimum concentration of the inhibitor PD173074 to inhibit HDF cells growth.
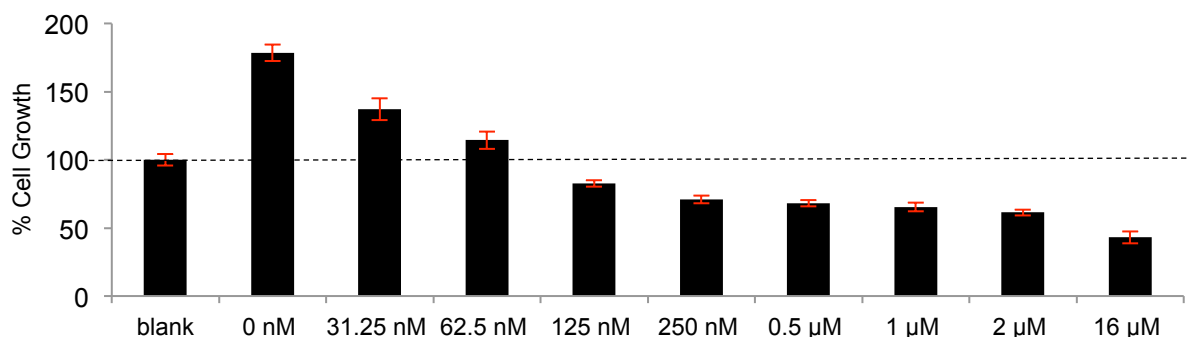
Figure 2.10. Screening for optimum concentration of the inhibitor PD173074 to inhibit HDF cells growth. Each sample group contained 1 ng/ml of bFGF except for the blank group. The x-axis shows increasing concentration of the PD173074 tested on HDF cells. 2,000 HDF cells/well was incubated with 100 μl of each of the samples for 72 hours. CellTiter®-Blue assay was performed to quantify the extent of cell growth. Data was normalized to blank sample group. Each sample group was measured with six replicates. Error bars are standard deviations. ⋯⋯ Denotes no induced proliferation by bFGF.
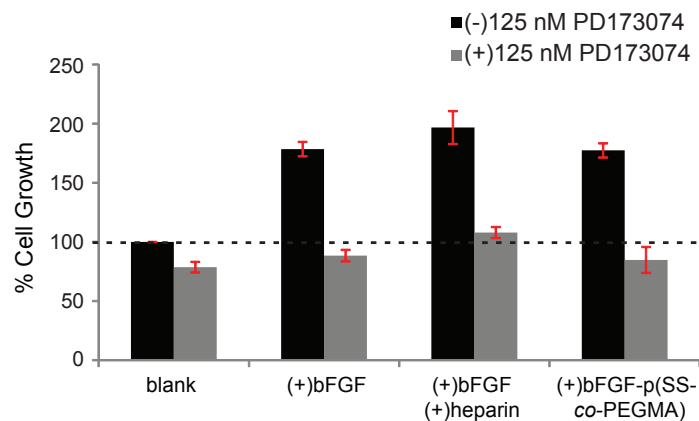
Figure 2.11. Inhibition of FGFR1 activation induced by bFGF and bFGF-heparin-mimicking polymer conjugate, bFGF-p(SS-*co*-PEGMA). The samples were prepared with and without 125 nM of PD173074. 2,000 HDF cells/well was incubated with 100 μl of each of the samples for 72 hours. CellTiter®-Blue assay was performed to quantify percent cell growth. Data was normalized to the blank sample group containing no PD173074. Each sample group was measured with six replicates, and the entire experiment was repeated three times. Error bars represent SEMs. ······· Denotes no induced proliferation by bFGF.

The following groups were tested: 1 ng/ml of bFGF, 1 ng/ml of bFGF with 1 μg/ml of heparin, and 1 ng/ml bFGF-p(SS-*co*-PEGMA). The data was normalized to the blank group containing no PD173074. Figure 2.11 shows that for 1 ng/ml of bFGF with no inhibitor present, the percent cell growth was $178 \pm 6\%$; while in the presence of 125 nM PD173074, the percent cell growth was decreased to $88 \pm 5\%$. Similarly for bFGF-p(SS-*co*-PEGMA), the percent cell growth without and with the addition of PD173074 were $177 \pm 6\%$ and $85 \pm 11\%$, respectively. In the presence of 1 μg/ml of heparin, cell proliferation at 197 ± 14 % was reduced to $108 \pm 5\%$ when 125 nM of PD173074 was added. This data indicated that the bFGF-heparin-mimicking

polymer conjugate triggered HDF cell proliferation through transmembrane tyrosine kinase receptor (FGFR) activation similar to native bFGF, since activity was abrogated by an inhibitor for this receptor.

2.3.5. Proliferation study of BaF3 cells

While bFGF interacts directly with cells by binding to FGFRs, signal transduction requires simultaneous interaction with HS proteoglycan cell surface receptors.[48,49] To investigate whether the heparin-mimicking polymer p(SS-*co*-PEGMA) stabilized the growth factor as anticipated or whether the observed activity resulted from participation of the polymer in the binding site, BaF3 cells (FR1C-11) were used. This BaF3 cell line is engineered to express FGFR1 and lacks cell-surface HS; addition of soluble heparin is required to activate the receptors with bFGF.[50] A 1 μg/ml concentration of heparin effectively stimulated cell proliferation as expected; percent cell growth was almost four times the blank control (384 ± 35%) (Figure 2.12). An addition of 1 μg/ml of the p(SS-*co*-PEGMA) did not show an increase in proliferation; the percent cell growth (128 ± 13%) was similar to the sample group where bFGF was added without heparin (127 ± 12%). Likewise, 1 ng/ml of the bFGF-p(SS-*co*-PEGMA) did not stimulate significant cell growth (147 ± 14%), suggesting that the heparin-mimicking polymer did not participate in receptor binding of the protein to FGFRs. Thus the role of the polymer was to stabilize the growth factor, not to activate the receptor.
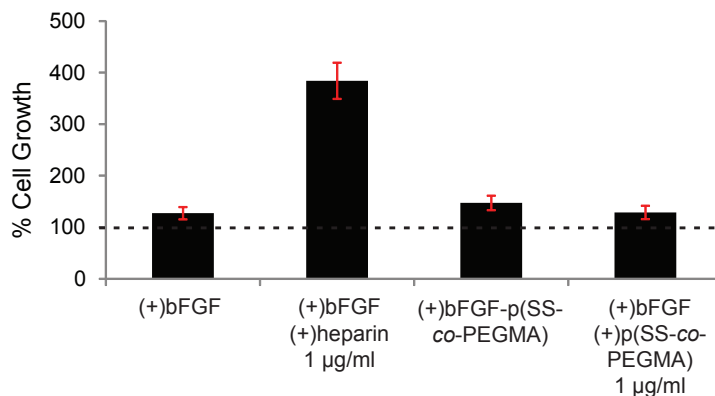
Figure 2.12. Proliferation study with BaF3 cells in response to the addition of the heparin-mimicking polymer and its bFGF conjugate. BaF3 cells (FR1C-11), which express FGFR1 but lack HS proteoglycans, were seeded at a density of 20,000 cells/well in culture medium lacking IL-3 in a 96-well plate. The samples were prepared in the working medium with the final concentrations: 1 ng/ml of bFGF, 1 ng/ml of bFGF with either 1 μg/ml of heparin or 1 μg/ml of p(SS-*co*-PEGMA), and 1 ng/ml of bFGF-p(SS-*co*-PEGMA). The cells were incubated for 42 hours. CellTiter®-Blue assay was performed to quantify percent cell growth. Data was normalized to blank the sample group. Each group was done with six replicates. Error bars are standard deviations. ⋯⋯ Denotes no induced proliferation by bFGF.

## 2.4. Discussion

For the past three decades, PEG conjugates have been widely utilized as biologic drugs;[51,52] yet these conjugates still suffer from environmental instability issues, and often require addition of large concentrations of excipients. We demonstrate herein that by careful design of a polymer to mimic a natural polysaccharide, a protein that is normally unstable can be rendered stable to numerous stresses that would typically inactivate the protein. bFGF has far reaching biological activity from wound healing to cardiac repair and as a result is an important drug target; thus, this stable construct may be useful therapeutically. Indeed, prior results have demonstrated that clinical trials of bFGF in wound healing have failed,[19] potentially due to issues with stability. The results also suggest that the bFGF-heparin-mimicking polymer conjugate does not require restrictive storage temperatures (freezing) or require loading of excipients as does the native protein. This is important when considering at-home patient use of any clinically relevant biologic, where storage in a freezer until just before use is not desirable and may not be feasible.

Interestingly, the bFGF-heparin-mimicking polymer conjugate, bFGF-p(SS-*co*-PEGMA), had superior stability compared to the control conjugate, bFGF-pPEGMA. bFGF-pPEGMA was significantly degraded after exposure to storage, heat and extreme acidic condition. With exposure to trypsin and mild acid, the experimental set-up required keeping samples refrigerated rather than frozen. Thus, it cannot be ruled out that the typical testing conditions for these stressors, i.e., keeping the samples at 4 ºC for 16 hours, caused the degradation, rather than the enzyme or acidic conditions. Yet, the data clearly showed that the heparin-mimicking polymer conjugate was superior to the PEGylated one, in that it could be heated to high temperature or stored in the refrigerator for weeks without loss of activity. The conjugate was also stable to

acidic conditions (that may be found in wounds for example), and to at least one proteolytic enzyme, which is a typical advantage of a PEGylated conjugate.

In the current study, the resulting conjugate outperformed addition of the same equivalent of non-conjugated polymer or heparin to bFGF. This suggests that the close proximity of the heparin-mimicking polymer protected bFGF from denaturation. This result is also useful because it shows that a very small amount of polymer can be used for stabilization. A large concentration of heparin stabilized the protein as expected. However, heparin itself has significant cross-bioactivity, and thus adding large amounts of the polysaccharide in vivo is not desirable.

Other heparin-binding proteins bind to heparin for stabilization. For example, non-conjugated PEG-polyanions (pentosan polysulfate and dextran sulfate) have been utilized to increase stability of a related protein keratinocyte growth factor-2 (KGF-2);[53] histidine-tagged FGF-8a has been non-covalently associated with nitrilotriacetic acid-nickel-modified poly(acrylamide).[54] These complexes are non-covalent. Non-covalent conjugates may not be useful in vivo because of the likelihood of detachment of the polymer upon dilution before reaching target sites. Thus, the strategy described herein, whereby a heparin-mimicking polymer is covalently, yet reversibly, attached to the protein, may be useful to stabilize other heparin-binding growth factors such as KGF-2. These studies are underway.

Although the inhibition assay indicated that the bFGF-heparin-mimicking polymer conjugate triggered HDF cells proliferation via the same signal transduction pathway as native bFGF, the heparin-mimicking polymer did not participate in receptor binding as does heparin. Heparin added at high concentrations to normal cells can inhibit the activity of these cells,[22,23] and this has been proposed to occur by competition of heparin with the HS. That p(SS-*co*-

PEGMA) mimicked heparin in that it bound to bFGF to stabilize it, but did not participate in receptor binding, could be advantageous: high concentrations of the polymer may not inhibit cellular activity as does heparin. It may be that the sulfonate groups do not bind to the receptor or that the PEG side chains prevented the polymer from fitting into the HS groove of the bFGF/FGFR tetramer complex.[49] Thus, it would also be interesting to identify a polymer that would stabilize the bFGF and bind in the HS receptor site, and this work is underway.

2.5. Conclusions

In this report, we describe a protein-polymer conjugate that has superior stability while retaining native activity after a variety of stressors. A cysteine-reactive heparin-mimicking polymer, PDS-p(SS-*co*-PEGMA), was prepared via RAFT polymerization. Conjugation of the polymer to bFGF via disulfide exchange was accomplished using an on-column technique to produce bFGF-p(SS-*co*-PEGMA). The conjugate exhibited significantly enhanced stability against heat, mild and harsh acidic conditions, storage, and proteolytic degradation compared to native bFGF and the analogous bFGF-pPEGMA conjugate. The conjugate targeted the same receptor as unmodified bFGF. While one equivalent of added polymer or heparin did not stabilize the growth factor, the same amount of conjugated polymer did. The results together demonstrate that the strategy of conjugating heparin-mimicking polymers to bFGF is valuable as a means to stabilize this clinically important protein.

2.6. References

1) Abuchowski, A.; Vanes, T.; Palczuk, N. C.; Davis, F. F. *J. Biol. Chem.* **1977**, *252*, 3578.

2) Duncan, R. *Nat. Rev. Drug Discov.* **2003**, *2*, 347.

3) Alconcel, S. N. S.; Baas, A. S.; Maynard, H. D. *Polym. Chem.* **2011**, *2*, 1442.

4) Keefe, A. J.; Jiang, S. *Nature Chem.* **2012**, *4*, 59.

5) Mancini, R. J.; Lee, J.; Maynard, H. D. *J. Am. Chem. Soc.* **2012**, *134*, 8474.

6) Capila, I.; Linhardt, R. J. *Angew. Chem. Int. Ed.* **2002**, *41*, 391.

7) Cardin, A. D.; Weintraub, H. J. R. *Arteriosclerosis* **1989**, *9*, 21.

8) Slack, J. M. W.; Darlington, B. G.; Heath, J. K.; Godsave, S. F. *Nature* **1987**, *326*, 197.

9) Cross, M. J.; Claesson-Welsh, L. *Trends Pharmacol. Sci.* **2001**, *22*, 201.

10) Kawai, K.; Suzuki, S.; Tabata, Y.; Ikada, Y.; Nishimura, Y. *Biomaterials* **2000**, *21*, 489.

11) Canalis, E.; Centrella, M.; McCarthy, T. *J. Clin. Invest.* **1988**, *81*, 1572.

12) Timmer, M.; Cesnulevicius, K.; Winkler, C.; Kolb, J.; Lipokatic-Takacs, E.; Jungnickel, J.; Grothe, C. *J. Neurosci.* **2007**, *27*, 459.

13) Levenstein, M. E.; Ludwig, T. E.; Xu, R. H.; Llanas, R. A.; VanDenHeuvel-Kramer, K.; Manning, D.; Thomson, J. A. *Stem Cells* **2006**, *24*, 568.

14) Barrientos, S.; Stojadinovic, O.; Golinko, M. S.; Brem, H.; Tomic-Canic, M. *Wound Repair Regen.* **2008**, *16*, 585.

15) Shipley, G. D.; Keeble, W. W.; Hendrickson, J. E.; Coffey, R. J.; Pittelkow, M. R. *J. Cell Physiol.* **1989**, *138*, 511.

16) Pittelkow, M. R.; Shipley, G. D. *J. Cell Physiol.* **1989**, *140*, 565.

17) Edelman, E. R.; Mathiowitz, E.; Langer, R.; Klagsbrun, M. *Biomaterials* **1991**, *12*, 619.

18) Whalen, G. F.; Shing, Y.; Folkman, J. *Growth Factors* **1989**, *1*, 156.

19) Richard, J. L.; Bringer, J.; Parerrichard, C.; Rodier, M.; Daures, J. P.; Jacob, C.; Clouet, S.; Comtebardonnet, M.; Vannereau, D. *Diabetes Care* **1995**, *18*, 64.

20) Gospodarowicz, D.; Cheng, J. *J. Cell Physiol.* **1986**, 475.

21) Sakiyama-Elbert, S. E. In *Comprehensive Biomaterials*; Ducheyne, P., Healy, K. E., Grainger, D. W., Hutmacher, D. W., Kirkpatrick, C. J., Eds.; Elsevier B.V.: 2011; Vol. 4, p 333.

22) Cariou, R.; Harousseau, J. L.; Tobelem, G. *Cell Biol. Int. Rep.* **1988**, *12*, 1037.

23) Ferrao, A. V.; Mason, R. M. *Biochim. Biophys. Acta* **1993**, *1180*, 225.

24) Liekens, S.; Leali, D.; Neyts, J.; Esnouf, R.; Rusnati, M.; Dell'Era, P.; Maudgal, P. C.; De Clercq, E.; Presta, M. *Mol. Pharmacol.* **1999**, *56*, 204.

25) Guan, R.; Sun, X. L.; Hou, S. J.; Wu, P. Y.; Chaikof, E. L. *Bioconjugate Chem.* **2004**, *15*, 145.

26) Christman, K. L.; Vazquez-Dorbatt, V.; Schopf, E.; Kolodziej, C. M.; Li, R. C.; Broyer, R. M.; Chen, Y.; Maynard, H. D. *J. Am. Chem. Soc.* **2008**, *130*, 16585.

27) Kolodziej, C. M.; Kim, S. H.; Broyer, R. M.; Saxer, S. S.; Decker, C. G.; Maynard, H. D. *J. Am. Chem. Soc.* **2012**, *134*, 247.

28) Wu, X.; Li, X.; Zeng, Y.; Zheng, Q.; Wu, S. *Protein Expres. Purif.* **2006**, *48*, 4.

29) Wu, X.; Liu, X.; Xiao, Y.; Huang, Z.; Xiao, J.; Lin, S.; Cai, L.; Feng, W.; Li, X. *J. Chromatogr. A* **2007**, *1161*, 5.

30) DeLong, S. A.; Moon, J. J.; West, J. L. *Biomaterials* **2005**, *26*, 3227.

31) Kang, C. E.; Tator, C. H.; Shoichet, M. S. *J. Control. Release* **2010**, *144*, 25.

32) Huang, Z. F.; Ye, C. H.; Liu, Z. J.; Wang, X. J.; Chen, H. B.; Liu, Y. L.; Tang, L.; Zhao, H. X.; Wang, J. F.; Feng, W. K.; Li, X. K. *Bioconj. Chem.* **2012**, *23*, 740.

33) Heredia, K. L.; Nguyen, T. H.; Chang, C. W.; Bulmus, V.; Davis, T. P.; Maynard, H. D. *Chem. Commun.* **2008**, 3245.

34) Murthy, N.; Campbell, J.; Fausto, N.; Hoffman, A. S.; Stayton, P. S. *Bioconjugate Chem.* **2003**, *14*, 412.

35) Kaddis, C. S.; Lomeli, S. H.; Yin, S.; Berhane, B.; Apostol, M. I.; Kickhoefer, V. A.; Rome, L. H.; Loo, J. A. *J. Am. Soc. Mass Spectr.* **2007**, *18*, 1206.

36) Saucy, D. A.; Ude, S.; Lenggoro, I. W.; de la Mora, J. F. *Anal. Chem.* **2004**, *76*, 1045.

37) Sumerlin, B. S. *ACS Macro Lett.* **2012**, *1*, 141.

38) Tolstyka, Z.; Maynard, H. D. In *Comprehensive Polymer Science*; Matyjaszewski, K., Möller, M., Eds.; Elsevier B.V.: 2012; Vol. 9, p 317.

39) Moad, G.; Rizzardo, E.; Thang, S. H. *Aust. J. Chem.* **2012**, *65*, 985.

40) Chang, C. W.; Bays, E.; Tao, L.; Alconcel, S. N. S.; Maynard, H. D. *Chem. Commun.* **2009**, 3580.

41) Maynard, H. D.; Hubbell, J. A. *Acta Biomater.* **2005**, *1*, 451.

42) Tao, L.; Kaddis, C. S.; Loo, R. R. O.; Grover, G. N.; Loo, J. A.; Maynard, H. D. *Macromolecules* **2009**, *42*, 8028.

43) Loo, J. A.; Berhane, B.; Kaddis, C. S.; Wooding, K. M.; Xie, Y. M.; Kaufman, S. L.; Chernushevich, I. V. *J. Am. Soc. Mass Spectr.* **2005**, *16*, 998.

44) Gethin, G. *Wounds UK* **2007**, *3*, 52.

45) Mohammadi, M.; McMahon, G.; Sun, L.; Tang, C.; Hirth, P.; Yeh, B. K.; Hubbard, S. R.; Schlessinger, J. *Science* **1997**, *276*, 955.

46) Mohammadi, M.; Froum, S.; Hamby, J. M.; Schroeder, M. C.; Panek, R. L.; Lu, G. H.; Eliseenkova, A. V.; Green, D.; Schlessinger, J.; Hubbard, S. R. *EMBO J.* **1998**, *17*, 5896.

47) Johnson, D. E.; Lu, J.; Chen, H.; Werner, S.; Williams, L. T. *Mol. Cell Biol.* **1991**, *11*, 4627.

48) Schlessinger, J.; Plotnikov, A. N.; Ibrahimi, O. A.; Eliseenkova, A. V.; Yeh, B. K.; Yayon, A.; Linhardt, R. J.; Mohammadi, M. *Mol. Cell* **2000**, *6*, 743.

49) Plotnikov, A. N.; Schlessinger, J.; Hubbard, S. R.; Mohammadi, M. *Cell* **1999**, *98*, 641.

50) Ornitz, D. M.; Leder, P. *J. Biol. Chem.* **1992**, *267*, 16305.

51) Fishburn, C. S. *J. Pharm. Sci.* **2008**, *97*, 4167.

52) Pasut, G.; Veronese, F. M. *Prog. Polym. Sci.* **2007**, *32*, 933.

53) Khondee, S.; Olsen, C. M.; Zeng, Y. H.; Middaugh, C. R.; Berkland, C. *Biomacromolecules* **2011**, *12*, 3880.

54) Griffith, B. R.; Allen, B. L.; Rapraeger, A. C.; Kiessling, L. L. *J. Am. Chem. Soc.* **2004**, *126*, 1608.

Chapter 3

bFGF-p(SS-*co*-PEGMA) Conjugates – Preclinical Study:

Cellular Uptake and Wound Healing Potential

3.1. Introduction

Protein-polymer conjugates have steadily proven to be a valuable class of therapeutics compared to small-molecule drugs in terms of high target specificity and low cytotoxicity and immunogenicity.[1] To date, there are eleven protein-polymer conjugates approved for clinical use by the FDA, and they are exclusively PEGylated proteins – proteins that are covalently conjugated to one or more PEG molecule(s).[2] Although PEGylated proteins have prolonged *in vivo* half-lives and decreased immunogenicities and antigenicities compared to their native counter parts,[3-5] there are limitations. First, while some of the therapeutic proteins have notoriously short shelf lives and are prone to degradation outside the body, PEG does not stabilize these proteins in their nonnative environments. Second, proteins are unique in their chemical structures and the environments in which they operate, while PEG being a linear, non-polar and inert polymer, is not tailored for maximizing interactions with individual protein. In fact, it is utilized because of its ability to repel proteins, which helps to enhance the pharmacokinetic properties of biomolecules.

The advancement in polymerization techniques have allowed for the synthesis of well-defined polymers, other than PEG, with complex architectures and functionalities to engage in specific applications. In early 2013, we reported for the first time a highly stable protein-heparin-mimicking polymer conjugate called basic fibroblast growth factor-p(SS-*co*-PEGMA) (bFGF-p(SS-*co*-PEGMA)) conjugate.[6] bFGF has a crucial role in diverse cellular functions;[7-11] however, the protein is extremely unstable during storage, delivery and handling making it yet inapplicable for clinical use in the USA.[12-14] We designed and synthesized a well-tunable p(SS-*co*-PEGMA) polymer that mimics heparin, a naturally occurring polysaccharide in many aspects; the polymer stabilizes bFGF *in vitro* and binds to the heparin-binding domain on the protein.[15,16]

We showed that bFGF-p(SS-*co*-PEGMA) conjugate exhibited superior stability to a variety of therapeutically and environmentally relevant stressors including: heat, mild and harsh acidic conditions, storage and proteolytic degradation, compared to native bFGF, PEGylated bFGF and bFGF with the heparin-mimicking polymer added noncovalently.[6] Equally important, the bioactivity of the protein was fully retained post synthesis.

Herein, we report a follow up study to investigate the preclinical value of the bFGF-p(SS-*co*-PEGMA) conjugate as a potential therapy for active wound healing. Specifically, we studied the efficacy of the conjugate in promoting chronic wound closure in a diabetic mouse model. The cellular uptake and trafficking of the conjugate was elucidated to better understand its mechanism of action. Long-term storage stability of the conjugate at 4 °C and 23 °C was also examined to determine the usefulness of the conjugate as a widely available therapeutic to patients, including at-home patients and patients in remote areas. In addition, we report for the first time the super-agonist characteristic of the heparin-mimicking polymer conjugate when used in the presence of exogenous heparin.

3.2. Experimental

3.2.1. Materials

Chemicals and reagents were purchased from Fisher or Sigma-Aldrich unless indicated otherwise. Basic FGF and ELISA Development DuoSet® kits were purchased from R&D Systems. Heparin was purchased from PromoCell. Rabbit anti-fibroblast growth factor basic antibody and goat anti-rabbit IgG-HRP conjugate for Western blot were purchased from CALBIOCHEM and Bio-Rad, respectively. Normal HDF cells were purchased from PromoCell. BaF3-FR1C cells expressing FGFR1 were kindly provided by Prof. David Ornitz (Washington University, Saint Louis). Media and supplements for cell culture were either purchased from PromoCell, Lonza or Invitrogen. CellTiter-Blue® cell viability assay were obtained from Promega. HiTrap™ Heparin HP 1 ml was purchased from GE Healthcare. PMMA standards for GPC calibration were purchased from Polymer Laboratories. AIBN was recrystallized twice from ethanol and dried prior to use. Prior to use, 4-styrene sulfonic acid, sodium salt hydrate monomer was pre-treated with Na^+-activated DOWEX 50WX8 200-400 mesh resin to produce the sodium salt. Diabetic db/db mice (female, 19-20 week old) were purchased from Jackson Laboratory.

3.2.2. Analytical Techniques

^{1}H NMR spectroscopy was performed on an Avance DRX 500 MHz spectroscopy instrument. UV-Vis spectrophotometry analyses were performed on a Biomate 5 Thermo Spectronic spectrometer. GPC was conducted on a Shimadzu HPLC system equipped with a refractive index detector RID-10A, one Polymer Laboratories PLgel guard column, and two Polymer Laboratories PLgel 5 μm mixed D columns. DMF containing 0.10 M LiBr at 40 °C

was used as the eluent and near-monodisperse poly(methyl methacrylate) standards were used for calibration at 0.6 ml/min. Chromatograms were processed using the EZStart 7.2 chromatography software. Gel electrophoresis was performed using Any kD™ Mini-PROTEAN® TGX™ precast gels with Tris-glycine as running buffer (Bio-rad, Hercules). ELISA assay results were read on the ELX800 Universal Microplate Reader (Bio-Tek Instrument Inc., Winooski) with $\lambda = 450$ nm and 630 nm for signal and background, respectively. Western blot was developed on a FluorChem® FC2 System version 3.2 (Cell Biosciences, Santa Clara). Fluorescent signals from CellTiter-Blue® assay were read using a SpectraMax M5 microplate reader (Molecular Devices, Sunnyvale). Fluorescent images for cell uptake studies were taken at UCLA CNSI Advanced Light Microscopy/Spectroscopy (ALMS) Imaging Facilities.

3.2.3. Methods

Preparation of Alexa Fluor® 488-labeled bFGF. Microscale Protein Labeling Kit (Life Technologies, Carlsbad, CA) was used to label bFGF with Alexa Fluor® 488 and purify the protein according to the manufacturer's protocol.

Preparation of Atto 590-labeled p(SS-co-PEGMA). Pyridyl disulfide (PDS)-p(SS-*co*-PEGMA) (5 mg, 0.19 μmol) was incubated with 400 μl of immobilized TCEP disulfide reducing gel (Thermo Scientific, Waltham, MA). The slurry solution was degassed by bubbling with argon. The reaction was monitored by UV-Vis absorbance at 343 nm for the release of the side product, pyridine-2-thione. After the reaction was complete, the slurry was centrifuged and the supernatant was collected. Atto 590 maleimide (1 mg, 1.3 μmol) was dissolved in 20 μl of degassed D-PBS. Then the dye solution was added to the polymer solution and incubated for

one hour in the dark. To purify the labeled polymer, the mixture was subjected to dialysis against Milli-Q water using MWCO 26,000 tubing. The resulting polymer was concentrated using a CentriPrep® centrifugal membrane MWCO 30,000. The polymer appeared red.

Synthesis of fluorescent heparin-mimicking polymer p(SS-co-PEGMA-co-RhoB). RAFT polymerization was employed to copolymerize sodium 4-styrenesulfonate (SS), poly(ethylene glycol) methyl ether methacrylate (PEGMA) and methacryloxyethyl thiocarbamoyl rhodamine B (RhoB). 2-(Pyridin-2-yldisulfanyl)ethyl 2-(((ethylthio)carbonothioyl)thio)propanoate was used as the CTA. The polymerization was started with an initial feed ratio of [SS]:[PEGMA]:[CTA]:[AIBN] = 105:30:1:0.5 using standard Schlenk techniques. The CTA (10 mg, 0.03 mmol), SS (0.57 g, 2.7 mmol), PEGMA (0.24 ml, 0.80 mmol), and AIBN (2.2 mg, 0.013 mmol) were dissolved in 3 ml of Milli-Q water and 3 ml of DMF in a Schlenk tube. The system was sealed and subjected to four freeze-pump-thaw cycles before immersion in a 60 °C oil bath. Conversions were calculated from the ^{1}H NMR spectra using the sum of the integral values of the vinylic protons of SS monomer and PEGMA monomer at 5.9 ppm and 6.2 ppm, respectively, and the sum of integral values of the regions where the monomer protons and the growing polymer protons overlap (8.0-6.3 ppm for SS and 4.3-2.9 ppm for PEGMA). The polymerization was allowed to progress for 4.5 hours reaching 47% conversion. In another 10-mL 2-neck round-bottom flask, two molar equivalents of RhoB (36.2 mg, 0.05 mmol) were subjected to vacuum and back-filled with argon three times. Subsequently, 200 μL of degassed DMF was added to the flask; 100 μL of the RhoB solution was quickly transferred via air-tight syringe to the polymerization flask. The polymerization continued for another 1.5 hours in the dark before stopping by exposing to air. The polymer was purified via dialysis first with 1:1 v/v water:acetonitrile followed by dialysis with Milli-Q water (MWCO 3000) and lyophilized to

remove solvent. The polymer appeared to be bright red after drying. δ ^{1}H NMR 500 MHz (D$_2$O): 8.7 (1H, end group C**H**N), 8.3 (1H, end group NCC**H**CH), 8.2 (1H, end group NCCH**CH**), 8.0-6.3 (Na$^+$SO$_3^-$C$_6$**H$_4$** side chains and RhoB's styrene ring protons), 4.3-2.9 (PEGMA side chains, RhoB's OC**H$_2$CH$_2$**O, RhoB's N(C**H$_2$**CH$_3$)$_2$ and RhoB's $^+$N(C**H$_2$**CH$_3$)$_2$), 2.9-0.0 (polymer backbone, RhoB's N(CH$_2$**CH$_3$**)$_2$ and RhoB's $^+$N(CH$_2$**CH$_3$**)$_2$). IR (cm^{-1}): 3422, 2982, 1642, 1445, 1151, 1031, 710. M$_n$ = 12.6 kDa by NMR, 17.8 kDa by GPC, PDI = 1.22 by GPC.

Preparation of dual fluorescent-labeled bFGF-p(SS-co-PEGMA-co-RhoB) conjugate. Alexa Fluor® 488-labeled bFGF (25 μg, 1.6 x 10^{-3} μmol) was diluted into 900 μl of D-PBS + 1mM EDTA, and loaded onto a hand-packed 1ml-heparin Sepharose® column. Subsequently, p(SS-*co*-PEGMA-*co*-RhoB) (5 mg, 0.4 μmol) was dissolved in 900 μl of D-PBS + 1mM EDTA and loaded onto the column. The column was allowed to incubate at 4 °C for 16 hours. The unconjugated polymer and weakly bound bFGF were washed off the column with 2 x 6 ml of 0 M NaCl D-PBS, and 1 x 3 ml of 0.5 M NaCl D-PBS, respectively. The conjugate was eluted off the column using 2 x 6 ml of 2 M NaCl D-PBS. The fractions were then desalted, concentrated using a CentriPrep® centrifugal membrane MWCO 3000 with D-PBS, and stored at -20 °C.

Cell culture. HDF primary cells were purchased from PromoCell and cultured in PromoCell fibroblast growth medium containing 2% fetal calf serum, 1 ng/ml bFGF, 5 μg/ml insulin, supplemented with 100 unit/ml penicillin and 100 μg/ml streptomycin at 37 °C, 5% CO$_2$. HDF cells were passaged every four days or after reaching 80% confluency. HDF cells were used up to passage 12. BaF3-FR1C cells were kindly provided by Dr. David Ornitz and cultured as recommended. Specifically, the cells were grown in RPMI1640 medium containing 10% newborn bovine calf serum, 2 mM L-glutamine, 0.5 ng/ml of recombinant mouse IL-3, 600

μg/ml of G418, 50 nM of 2-mercaptoethanol, supplemented with 100 unit/ml penicillin and 100 μg/ml streptomycin at 37 °C, 5% CO_2. The medium was changed every two days.

Cell treatment and confocal microscopy. HDF cells were seeded on cover glasses in 6-well plates at a density of 0.3 x 10^6/well. The cells were incubated over 12 hours to allow attachment. Then the cells were incubated for 4 hours with various formulations, including Alexa Fluor® 488-labeled bFGF (40 nM), Atto 590-labeled p(SS-*co*-PEGMA) (40 nM), Alexa Fluor® 488-labeled bFGF (40 nM) with Atto 590-labeled p(SS-*co*-PEGMA) (40 nM), and dual fluorescent-labeled bFGF-p(SS-co-PEGMA-co-RhoB) conjugate. Untreated cells were used as controls. After incubation, the cells were washed with cold PBS, fixed with 4% paraformaldehyde and mounted in a medium containing DAPI (Vector Lab). Images were captured using an Leica TCS SP2 spectral confocal microscope under three channels: DAPI for nuclei, Alexa Fluor 488 for bFGF, Atto 590 for p(SS-*co*-PEGMA), and Rhodamine B for p(SS-*co*-PEGMA-*co*-RhoB).

Preparation of samples for long-term storage activity studies. A volume of 45 μl in D-PBS was prepared to contain either 0.5 ng/mL of bFGF, 0.5 ng/ml of bFGF-p(SS-*co*-PEGMA), or 0.5 ng/mL of bFGF with 0.5 μg/mL of heparin. Each 45 μL sample was divided into 15 vials of 3 μL/aliquot further diluted with 27 μL of D-PBS. All of the aliquots were stored at 4 °C or 23 °C for long-term storage treatment.

Stability studies with HDF cells. At predetermined time points, a set of aliquots was diluted to 1.5 ml with UltraCULTURE™ serum-free medium, which brought the final concentration of bFGF/bFGF-p(SS-*co*-PEGMA) to 1 ng/mL and heparin to 1 μg/mL. The untreated samples were prepared fresh at the same final concentrations at the start of the assay.

HDF cells were trypsinized and resuspended in UltraCULTURE^{TM} serum-free medium supplemented with 2 mM L-Glutamine, 100 unit/mL penicillin and 100 μg/mL streptomycin. The cells were plated at 2,000 cells/well in a 96-well plate and allowed to adhere for 16 hours at 37 °C, 5% CO_2. At the end of the 16-hour incubation, 100 μL of medium containing bFGF or the tested compounds were replaced in each well. After incubation of 72 hours at 37 °C, 5% CO_2, CellTiter-Blue® assay was carried out to evaluate cell proliferation. All experimental groups were set relative to the untreated bFGF, which was set at 100%. Each group was done with six replicates.

Western blot analysis. Multiple stored aliquots of the same samples were concentrated via CentriPrep® centrifugal membrane MWCO 3,000 and then assessed via native PAGE. Fresh samples taken from -80 °C freezer were used as controls. The procedure for Western blot was followed as described in Chapter 2.

Proliferation studies with BaF3-FR1C. BaF3-FR1C cells were collected and washed three times with culture medium lacking interleukin 3 (IL-3). The cells were plated with 50 μL at a density of 20,000 cells/well in a 96-well plate. The samples were prepared in the working medium to contain various concentrations of bFGF or bFGF-p(SS-*co*-pPEGMA) (2 ng/mL – 0.25 ng/mL) with or without 2 μg/ml of heparin. Subsequently, 50 μL of each sample was added into each corresponding well. After incubation for 42 hours at 37 °C, 5% CO_2, CellTiter-Blue® assay was carried out to evaluate the extent of cell growth. All of the groups were normalized to the control group, which had only medium. Each group was performed with four replicates and the experiment was repeated four times.

Release studies from Pluronic F127 gel. A solution of 22% w/v Pluronic F127 was prepared by diluting the powder in D-PBS and kept at 4 °C. An equal amount of bFGF and the conjugate was loaded into the each gel solution at 4 °C. A 100 µL of each solution containing 46.5 ng of bFGF or the conjugate was pipetted out in a 96-well-plate at 23 °C for one hour to form an opaque gel (n = 4). A 100 µL of 1 mg/mL BSA solution was pipetted on top of each gel and the plate was shaken slightly. Aliquots of 10 µL were collected every 30 min to quantify the released bFGF/conjugate via ELISA. The procedure for ELISA is described in Chapter 2. The percent bFGF released was the cumulative released bFGF or the conjugate at the indicated time point relative to the known amount of bFGF or the conjugate loaded initially.

Wound healing study. Animal study was conducted in compliance with the UCLA Animal Care Committee. The 12 db/db mutant female mice ages 19-20 weeks were utilized. Twelve mice were maintained under fasting conditions for 4 hours and subsequently anesthetized with a mixture of isoflurane and oxygen. After induction of anesthesia, the dorsal skin was shaved. A 5-mm punch biopsy was created on the dorsal skin of each mouse using a sterile, disposable biopsy punch (Miltex, Inc.). After wounding, mice were maintained in separate cages. To the injured site, 100 µL of Pluronic gel containing 0.5 µg of either bFGF, bFGF-p(SS-*co*-PEGMA) or D-PBS (blank) was applied. The mice were treated once a day for five days consecutively post wounding. The experiment was blinded, in which the samples were given arbitrary letters and the keys were revealed after the data had been obtained. The total lesion size was measured by analyzing digital photographs (Nikon Coolpix) of mice taken at various time points after the 5-mm punch biopsy using the software program, ImageJ (http://rsbweb.nih.gov/ij/).

3.3. Results and Discussion

3.3.1. Cellular uptake studies

Understanding cellular uptake and trafficking is essential to validate the biological function of a protein drug. In order to conduct the studies, fluorescent-labeled heparin-mimicking polymer p(SS-*co*-PEGMA), bFGF and the conjugate were prepared. A maleimide-functionalized Atto 590 dye was utilized to label the polymer because of its robust reactivity toward thiol (Scheme 3.1).[17] PDS-p(SS-*co*-PEGMA) was first reduced to thiol-p(SS-*co*-PEGMA) using TCEP resin. Since TCEP is a mild reducing agent, only the PDS group would be reduced to thiol and react with the maleimide-Atto 590 to form a mono-labeled polymer. After the reaction with the maleimide-Atto 590 and extensive purification, the polymer appeared to be red indicating the success of the labeling.

Scheme 3.1. Synthesis of Atto 590-labeled p(SS-*co*-PEGMA).

95
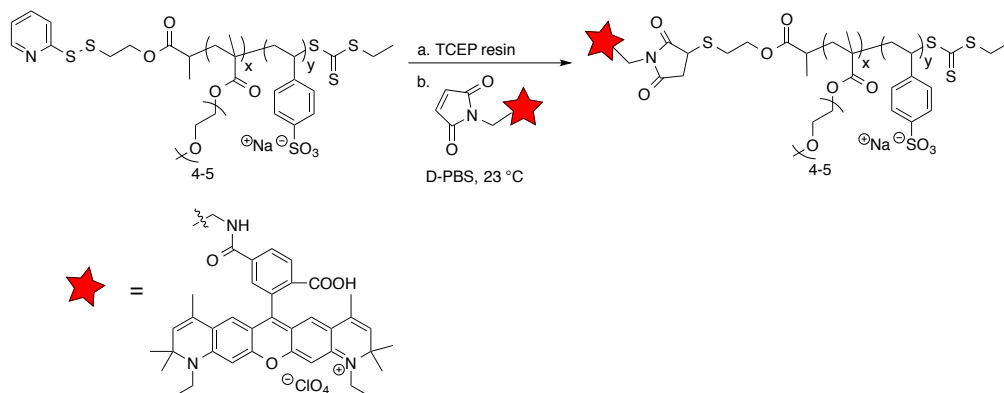
In order to label both the protein and the heparin-mimicking polymer in the conjugate form for the dual tracking, a different synthetic approach was needed. Since the PDS end group on the polymer was originally utilized as a thiol activation for disulfide exchange with another free thiol on bFGF, maleimide-Atto 590 was not applicable. Instead, the heparin-mimicking polymer was synthesized in the presence of a RhoB-based methacrylate monomer as a way to label the polymer red (Scheme 3.2). RhoB-based methacrylate was chosen because of its compatible rate of polymerization with SS and PEGMA, and rate of transfer with the CTA. One molar equivalent of the RhoB-based methacrylate monomer was added to the reaction after the polymerization between SS and PEGMA reached 45% conversion in order to not disturb the heparin-mimicking structure of the polymer. The polymer was subjected to dialysis to remove unreacted dye; the dialysis water was changed until it remained colorless. The ^{1}H NMR spectrum of the polymer however did not show evidence for the incorporation of RhoB (Figure 3.1). The protons from the RhoB segment were possibly hidden underneath the peaks for SS and PEGMA segments, which stretched from 8 ppm to 2.9 ppm. However, the polymer was fluorescent indicating that the dye was successfully incorporated. The MW of the fluorescent heparin-mimicking polymer p(SS-*co*-PEGMA-*co*-RhoB) was 12.6 kDa by NMR, assuming the DP of the RhoB-based methacrylate monomer was negligible compared to the DPs of SS and PEGMA (see Chapter 2's Methods section for how to calculate the MW of the polymer). The M_n and PDI of the polymer by GPC were 17.8 kDa and 1.22, respectively. The GPC trace of the polymer appeared to be unimodal and the narrow PDI indicating that the polymerization was well controlled (Figure 3.1).

Scheme 3.2. Syntheses of p(SS-*co*-PEGMA-*co*-RhoB) via RAFT polymerization and dual fluorescent-labeled Alexa Fluor® 488-bFGF-p(SS-*co*-PEGMA-*co*-RhoB) conjugate.

a

b

98

c
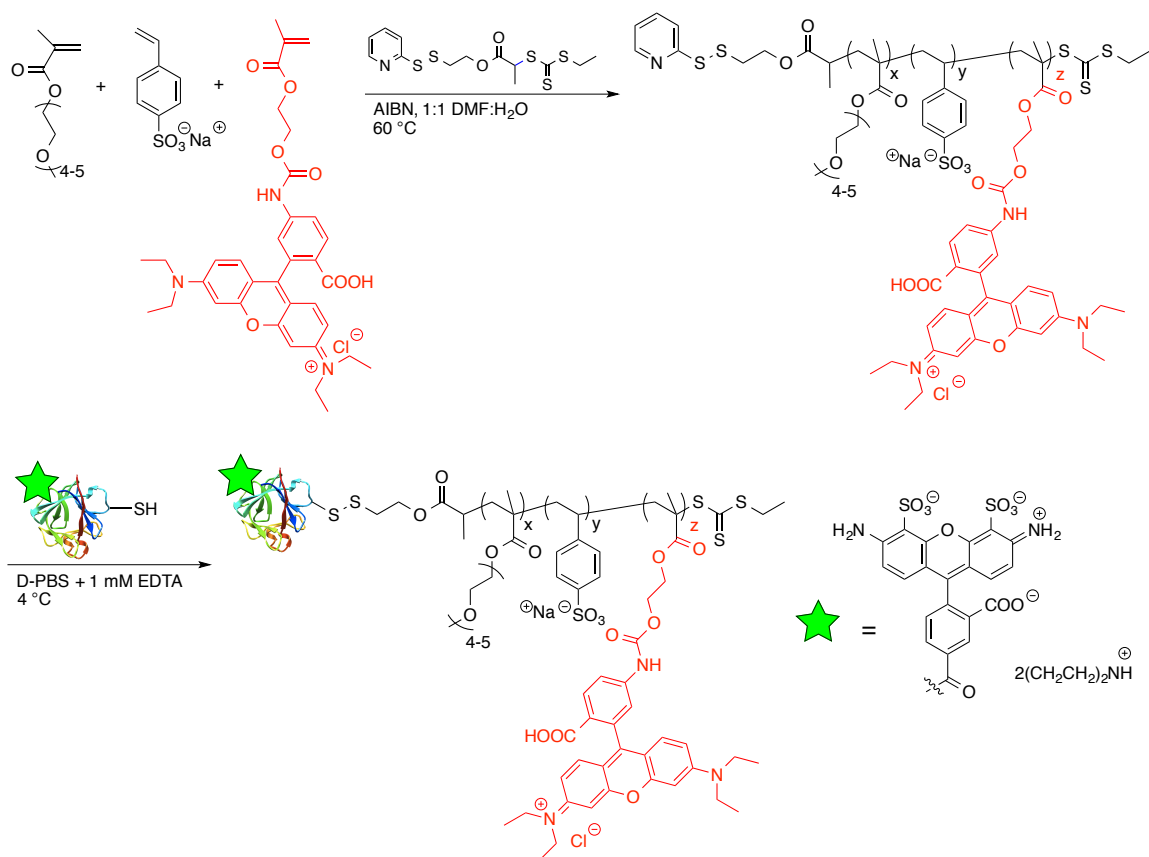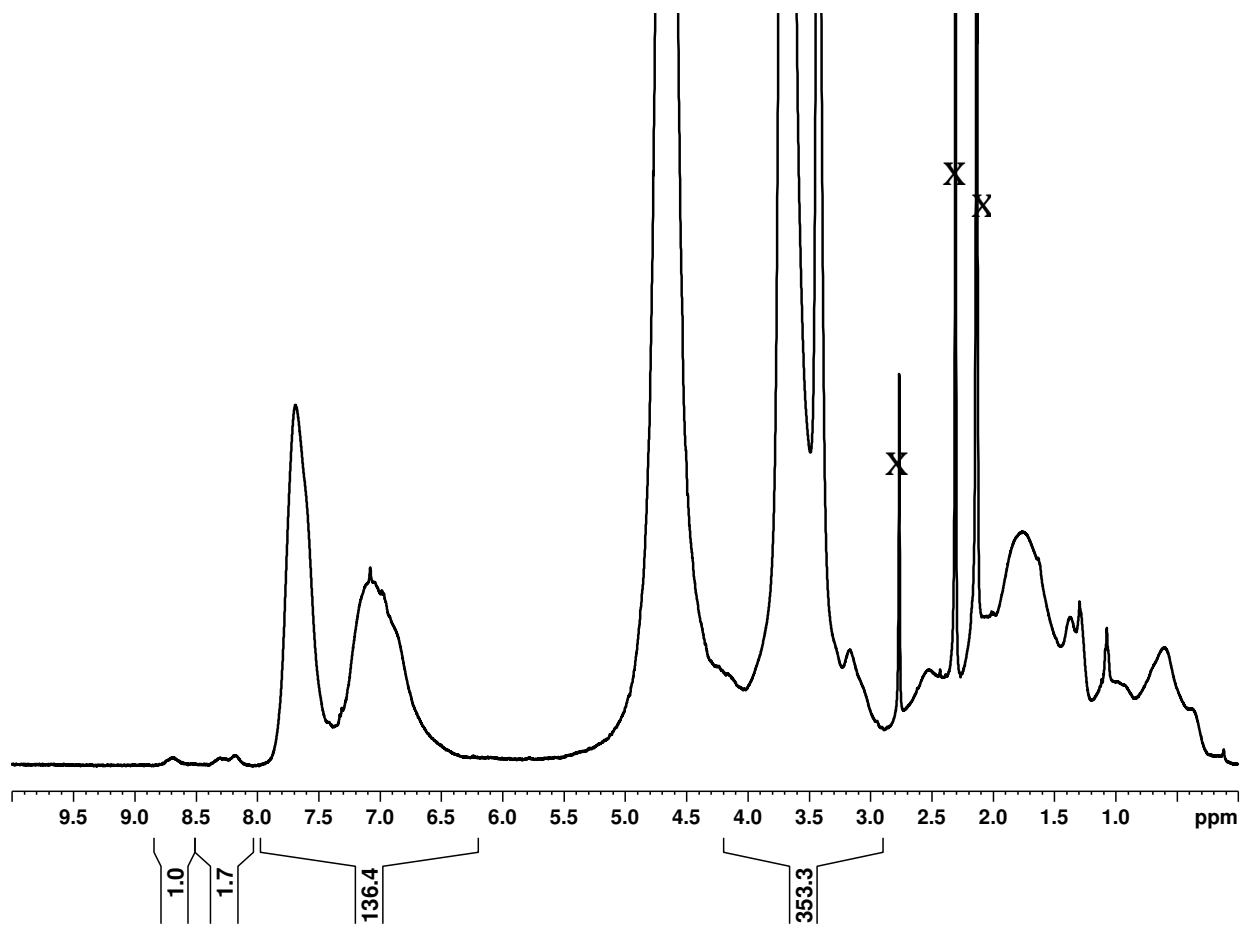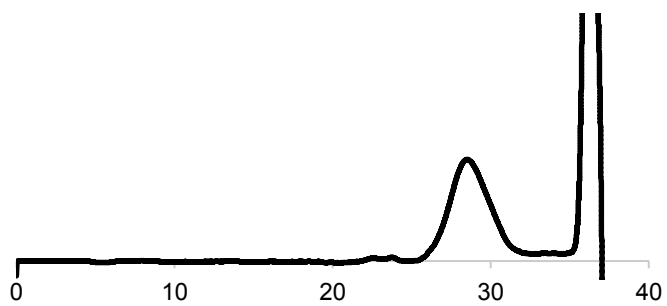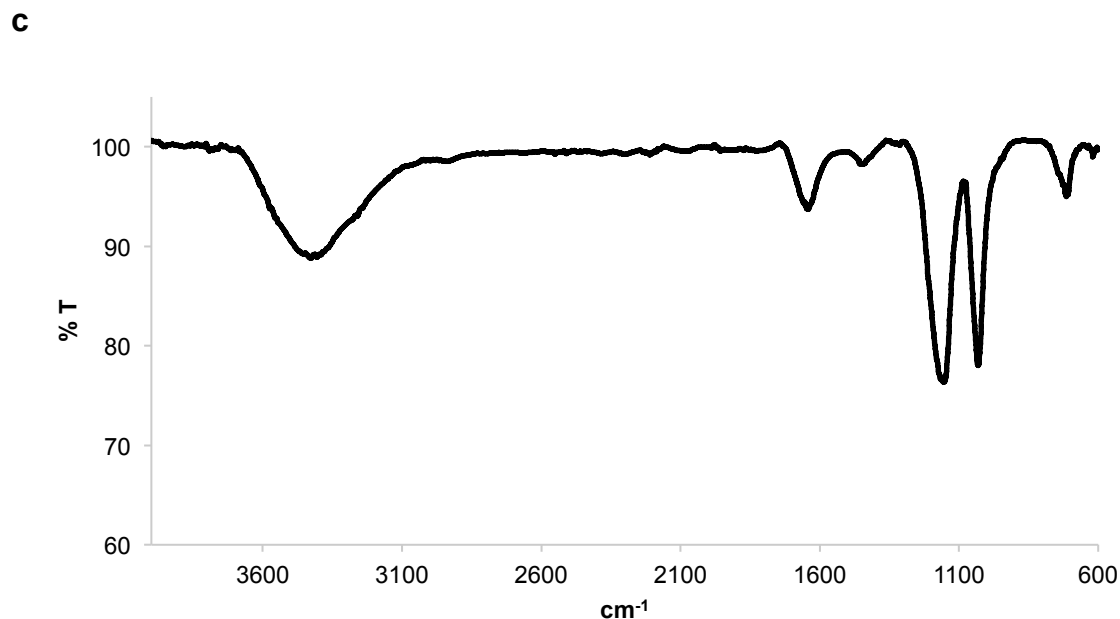
Figure 3.1. Characterization of p(SS-*co*-PEGMA-*co*-RhoB). a) ^{1}H NMR spectrum of the polymer in D$_2$O, b) GPC trace of the polymer in DMF 0.1 M LiBr, and c) FT-IR spectrum of the polymer.

We previously showed that the bFGF-heparin-mimicking polymer conjugate was bioactive when tested on HDF cells.[6] In this follow up study, we investigated the cellular uptake and trafficking of bFGF, p(SS-*co*-PEGMA) and the conjugate in the same cell line. The cells were incubated with various formulations. As shown in Figure 3.2, bFGF was internalized by HDF cells and localized in the cytoplasm, indicated by the green signals. bFGF is internalized via receptor-mediated pathway and has been shown to be co-internalized with its fibroblast growth factor receptor, FGFR, in a dual labeling experiment;[18] thus this result was expected. When the cells were treated with Atto 590 labeled-p(SS-*co*-PEGMA), the red signals were not detected inside the cytoplasm indicating that the polymer alone was not able to enter HDF cells.

This was also expected since the polymer is highly negatively charged, thus likely repelled by the negatively rich cellular surface. In the presence of Alexa Fluor® 488-labeled bFGF, Atto 590-labeled p(SS-*co*-PEGMA) was taken up by HDF cells as indicated by both red and green signals located in the cells (appeared as orange). This result suggested that bFGF bound to p(SS-*co*-PEGMA),[15] and the whole complex interacted with FGFR and was internalized. After treatment with the dual-fluorescent labeled conjugate, HDF cells showed strong fluorescent intensity of both Alexa 488 (bFGF) and Rhodamine (polymer) in the cytoplasm. The two signals were not sequestered in any subcellular compartment and generally overlapping. This suggested that the intact conjugate could be up taken into the cytoplasm even after four hours of incubation at 37 °C. The intact integrity of the conjugate further demonstrated the strong binding between the polymer and bFGF that was observed in a previous report.[19] The data also further proved that the conjugated heparin-mimicking polymer did not inhibit the binding of bFGF to its high affinity receptors.

Figure 3.2. The cellular uptake studies. HDF cells were treated with (from left to right): Alexa Fluor® 488-labeled bFGF, Atto 590-labeled p(SS-*co*-PEGMA), Alexa Fluor® 488-labeled bFGF (+) Atto 590-labeled p(SS-*co*-PEGMA), dual fluorescent-labeled Alexa Fluor® 488-bFGF-(pSS-*co*-PEGMA-*co*-RhoB) conjugate and magnified image of the conjugate. Images were captured
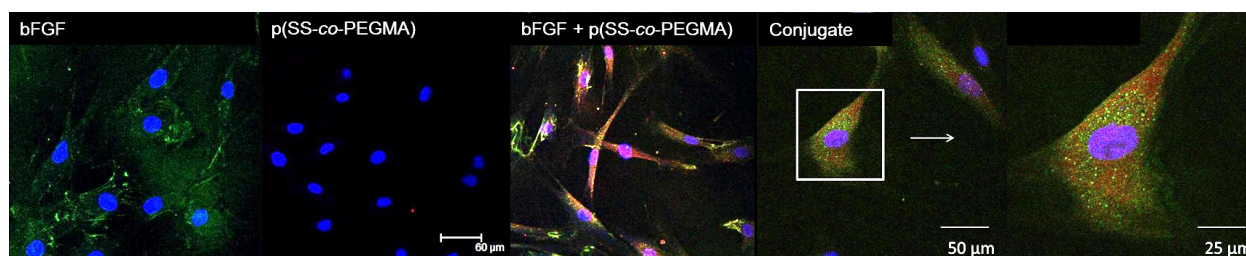
100

under three channels: DAPI for nuclei (blue), Alexa Fluor 488 for bFGF (greene), Atto 590 for p(SS-*co*-PEGMA) (red), Rhodamine B for (pSS-*co*-PEGMA-*co*-RhoB) (red).

3.3.2. Long-term storage stability studies

One of the imperative factors for effective commercialization of protein drugs is to maintain their bioactivity throughout the manufacturing processes, storage and handling. According to Pierce Biotechnology Inc., a typical shelf life of a protein is one month providing that it is kept at 4 °C to avoid degradation of the protein due to temperature fluctuations.[20] bFGF retained about 5% of its original bioactivity after storing at 4 °C for 4 weeks.[12] The high instability of a protein drugs leads to higher costs, because additional approaches, such as chemical modification, protein engineering, and formulation (adding excipient or additive) have to be explored for each specific protein drug.[21] Thus far, utilizing excipients in drug formulations is the most common and least expensive method to counter the inherit instability of proteins.[21] Even so, excipients are generally not effective in prolonging the shelf lives of proteins in the liquid form. For example, Herceptin® – a FDA approved protein therapeutic to treat breast cancer formulated with α, α-trehalose dehydrate as an excipient – is only effective for 48 hours (when stored at 4 °C) after reconstitution with sterile water.[22] The reconstituted drug must be discarded after 48 hours. Having to reconstitute proteins prior to use can further increase inconvenience and costs to patients.
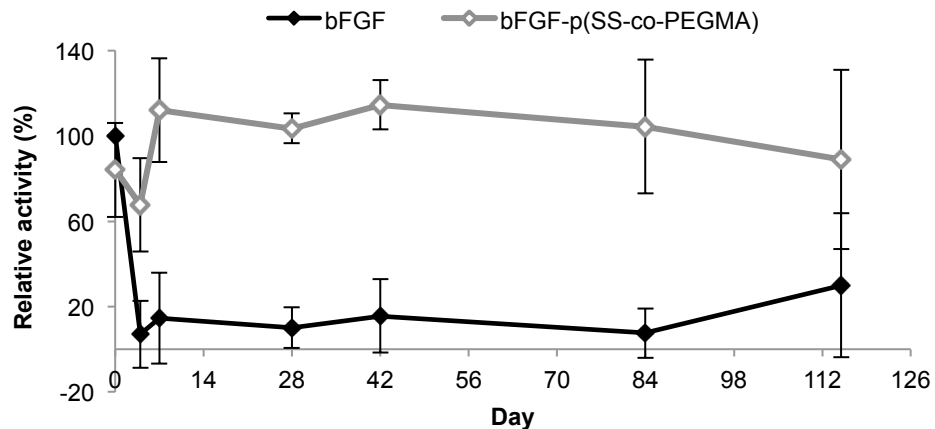
Figure 3.3. Long-term storage stability of bFGF-p(SS-*co*-PEGMA) compared to native bFGF tested on HDF cells. Preparation of the treated samples and untreated samples is detailed in the Methods section. The concentrations of bFGF and bFGF conjugate under storage were 0.05 ng/µL. The final concentrations of bFGF and bFGF conjugate in the medium were 1 ng/ml. Incubation of 2,000 cells/well in 96-well plate with each of the samples was carried out for 72 hours. CellTiter®-Blue assay was performed to quantify the extent of cell growth. Data showed the percent activity of each group relative to untreated bFGF, which was set at 100%. Each sample was done with six replicates. Error bars are STDEV.

The bFGF-heparin-mimicking polymer conjugates may be used in topical applications to treat dermal wounds; therefore, its stability in a liquid form needs to be addressed. Thus, we challenged the bFGF-heparin-mimicking polymer conjugate to long-term storage stability at 4 °C and 23 °C (typical room temperature). The solutions of bFGF and the conjugate were prepared using sterile D-PBS, split into multiple aliquotes and stored at 4 °C or 23 °C. Aliquots were taken at various times for either cell proliferation assay on HDF cells or for Western blot analysis. In the proliferation assays, our results indicated that bFGF-p(SS-*co*-PEGMA)

102

conjugate had superior storage stability compared to native bFGF up to at least 16 weeks at 4 °C (Figure 3.3). After 4 weeks (28 days), the activity of the stored conjugate was $103 \pm 7\%$ relative to untreated bFGF while the activity of stored bFGF was measured at $10 \pm 9\%$. Literature reported $5.4 \pm 1.6\%$ of activity remained when bFGF was stored at 4 °C for 4 weeks. After 6 weeks and 16 weeks, the activities of the conjugate were $114 \pm 12\%$ and $89 \pm 42\%$, respectively.
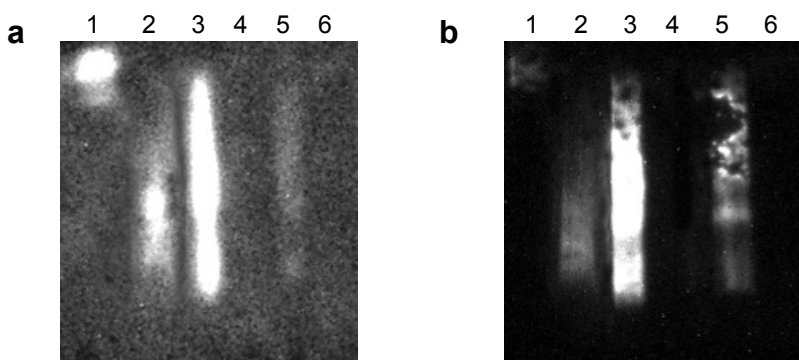
Figure 3.4. Western blot of Native PAGE of long-term storage samples for 19 weeks at 4 °C (a) and 23 °C (b): lane 1, untreated bFGF; lane 2, untreated bFGF (+) heparin; lane 3, untreated bFGF-p(SS-*co*-PEGMA); lane 4, bFGF in storage; lane 5, bFGF-p(SS-*co*-PEGMA) in storage; lane 6,bFGF (+) heparin in storage.

We investigated the immunochemical viability of bFGF and the conjugate after being stored at 4 °C and 23 °C for extended period of time via Western blot. In Figure 3.4, the first 3 lanes (a and b) showed the staining of untreated bFGF, bFGF with about 700 molar excess of heparin and the conjugate, respectively. bFGF in the presence of heparin and the conjugate ran lower than bFGF in the native PAGE due to the change in the overall surface charge of the

complexes in the presence of the highly negatively charged heparin and the polymer, respectively. Lane 4, 5 and 6 were the bFGF, the heparin-mimicking polymer conjugate and the bFGF with excess heparin, respectively after being stored for 19 weeks at 4 °C (Figure 3.4a) and 23 °C (Figure 3.4b). Only the conjugate in lane 5 for both gels was visible indicating that the conjugate was still immunochemically viable up to at least 19 weeks at 4 °C and 23 °C. This result is important because it also demonstrated that the conjugate remained intact for that time period, meaning that the disulfide bond had not cleaved.

3.3.3. Proliferation studies with BaF3-FR1C cells

As previously reported, p(SS-*co*-PEGMA) bound to bFGF, likely at the heparin-binding domain, which resulted in a stable hybrid with bFGF. The polymer was proven not capable of replacing the facilitating role of HS proteoglycan in FGFR dimerization when tested on BaF3-FR1C cell line – cells that express FGFR1 but lack HS.[6] Therefore, it was concluded that the observed bioactivity of the conjugate post-stress was that it retained native bioactivity; the conjugated heparin-mimicking polymer did not bind to the receptors to increase the native bioactivity of the protein overall.
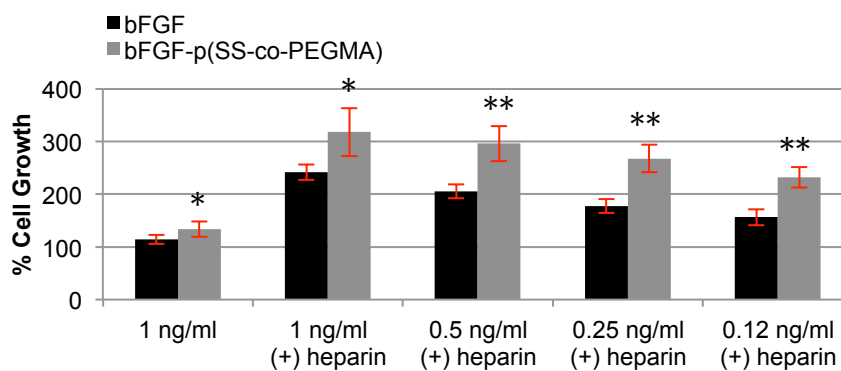
Figure 3.5. Bioactivity study of bFGF-p(SS-*co*-PEGMA) conjugate and native bFGF tested on BaF3-FR1C cells in the absence and presence of heparin. The concentration of heparin in the medium was 1 µg/mL. Incubation of 20,000 cells/well in 96-well plate with each of the samples was carried out for 48 hours. CellTiter®-Blue assay was used to quantify the extent of cell growth. Data was normalized to the blank medium group, which was set at 100%. Each sample was done with four replicates, and the whole experiment was repeated four times. Error bars represent SEM. Statistical analysis was done using Student's t-test. * $p < 0.5$, ** $p < 0.05$ for bFGF-p(SS-*co*-PEGMA) compared to bFGF at the same concentration.

The BaF3-FR1C cells responded slightly better to 1 ng/mL of bFGF-p(SS-*co*-PEGMA) conjugate (134 ± 14%) compared to 1 ng/mL of native bFGF (114 ± 9%) (Figure 3.5); this result is similar to our previous reports (see Chapter 2).[6] When 1 µg/mL of heparin was added to 1 ng/mL of bFGF-p(SS-*co*-PEGMA) conjugate (318 ± 45%), the cell proliferation surpassed that of when heparin was added to the same concentration of bFGF (242 ± 15%). The difference in proliferation was much more exaggerated when the concentrations of bFGF and the conjugate were lowered to 0.5, 0.25, and 0.12 ng/mL ($p < 0.05$ for all concentrations). The cell proliferation values at 0.25 ng/mL for the conjugate and bFGF were 268 ± 27% and 178 ± 13%,

respectively. To explain this phenomenon, we hypothesized that the conjugated heparin-mimicking polymer enhanced the binding of bFGF to its receptors in the presence of heparin resulting in faster cell proliferation cycles. When the same experiment was conducted on HDF cells, no difference in cell growth was observed (Figure 3.6). This phenomenon could be explained in two ways. First, it is likely because HDF cells express HS, which functions similarly to heparin but has closer proximity to the receptors than heparin; therefore, HS could better participate in receptor dimerization, no extra assistance from heparin was required. Second, HS is very heterogeneous in term of its chemical structure. The chemical structure of HS in HDF cells could possibly better fit to the heparin-binding site in the receptors; therefore, it outcompeted heparin in the receptor dimerization. However, this result led to the design of a next generation heparin-mimicking polymer that contained both bFGF and receptor-binding segments as described in Chapter 4.
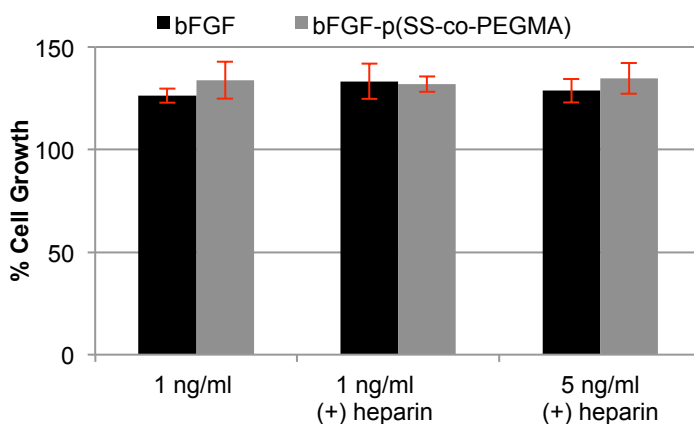

Figure 3.6. Bioactivity study of bFGF-p(SS-*co*-PEGMA) conjugate compared to native bFGF tested on HDF cells in the absence and presence of heparin. The concentration of bFGF and the conjugate was either 1 ng/mL or 5 ng/mL. The concentration of heparin in the medium was 1

µg/mL. Incubation of 2,000 cells/well in 96-well plate with each of the samples was carried out for 72 hours. CellTiter®-Blue assay was performed to quantify the extent of cell growth. Data was normalized to the blank medium group, which was set at 100%. Each sample was done with six replicates. Error bars represent standard deviations.

3.3.4. Wound healing study

In our current 21st century, wound care and wound treatment remain a tremendous hurdle to individuals and society worldwide. A study in 2010 showed that chronic wounds affected three to six million people in the USA alone.[23] It has been estimated that the annual wound care expenditures in the USA are $20 billion, which includes the cost of wound care products, treatment of complications such as infection, extended physician care, and lengthy hospital stays.[24] Wound care products aim to minimize infections and to heal wounds in a timely manner. Passive wound care products to control and treat infections following wounding such as wound cleansers, dressings, and films make up the majority of the wound care product market.[25,26] However, it is predicted that active wound care products aimed to accelerate wound healing, such as biological growth factors, is the fastest growing segment in the wound care product market.[27] This prediction is based on the realization of the power of growth factors such as bFGF in stimulating wound closing. It has previously shown that adding bFGF topically can increase rate of wound healing and the integrity of the healing wounds on mice.[28-32] bFGF is approved in Japan under the trade name Fiblast® for treatment of pressure ulcers and skin ulcers.[33] In this report, we demonstrated the potential of the bFGF-heparin-mimicking polymer conjugate as a wound healing promoter.
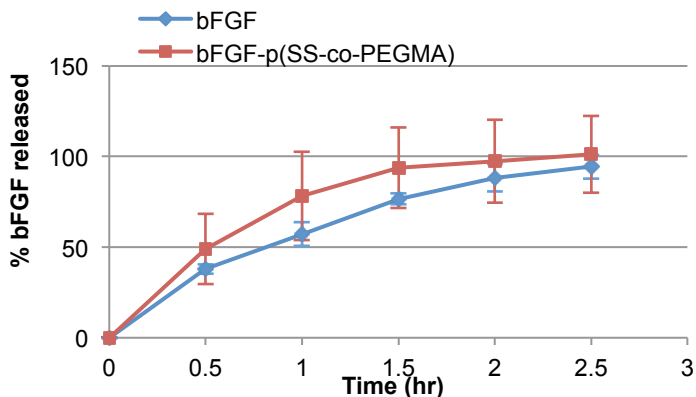
Figure 3.7. Release kinetic studies of bFGF and bFGF-p(SS-*co*-PEGMA) from Pluronic F127 22% gel. Preparation of the samples is detailed in the Methods section. The percent bFGF released was the cumulative released bFGF or the conjugate at the indicated time point relative to the known amount of bFGF or the conjugate loaded initially. Error bars represent STDEV.

First, we developed a vehicle to deliver bFGF and the conjugates to the wound site using Pluronic F127. Pluronic F127 is a hydrophilic polyol that can form thermo-responsive gel; it is in a liquid form at 4 °C and solidifies at temperature higher than 20 °C.[34] It has been used in topical applications for skin wound healing and shown to release captured growth factors with up to 70% within a day.[34,35] We tested various concentrations of Pluronic F127 gel: 19, 20, 22, 25 and 30% and determined that the 22% gel was the most optimal for capturing and releasing bFGF and the conjugate. Figure 3.7 shows that the protein and the conjugate have similar release profiles. Complete release of bFGF and the conjugate was achieved after 2.5 hours.

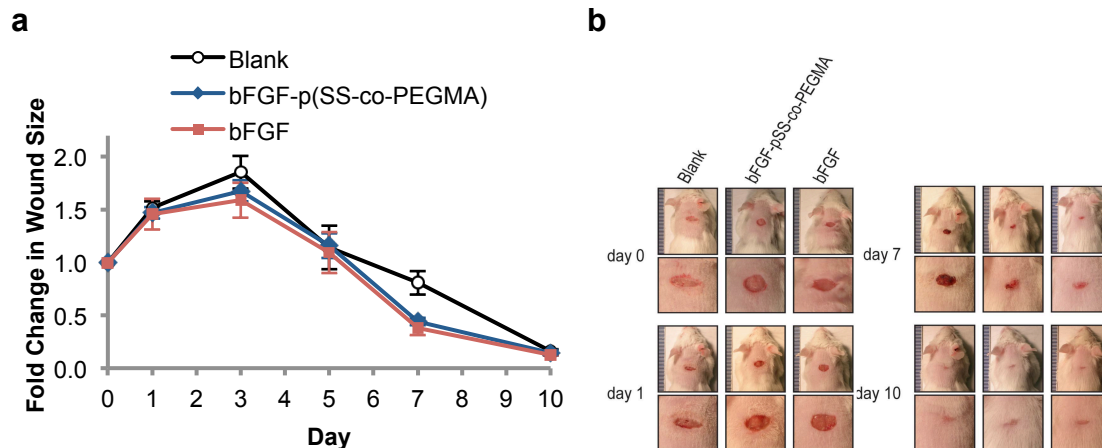**Figure 3.8.** Wound healing study. A 5-mm punch biopsy was performed on the back of db/db mice. 100 μL of Pluronic gel containing 0.5 μg of either bFGF, bFGF-p(SS-*co*-PEGMA) or D-PBS (Blank) was applied daily for 5 days continuously post wounding. Measurements of total lesion size were made by analyzing digital photographs of mice using the ImageJ software. a) Fold change in wound size was calculated by dividing the wound size measured on the specific day by the wound size measured on day 0. b) Representative lesions on the backs of mice. Shown are entire dorsal backs (top) and close-ups of lesions (bottom).

Three groups of four db/db mice, which have persistent non-healing wounds[36] were employed and prepared as detailed under the Methods section. A 5-mm punch biopsy was created on the dorsal skin of each mouse. Immediately after wounding, 100 μL of Pluronic gel containing 0.5 μg of either bFGF, bFGF-p(SS-*co*-PEGMA) or D-PBS (Blank) was applied; treatment was repeated for the next 4 consecutive days. Figure 3.8 shows the results of wound closing rate and representative photographs of the wounds taken at day 0, 1, 7 and 10. The difference in healing rate was observed at day 7; the bFGF and bFGF-p(SS-*co*-PEGMA) groups had faster wound healing rate than the Blank group ($p < 0.05$ for both). This result indicated that

the bFGF-heparin-mimicking polymer conjugate could promote wound healing as does pristine bFGF. This indicates that the polymer does not inhibit wound healing and the bFGF conjugate is able to act as bFGF alone, corroborating the *in vitro* results. We believed that a difference in wound size was only observed on day 7 because of the hard crust formed by the Pluronic gel after the first day of treatment. This, which covered the lesion, prevented the penetration of the growth factor in subsequent treatments and thus needed to be removed each day, altering the response. Thus, different delivery vehicles need to be developed in order to obtain reproducible and accurate *in vivo* data. This work is ongoing in the Maynard group.

3.4. Conclusions

In this report, we elucidated the cellular uptake and trafficking of the heparin-mimicking polymer conjugate, bFGF-p(SS-*co*-PEGMA). We showed that the intact conjugate was able to be internalized to cytoplasm in HDF cells via the receptor-mediated pathway, thus validating its biological function as a cell proliferation promoter. In parallel, we found that the conjugate was a superagonist compared to bFGF in the presence of exogenous heparin when tested on HS-deficient cells. We also showed that the conjugate was applicable for long-term storage both at 4 °C and 23 °C, an important consideration in developing useful protein therapeutics. Furthermore, we demonstrated the potential of the conjugate as an active wound healing promoter in mice. This is significant because active wound healing agents are really needed to heal chronic wounds caused by diabetes, HIV and other disease in order to heal patients and lower the cost of health care in general.

3.5. References

1) Leader, B.; Baca, Q. J.; Golan, D. E. *Nat. Rev. Drug Discov.* **2008**, *7*, 21.

2) Alconcel, S. N. S.; Baas, A. S.; Maynard, H. D. *Polym. Chem.* **2011**, *2*, 1442.

3) Caliceti, P.; Veronese, F. M. *Adv. Drug Deliv. Rev.* **2003**, *55*, 1261.

4) Fishburn, C. S. *J. Pharm. Sci.* **2008**, *97*, 4167.

5) Roberts, M. J.; Bentley, M. D.; Harris, J. M. *Adv. Drug Deliv. Rev.* **2002**, *54*, 459.

6) Nguyen, T. H.; Kim, S. H.; Decker, C. G.; Wong, D. Y.; Loo, J. A.; Maynard, H. D. *Nature Chem.* **2013**.

7) Barrientos, S.; Stojadinovic, O.; Golinko, M. S.; Brem, H.; Tomic-Canic, M. *Wound Repair Regen.* **2008**, *16*, 585.

8) Canalis, E.; Centrella, M.; McCarthy, T. *J. Clin. Invest.* **1988**, *81*, 1572.

9) Cross, M. J.; Claesson-Welsh, L. *Trends Pharmacol. Sci.* **2001**, *22*, 201.

10) Kawai, K.; Suzuki, S.; Tabata, Y.; Ikada, Y.; Nishimura, Y. *Biomaterials* **2000**, *21*, 489.

11) Levenstein, M. E.; Ludwig, T. E.; Xu, R. H.; Llanas, R. A.; VanDenHeuvel-Kramer, K.; Manning, D.; Thomson, J. A. *Stem Cells* **2006**, *24*, 568.

12) Edelman, E. R.; Mathiowitz, E.; Langer, R.; Klagsbrun, M. *Biomaterials* **1991**, *12*, 619.

13) Richard, J. L.; Bringer, J.; Parerrichard, C.; Rodier, M.; Daures, J. P.; Jacob, C.; Clouet, S.; Comtebardonnet, M.; Vannereau, D. *Diabetes Care* **1995**, *18*, 64.

14) Whalen, G. F.; Shing, Y.; Folkman, J. *Growth Factors* **1989**, *1*, 156.

15) Christman, K. L.; Vazquez-Dorbatt, V.; Schopf, E.; Kolodziej, C. M.; Li, R. C.; Broyer, R. M.; Chen, Y.; Maynard, H. D. *J. Am. Chem. Soc.* **2008**, *130*, 16585.

16) Gospodarowicz, D.; Cheng, J. *J. Cell Physiol.* **1986**, 475.

17) Hermanson, G. T. *Bioconjugate Techniques*; 1st ed.; Elsevier Science: San Diego, 1996.

18) Reilly, J. F.; Mizukoshi, E.; Maher, P. A. *DNA Cell Biol.* **2004**, *23*, 538.

19) Kolodziej, C. M.; Kim, S. H.; Broyer, R. M.; Saxer, S. S.; Decker, C. G.; Maynard, H. D. *J. Am. Chem. Soc.* **2012**, *134*, 247.

20) "Protein Stability and Storage." Pierce Biotechnology, Inc., 1 Sept. 2005. Web. 1 Aug. 2014. <http://sites.bio.indiana.edu/~chenlab/protocol_ files/protein_storage.pdf>.

21) Patro, S. Y.; Freund, E.; Chang, B. S. *Biotechnol. Annu. Rev.* **2002**, *8*, 55.

22) "Data Sheet Herceptin." Roche, 25 June 2014. Web. 1 Aug. 2014. <http://www.med-safe.govt.nz/profs/datasheet/h/Herceptininf.pdf>.

23) Guo, S.; Dipietro, L. A. *J. Dent. Res.* **2010**, *89*, 219.

24) Zaleski, Toby. ""Active" Products Drive Wound-Care Market." Genetic Engineering & Biotechnology News, 1 May 2008. Web. 1 Aug. 2014. <http://www.genengnews.com/gen-articles/active-products-drive-wound-care-market/2459/>.

25) Ovington, L. G. *Clin. Dermatol.* **2007**, *25*, 33.

26) Stojadinovic, A.; Carlson, J. W.; Schultz, G. S.; Davis, T. A.; Elster, E. A. *Gynecol. Oncol.* **2008**, *111*, S70.

27) "Wound Management: An $18.5 Billion Worldwide Market in 2021." MedMarket Diligence, LLC, 10 June 2013. Web. 1 Aug. 2014. <http://blog.mediligence.com/2013/06/10/wound-management-an-18-5-billion-worldwide-market-in-2021/>.

28) Sprugel, K. H.; McPherson, J. M.; Clowes, A. W.; Ross, R. *Am. J. Pathol.* **1987**, *129*, 601.

29) McGee, G. S.; Davidson, J. M.; Buckley, A.; Sommer, A.; Woodward, S. C.; Aquino, A. M.; Barbour, R.; Demetriou, A. A. *J. Surg. Res.* **1988**, *45*, 145.

30) Greenhalgh, D. G.; Sprugel, K. H.; Murray, M. J.; Ross, R. *Am. J. Pathol.* **1990**, *136*, 1235.

31) Tsuboi, R.; Rifkin, D. B. *J. Exp. Med.* **1990**, *172*, 245.

32) Okumura, M.; Okuda, T.; Nakamura, T.; Yajima, M. *Biol. Pharm. Bull.* **1996**, *19*, 530.

33) "Kaken's Innovation Product for Regeneration." Kaken Pharmaceutical Co., Ltd., 1 Dec. 2012. Web. 1 Aug. 2014. <http://www.kaken.co.jp/english/rd_pipeline.html>.

34) Schmolka, I. R. *J. Biomed. Mater. Res.* **1972**, *6*, 571.

35) Puolakkainen, P. A.; Twardzik, D. R.; Ranchalis, J. E.; Pankey, S. C.; Reed, M. J.; Gombotz, W. R. *J. Surg. Res.* **1995**, *58*, 321.

36) Park, S.; Rich, J.; Hanses, F.; Lee, J. C. *Infect. Immun.* **2009**, *77*, 1008.

Chapter 4

Heparin-Mimicking Polymer Conjugate

Increases Bioactivity of bFGF

4.1. Introduction

The study of polymers in pharmaceutical and biomedical sciences, generally referred to as biomaterial research, has matured over the years.[1] Biomaterials are traditionally explored as medical implant materials.[1] Although synthetic polymers that bear non-specific cell-biomaterial interactions such as in pacemakers, silicone and dental composite resins have saved lives and improved standard of living, there are limitations such as poor biocompatibility and host-tissue response.[2] For example, fibrous capsules can form around vascular grafts, pacemakers or breast implants leading to complications called capsular contracture, which is a form of the body's immune responses rejecting the foreign materials. Therefore, the focus of modern research has shifted towards designing biomaterials that possess specific cell-biomaterial interactions to achieve control over cellular behaviors such as cell proliferation, differentiation and adhesion.[3] Such biomaterials have defined chemical structures, functions or can form a system closely related to those that found in nature, so-called biomimetic polymers, that should perform better in their intended purposes.

Hermann Staudinger first proposed polymers to mimic naturally occurring compounds in the 1920s. Currently, research in biomimetic polymers for applications in tissue engineering[3,4] and drug delivery has gained much attention.[3,5] Polysaccharide-mimicking polymers make up a large area in biomimetic polymer research.[6] Polysaccharides were discovered in the late 1930s and were found to be abundant in every living organism.[6] In addition to their heterogeneous chemical structures, polysaccharides display a variety of biological functions ranging from energy storage or structural materials to inducing biological responses such as blood anticoagulation (heparin) or anti-inflammation (hyaluronic acid).[7,8] Specifically in biomimetic polymer research, heparin, a highly sulfated polysaccharide, has gained much interest (see

116

Chapter 1).   Originally, heparin-mimicking polymers such as carboxymethyl benzylamide sulfonate dextrans (CMDBS) were developed as antithrombotic alternatives to heparin.[9,10]   Over the years, heparin was recognized for its functions in diverse biological processes including: cell differentiation, angiogenesis, inflammation, host defense and viral infection mechanisms, lipid transport and clearance, and cell adhesion and interaction.[11]   Researchers have developed heparin-mimicking polymers such as CMDBS,[12] poly(4-hydroxyphenoxyacetic acid),[13,14] sulfated glycopolymers,[15,16] and polysulfonated polymers[17-20] to harvest other heparin-like properties.

We first reported the synthesis of a heparin-mimicking polysulfonated polymer named poly(sodium 4-styrenesulfonate-co-poly(ethylene glycol) methyl ether methacrylate) (p(SS-*co*-PEGMA)) via reversible addition-fragmentation chain transfer (RAFT) polymerization.[17]   The polymer was shown to bind basic fibroblast growth factor (bFGF) at the heparin-binding domain.[17,21]   Heparin is a natural stabilizer for many heparin-binding proteins including bFGF, an extremely unstable therapeutic protein.[22]   Recently, we reported the synthesis of a covalent conjugate of bFGF and the heparin-mimicking polymer (bFGF-p(SS-*co*-PEGMA)) and showed that the hybrid can withstand a variety of environmentally and therapeutically relevant stressors including: heat, mild and harsh acidic conditions, long-term storage and proteolytic degradation, unlike the native protein (see Chapter 2).[20]   The conjugate was also shown to have potential in healing skin wounds through studies on a diabetic mouse wound healing model (see Chapter 3).

Herein, we report the designs and syntheses of a 2nd-generation and 3rd-generation heparin-mimicking polymers that mimic the biological role of heparin in facilitating fibroblast growth factor receptor (FGFR) dimerization.   Heparan sulfate (HS) proteoglycan, a form of heparin, is known as a low affinity receptor to bFGF.[23]   Upon binding of two bFGF molecules to

heparin and to two of its high affinity FGFRs, dimerization and subsequently phosphorylation of the receptors occur.[24,25] This event cascades the cellular signals leading to cellular responses. Covalent conjugates between bFGF and the newly developed heparin-mimicking polymers were prepared. The proliferation and migration effects of the conjugates on HDF and HUVEC were studied. We report here that the 3rd-generation heparin-mimicking polymer-bFGF conjugate showed increase proliferation and migration effects when tested on HUVECs compared to the native protein. To our best knowledge, a protein-polymer conjugate that is more bioactive than its native protein has never been reported. This novel conjugate could be employed to accelerate angiogenesis, an important process in tissue engineering.

4.2. Experimental

4.2.1. Materials

Chemicals and reagents were purchased from Fisher or Sigma-Aldrich unless indicated otherwise. Poly(sodisum sulfonate styrene) (pSS) polymers and poly(2-acrylamido-2-methylpropane sulfonic acid) (pAMPS) 70 kDa were purchased from Polymer Laboratories and Monomer-Polymer & Dajac Labs (Trevose, PA), respectively. The plasmid pET29c(+)hFGF-2 was obtained from Prof. Thomas Scheper (Leibniz University of Hannover, Germany), and the expression and purification procedures of bFGF were performed as described.[26] ToxinSensorTM Chromogenic LAL Endotoxin assay kit was purchased from Genscript (Piscataway, NJ). Recombinant human FGFR1α(IIIc) Fc chimera, and ELISA Development DuoSet[®] kits were purchased from R&D Systems. Heparin was purchased from PromoCell. Rabbit anti-fibroblast growth factor basic antibody and goat anti-rabbit IgG-HRP conjugate for Western blot were purchased from CALBIOCHEM and Bio-Rad, respectively. Normal HDF and HUVEC cells were purchased from Lonza. BaF3-FR1C cells expressing FGFR1 were provided by Prof. David Ornitz (Washington University, Saint Louis).[27] Chinese Hamster Ovary (CHO) cells were a gift from Prof. Sherie Morrison (UCLA). Media and supplements for cell culture were either purchased from Lonza or Invitrogen. CellTiter-Blue[®] cell viability assay were obtained from Promega. HiTrap[TM] Heparin HP 1 ml was purchased from GE Healthcare. Poly(methyl methacrylate) standards for GPC calibration were purchased from Polymer Laboratories. Merck 60 (230-400 mesh) silica gel was used for column chromatography. THF and DCM were distilled over CaH_2 prior to use. Prior to polymerizations, 4-styrene sulfonic acid, sodium salt hydrate monomer and vinyl sulfonic acid, sodium salt was pre-treated with Na^+-activated DOWEX 50WX8 200-400 mesh resin then dried to produce the sodium salt. AIBN was

recrystallized twice from ethanol and dried prior to use. V501 initiator was dried prior to use. p(SS-*co*-PEGMA-*co*-RhoB) used in cellular uptake studies was synthesized as described in Chapter 3. 2-(Pyridin-2-yldisulfanyl)ethanol[28] were synthesized as previously described.

4.2.2. Analytical Techniques

^{1}H NMR and ^{13}C NMR spectroscopy were performed on an Avance DRX 400 or 500 MHz spectroscopy instruments. UV-Vis spectrophotometry analyses were performed on a Biomate 5 Thermo Spectronic spectrometer. GPC was conducted on a Shimadzu HPLC system equipped with a refractive index detector RID-10A, one Polymer Laboratories PLgel guard column, and two Polymer Laboratories PLgel 5 μm mixed D columns. DMF containing 0.10 M LiBr at 40 °C was used as the eluent and near-monodisperse poly(methyl methacrylate) standards were used for calibration at 0.6 ml/min. Chromatograms were processed using the EZStart 7.2 chromatography software. Gel electrophoresis was performed using Any kD™ Mini-PROTEAN® TGX™ precast gels with Tris-glycine as running buffer (Bio-rad, Hercules). ELISA assay results were read on the ELX800 Universal Microplate Reader (Bio-Tek Instrument Inc., Winooski) with $\lambda = 450$ nm and 630 nm for signal and background, respectively. Western blot was developed on a FluorChem® FC2 System version 3.2 (Cell Biosciences, Santa Clara). Fluorescent signals from CellTiter-Blue® assay were read using a SpectraMax M5 microplate reader (Molecular Devices, Sunnyvale). Fluorescent images for cell uptake studies were taken at UCLA CNSI Advanced Light Microscopy/Spectroscopy (ALMS) Imaging Facilities. Fluorescent images of the cells from LIVE/DEAD® viability/cytotoxicity assays and images of cells migration studies were acquired on an Axiovert 200 microscope equipped with an AxioCam MRm camera and FluoArc mercury lamp (Carl Zeiss, Thornwood). NIH ImageJ software was used to assist cell counting and to measure distances of cell-free paths.

4.2.3. Methods

Synthesis of poly(potassium 3-sulfopropyl methacrylate) (pSPM), poly(sodium 1-allyloxy-2 hydroxypropyl sulfonate) (pAHPS) and poly(sodium vinyl sulfonate) (pVS) polymers for screening studies. Free radical polymerization in water was employed to synthesize all of the polymers for screening studies; V501 was used as the initiator. Three pSPM polymers were prepared by varying the ratio of [SPM]:[V501] = 4/20/200:1 at 80 °C. Two pAHPS polymers were prepared by varying the ratio of [AHPS]:[V501] = 10/20:1 at 60 °C. pVS was synthesized with a ratio of [VS]:[V501] = 40:1 at 60 °C. Prior to screening studies, all of the polymers were purified extensively by dialysis against MilliQ-water using MWCO 2,000 tubing and dried.

Synthesis of 2-((ethoxycarbonothioyl)thio)propanoic acid, **CTA1**. In a three-neck round-bottom flask, 40 mL of dry THF under argon was pre-cooled to 0 °C in an ice-bath. Sodium hydride 60% in oil (1.76 g, 73.3 mmol) was added into the flask. Dry ethanol (2.6 mL, 44.4 mmol) was added drop-wise into the reaction flask for 10 minutes following by carbon disulfide (3 mL, 49.9 mmol). The reaction was allowed to stir for 20 minutes. Subsequently, 2-bromopropionic acid (1.0 mL, 11.1 mmol) was added into the reaction flask. The reaction solution was stirred for 48 hours and allowed to warm to 23 °C. The reaction was quenched with methanol, then water. THF was removed via rotavap; the reaction crude was washed twice with DCM. The aqueous layer was acidified and extracted three times with DCM. The collected organic layer was dried over anhydrous magnesium sulfate and rotavaped to remove solvent. The crude product was purified by silica column chromatography (9:1 v/v hexane: acetic acid), and lyophilized to give a slightly yellow solid (1.86 g, 86% yield). δ ^{1}H NMR (400 MHz, CDCl$_3$): 11.58 (1H, s, COO**H**), 4.67-4.61 (2H, qd, J = 7.18, 2.00 Hz, OC**H$_2$**CH$_3$), 4.44-4.38 (1H, q, J = 7.43 Hz, C**H**CH$_3$), 1.61-1.59 (3H, d, J = 7.44 Hz, CHC**H$_3$**), 1.43-1.39 (3H, t, J = 1.11 Hz,

OCH$_2$**CH$_3$**). δ ^{13}C NMR (400 MHz, CDCl$_3$): 211.67, 178.10, 70.64, 46.91, 16.60, 13.72. FT- IR (cm^{-1}): 2980, 2933, 2628, 2486, 1698, 1628, 1457, 1450, 1435, 1408, 1363, 1301, 1258, 1237, 1153, 1113, 1078, 1059, 1040, 1002, 984, 855, 805, 716, 696.

*Synthesis of 2-(((neopentyloxy)carbonothioyl)thio)acetic acid, **CTA2**.* In a three-neck round-bottom flask, 35 mL of dry THF under argon was pre-cooled to 0 °C in an ice-bath. Sodium hydride 60% in oil (1.14 g, 47.5 mmol) was added into the flask. Dry ethanol (2.6 mL, 44.4 mmol) was added drop-wise into the reaction flask for 10 minutes following by carbon disulfide (1.95 mL, 32.4 mmol). The reaction was allowed to stir for 20 minutes. Subsequently, 2-bromoacetic acid (2.54 g, 28.8 mmol) was added into the reaction flask. The reaction solution was stirred for 5 hours and allowed to warm to 23 °C. The reaction was quenched with methanol, then water. THF was removed via rotavap; the reaction crude was washed twice with DCM. The aqueous layer was acidified and extracted three times with DCM. The collected organic layer was dried over anhydrous magnesium sulfate and rotavaped to remove solvent. The crude product was purified by recrystallization in warm water; the obtained crystals were washed with 20 mL of pre-chilled water, and lyophilized (1.2 g, 70% yield). δ ^{1}H NMR (400 MHz, CDCl$_3$): 9.95 (1H, s, COO**H**), 4.26 (2H, s, OC**H$_2$**C), 3.97 (2H, s, **CH$_2$**S), 1.01 (9H, s, C(**CH$_3$)$_3$**). δ ^{13}C NMR (400 MHz, CDCl$_3$): 212.11, 174.24, 84.22, 37.44, 31.84, 26.50. FT- IR (cm^{-1}): 2955, 2868, 2701, 2594, 1717, 1467, 1419, 1398, 1357, 1303, 1273, 1228, 1173, 1066, 1028, 955, 933, 913, 880, 793, 665.

Synthesis of 2-(pyridin-2-yldisulfanyl)ethyl 2-(((neopentyloxy)carbonothioyl)thio)acetate, ***CTA3***. In a three-neck round-bottom flask, 2-(pyridin-2-yldisulfanyl)ethan-1-ol (0.31 g, 1.65 mmol) and **CTA2** (0.24 g, 1.1 mmol) were dissolved with 15 mL of dry DCM under argon. The reaction flask allowed to cool to 0 °C in an ice-bath. Then, EDC (0.21 g, 1.32 mmol) and

DMAP (27 mg, 0.22 mmol) were added at once to the reaction flask. The aqueous layers were combined and dried over anhydrous magnesium sulfate. The reaction solution was stirred for 5 hours and allowed to warm to 23 °C. The reaction solution was washed with two times with $NaHCO_3$ and two times with water. After removal of solvent, the crude product was purified by silica column chromatography (2:1 v/v hexane: ethyl acetate, Rf = 0.4), and lyophilized to give a slightly yellow oil (272 mg, 61% yield). δ ^{1}H NMR (400 MHz, $CDCl_3$): 8.44-8.43 (1H, dq, J = 4.88, 0.87 Hz, C**H**N), 7.67-7.59 (2H, m, C**H**C**H**CN), 7.09-7.05 (1H, ddd, J = 6.64, 4.92, 1.6 Hz, C**H**CHN), 4.40-4.37 (2H, t, J = 6.44 Hz, OC**H₂**), 4.22 (2H, s, OC**H₂**C), 3.89 (2H, s, COC**H₂**S), 3.05-3.01 (2H, t, J = 6.43 Hz, C**H₂**O), 0.97 (9H, s, C(C**H₃**)₃). δ ^{13}C NMR (400 MHz, $CDCl_3$): 212.51, 167.62, 159.59, 149.75, 137.15, 120.97, 119.93, 84.04, 63.55, 37.57, 37.12, 31.85, 26.55. FT- IR (cm^{-1}): 2959, 2871, 1739, 1572, 1446, 1416, 1365, 1273, 1225, 1147, 1116, 1059, 1029, 986, 950, 931, 906, 880, 759, 716, 616, 555, 529, 508, 486, 479, 462.

Synthesis of 2-((ethoxycarbonothioyl)thio)-2-methylpropanoic acid, CTA4. In a three-neck round-bottom flask, 40 mL of acetone and 40 mL of water under argon was pre-cooled to 0 °C in an ice-bath. Sodium hydroxide (2.5 g, 63 mmol) was added into the flask. Dry ethanol (3.15 mL, 54.0 mmol) was added drop-wise into the reaction flask for 10 minutes following by carbon disulfide (3.80 mL, 63.0 mmol). The reaction was allowed to stir for 20 minutes. Subsequently, 2-bromo-2-methylpropanoic acid (3.0 g, 18.0 mmol) was added into the reaction flask. The reaction solution was stirred for 48 hours and allowed to warm to 23 °C. The workup and purification of the product was similar to those of **CTA2** (0.9 g, 23% yield). δ ^{1}H NMR (400 MHz, $CDCl_3$): 4.64-4.59 (2H, q, J = 7.15 Hz, OC**H₂**CH₃), 1.66 (6H, s, C(C**H₃**)₂), 1.41-1.37 (3H, t, J = 7.12 Hz, CHC**H₃**). δ ^{13}C NMR (400 MHz, $CDCl_3$): 210.32, 179.43, 70.01, 53.86,

25.51, 13.32. FT- IR (cm^{-1}): 2986, 2867, 2653, 2553, 1704, 1466, 1416, 1362, 1284, 1249, 1175, 1108, 1037, 999, 922, 850, 806, 691, 631, 610, 590, 561, 538, 519, 509, 485, 471, 458.

*Synthesis of 2-(pyridin-2-yldisulfanyl)ethyl 2-((ethoxycarbonothioyl)thio)-2-methyl propanoate, **CTA5***. In a three-neck round-bottom flask, 2-(pyridin-2-yldisulfanyl)ethan-1-ol (0.35 g, 1.87 mmol) and **CTA4** (0.26 g, 1.25 mmol) were dissolved with 10 mL of dry DCM under argon. The reaction flask allowed to cool to 0 °C in an ice-bath. Then, EDC (0.23 g, 1.5 mmol) and DMAP (31 mg, 0.25 mmol) were added at once to the reaction flask. The reaction solution was stirred for 5 hours and allowed to warm to 23 °C. The reaction solution was washed with two times with NaHCO$_3$ and two times with water. The aqueous layers were combined and dried over anhydrous magnesium sulfate. After removal of solvent, the crude product was purified by silica column chromatography (2:1 v/v hexane: ethyl acetate, Rf = 0.5), and lyophilized to give a yellow oil (182 mg, 39% yield). δ ^{1}H NMR (400 MHz, CDCl$_3$): 8.43-8.43 (1H, dq, J = 4.85, 0.92 Hz, C**H**N), 7.68-7.60 (2H, m, C**H**C**H**CN), 7.08-7.05 (1H, ddd, J = 6.61, 4.82, 1.32 Hz, C**H**CHN), 4.56-4.51 (2H, q, J = 7.15 Hz, OC**H₂**CH$_3$), 4.36-4.33 (2H, t, J = 6.42 Hz, OC**H₂**CH$_2$), 3.02-2.99 (2H, t, J = 6.40 Hz, C**H₂**S), 1.58 (6H, s, C(C**H₃**)₂), 1.34-1.30 (3H, t, J = 7.08 Hz, OCH$_2$C**H₃**). δ ^{13}C NMR (400 MHz, CDCl$_3$): 210.80, 172.82, 159.53, 149.74, 137.15, 120.94, 119.88, 69.84, 63.18, 54.08, 37.11, 25.74, 13.42. FT- IR (cm^{-1}): 2960, 2870, 1736, 1572, 1447, 1416, 1366, 1274, 1224, 1154, 1116, 1056, 1029, 986, 950, 931, 905, 806, 759, 731, 716, 616, 579, 565, 529, 508, 497, 492, 487, 471, 457.

Synthesis of pVS polymers for size-dependent studies. Reversible addition- fragmentation chain transfer (RAFT) polymerization was employed to polymerize VS monomer. The polymerizations were performed with the initial feed ratio of [VS]:[**CTA1**]:[V501] = 40/80/160/320/500:2:1 using standard Schlenk techniques. The concentration of the monomer

was 1.4 – 2.0 M. For a typical polymerization of the system [VS]:[**CTA1**]:[V501] = 40:2:1, the **CTA1** (27.7 mg, 0.14 mmol), VS monomer (372 mg, 2.86 mmol), and V501 (20 mg, 0.07 mmol) were dissolved in 1 mL of Milli-Q water and 1 mL of DMF in a Schlenk tube. The system was sealed and subjected to four freeze-pump-thaw cycles before immersion in a 70 °C oil bath. Aliquots were removed at predetermined time points and diluted in D_2O for ^1H NMR. The progress of the polymerization was monitored from the ^1H NMR spectra using the integral value of the vinylic proton of VS monomer at 6.6 ppm and the integral value of the growing polymer protons (3.8-3.4 ppm, part of C**H**SO_3Na polymer backbone). The polymerization was stopped after 3.5 hours. The polymer was purified by dialysis with Milli-Q water (MWCO 1000) and lyophilized to remove solvent. δ ^1H NMR 500 MHz (D_2O): 4.2-2.9 (CH_2C**H**SO_3Na polymer backbone), 2.9-1.4 (C**H_2**CHSO$_3$Na polymer backbone), 1.45 (1H, OC**H_2**C**H_3**), 1.45-1.20 (3H, CHC**H_3**). IR (cm^{-1}): 3435, 2942, 1642, 1544, 1525, 1499, 1453, 1156, 1031, 711, 613, 572, 540, 515, 496, 485. The M_n = 6.6 kDa by NMR. The NMR spectrum of each polymer was calibrated to the peak at 1.45-1.20 ppm, and the M_n of the polymers were calculated using the formula:

$$Mn = \Sigma \text{ polymer backbone integrals}/3 \times MW \text{ monomer} + MW \text{ CTA}.$$ Five pVS polymers were synthesized with M_n = 6.6, 14.4, 24.6, 35.9, and 80.3 kDa.

Synthesis of PDS-pVS. The RAFT polymerizations were performed with the initial feed ratio of [VS]:[**CTA3**]:[V501] = 100/300:1:0.5 using standard Schlenk techniques. The concentration of the monomer was 2.2 – 2.5 M. For a typical polymerization of the system [VS]:[**CTA3**]:[V501] = 100:1:0.5, the **CTA3** (50.0 mg, 0.13 mmol), VS monomer (1.66 g, 12.77 mmol), and V501 (18.0 mg, 0.064 mmol) were dissolved in 2.5 mL of Milli-Q water and 2.5 mL of DMF in a Schlenk tube. The system was sealed and subjected to four freeze-pump-thaw cycles before immersion in a 70 °C oil bath. The polymerization was stopped after 17 hours.

The polymer was purified by dialysis first with 1:1 v/v acetonitrile:Milli-Q water followed by dialysis with 100% Milli-Q water (MWCO 1000), and lyophilized to remove solvent. δ ^{1}H NMR 500 MHz (D$_2$O): 8.82-8.81 (1H, d, J = 5.67 Hz, C**H**N), 8.50-8.46 (1H, td, J = 8.04, 1.67, C**H**CHCN), 8.36-8.34 (1H, d, J = 8.36, CHC**H**CN), 7.90-7.88 (1H, ddd, J = 7.06, 5.71, 0.95, C**H**CHN), 4.52 (2H, s, OC**H$_2$**C), 4.19 (2H, s, COC**H$_2$**), 4.2-2.9 (C**H$_2$**C**H**SO$_3$Na polymer backbone), 3.41-3.39 (2H, t, J = 5.83, SC**H$_2$**), 2.9-1.4 (C**H$_2$**C**H**SO$_3$Na polymer backbone), 1.20 (9H, s, C(C**H$_3$**)**$_3$**) . IR (cm^{-1}): 3419, 2957, 2878, 1725, 1642, 1448, 1366, 1148, 1027, 710, 610, 508. The M$_n$ = 10.2 kDa by NMR. The NMR spectrum of each polymer was calibrated to the peak at 8.82-8.81 ppm, and the M$_n$ of the polymers were calculated using the formula:

$$\text{Mn} = \frac{(Polymer\ backbone\ integrals\ at\ 4.2-2.9\ ppm) - 4}{1} \times \text{MW monomer} + \text{MW CTA}.$$ Three PDS-pVS

polymers were synthesized with M$_n$ = 7.6, 10.2, and 16.3 kDa.

Synthesis of p(VS-co-RhoB). RAFT polymerization was employed to copolymerize VS monomer and methacryloxyethyl thiocarbamoyl rhodamine B (RhoB) monomer. The polymerization was started with an initial feed ratio of [VS]: [RhoB]:[**CTA3**]:[V501] = 200:0.1:1:0.5 using standard Schlenk techniques. The **CTA3** (15 mg, 0.04 mmol), VS (996 mg, 7.67 mmol), and V501 (5.0 mg, 0.02 mmol) were dissolved in 1.5 mL of Milli-Q water and 1.5 mL of DMF in a Schlenk tube. The system was sealed and subjected to four freeze-pump-thaw cycles before immersion in a 60 °C oil bath. The polymerization was allowed to progress for 2.5 hours. In another 5-mL 2-neck round-bottom flask, three molar equivalents of RhoB monomer (7.8 mg, 0.012 mmol) were dissolved in 600 μL of degassed DMF and subjected to three freeze-pump-thaw cycles. Subsequently, 200 μL of the RhoB monomer solution was quickly transferred via air-tight syringe to the polymerization flask. The polymerization continued for another hour in the dark before stopping by exposing to air. The polymer was purified via

dialysis first with 1:1 v/v Milli-Q water:methanol followed by dialysis with Milli-Q water (MWCO 1000) and lyophilized to remove solvent. The polymer appeared to be bright red after drying.

Synthesis of p(SS-co-PEGMA)-xanthate. The RAFT polymerizations were performed with the initial feed ratio of [SS]:[PEGMA]:[**CTA5**]:[AIBN] = 35:10:1:0.2 using standard Schlenk techniques. SS monomer (382 mg, 1.84 mmol) and PEGMA monomer (159 mg, 0.53 mmol) were dissolved in 1.2 mL of Milli-Q water and 1.0 mL of DMF in a Schlenk tube. The **CTA5** (20.0 mg, 0.05 mmol) and AIBN (1.74 mg, 0.01 mmol) were dissolved with 0.2 mL of DMF in a small vial and transferred to the Schlenk tube. The system was sealed and subjected to four freeze-pump-thaw cycles before immersion in a 60 °C oil bath. The polymerization was stopped after 4 hours. The polymer was purified by dialysis first with 1:1 v/v Milli-Q water:methanol (MWCO 1000) and lyophilized to remove solvent. δ ^{1}H NMR 500 MHz (D$_2$O): 8.40 (1H, s, C**H**N), 8.2-6.2 (NaSO$_3$C$_6$**H$_4$** side chains), 4.2-2.8 (PEGMA side chains), 2.8-0.0 (polymer backbone). IR (cm^{-1}): 3420, 2926, 1702, 1660, 1453, 1411, 1176, 1124, 1036, 1008, 948, 834, 774, 674, 612, 574, 499, 487. The M$_n$ = 33.0 kDa by NMR, 25.6 kDa by GPC, PDI = 1.56 by GPC. The NMR spectrum of the resulted polymer was calibrated to the peak at 8.40 ppm, and the M$_n$ of the polymers were calculated using the formula:

$$\text{Mn} = \left[\frac{(\text{integral value at 8.2}-6.2 \text{ ppm})}{4} \times MW\ SS\ monomer \right] + \left[\frac{(\text{integral value at 4.2}-2.8 \text{ ppm})}{20.4} \times \right.$$

$$\left. MW\ PEGMA\ monomer \right] + \text{MW CTA}.$$

Synthesis of p(SS-co-PEGMA-b-VS). The RAFT polymerizations were performed with the initial feed ratio of [VS]:[**p(SS-*co*-PEGMA)-xanthate**]:[V501] = 333:1:0.7 using standard Schlenk techniques. The **p(SS-*co*-PEGMA)-xanthate** (50.0 mg, 0.0015 mmol), VS monomer

(65 mg, 0.5 mmol), and V501 (0.4 mg, 0.001 mmol) were dissolved in 0.5 mL of Milli-Q water in a Schlenk tube. The system was sealed and subjected to three freeze-pump-thaw cycles before immersion in a 70 °C oil bath. The polymer was purified by washing for 20 cycles using a CentriPrep centrifugal membrane MWCO 10,000 with MilliQ-water at 12,000 relative centrifugal force (rcf) for 10 min/cycle and lyophilized to remove solvent. δ ^{1}H NMR 500 MHz (D_2O): 8.40 (1H, s, C**H**N), 8.2-6.2 (SS side chains), 4.2-2.8 (PEGMA side chains and $CH_2C\textbf{H}SO_3Na$ polymer backbone), 2.8-0.0 (SS and PEGMA polymer backbone and $C\textbf{H}_2CHSO_3Na$ polymer backbone). IR (cm^{-1}): 3420, 2941, 1702, 1656, 1452, 1411, 1351, 1168, 1124, 1032, 1007, 835, 674, 612, 587, 573, 514, 495, 482. The M_n = 57.2 kDa by NMR, 31.6 kDa by GPC, PDI = 1.46 by GPC.

Synthesis of bFGF-pVS and bFGF-p(SS-co-PEGMA-b-VS) conjugates. The syntheses of the bFGF conjugates were similar to the procedure described in Chapter 2; except for 100 μg of bFGF (5.9 X 10^{-3} μmol) was used at a time, and 100 molar equivalents of PDS-pVS or PDS-p(SS-*co*-PEGMA-*b*-VS) was employed for each conjugation. To purify the conjugates, the 2 M NaCl fractions were washed for 10 cycles using a CentriPrep centrifugal membrane MWCO 30,000 with D-PBS at 12,000 rcf for 8 min/cycle. The collected conjugate was then characterized by western blot and quantified by ELISA. (The procedure for western blot and ELISA were described in Chapter 2).

ELISA-based FGFR binding assay. A 96-well-plate was incubated with 100 μL of 0.5 μg/mL of rhFGFR1α(IIIc) prepared in D-PBS for 16 hours at 23 °C, then blocked with 1% BSA solution for 2 hours. A solution of 1 ng/mL of bFGF with or without 1 μg/mL of heparin or the polymers was added to the wells and incubated for 2 hours. Subsequently, bFGF antibody-biotin conjugate solution was probed for 2 hours before streptavidin-horseradish peroxidase solution

was added for 20 minutes. The colorimetric signals were developed by incubating the wells with 1-Step Ultra TMB solution (Pierce Biotechnology, Rockford) for 6 minutes. The assay was stopped by addition of 50 μL of 1 M H_2SO_4 in to each well. The absorbance signals was recorded at $\lambda = 450$ nm, and the background at $\lambda = 630$ nm was subtracted. Each group was done with three replicates, and the experiment was repeated three times.

Cell cultures. HDF primary cells were cultured in Lonza FGM-2 medium containing 2% fetal calf serum (FCS), bFGF, insulin, 30 μg/ml Gentamicin and 15 ng/ml Amphotericin at 37 °C, 5% CO_2. HDF cells were passaged every four days or after reaching 80% confluency. HDF cells were used up to passage 12. BaF3-FR1C cells were kindly provided by Dr. David Ornitz and cultured as recommended. Specifically, the cells were grown in RPMI1640 medium containing 10% newborn bovine calf serum, 2 mM L-glutamine, 0.5 ng/ml of recombinant mouse IL-3, 600 μg/ml of G418, 50 nM of 2-mercaptoethanol, supplemented with 100 unit/ml penicillin and 100 μg/ml streptomycin at 37 °C, 5% CO_2. The medium was changed every two days. HUVEC cells were cultured in Lonza EGM-2 medium containing 5% FCS, recombinant human endothelial growth factor (rhEGF), bovine brain extract (BBE), 30 μg/ml Gentamicin and 15 ng/ml Amphotericin at 37 °C, 5% CO_2. HUVEC cells were passaged every three days or after reaching 80% confluency. CHO cells cultured in ATCC F-12K medium containing 10% FCS. CHO cells were passaged every three days.

Cytotoxicity study on HDF cells. LIVE/DEAD® viability/cytotoxicity assay kit was employed. The procedure was followed as described in Chapter 2, except the cells were treated with various concentrations of pVS 80.3 kDa ranging from 1 mg/mL to 1 ng/mL in FGM-2 medium (-) bFGF. Each sample group had four repeats, and the whole experiment was repeated three times.

Cellular uptake study. CHO cells were seeded on cover glasses in 6-well plates at a density of 5 x 10^5/well. The cells were incubated over 12 hours to allow attachment. Then the cells were incubated for 4 hours with various formulations, including p(SS-*co*-PEGMA-*co*-RhoB) or p(VS-*co*-RhoB) (25 µg/ml) with or without bFGF (0.1 µg/ml). After incubation, the cells were washed with cold PBS, fixed with 4% paraformaldehyde and mounted in a medium containing DAPI (Vector Lab). Images were captured using an Leica TCS SP2 spectral confocal microscope under three channels: DAPI for nuclei, and Rhodamine B for p(SS-*co*-PEGMA-*co*-RhoB) and p(VS-*co*-RhoB).

Proliferation assays. HDF cells were trypsinized and resuspended in UltraCULTURE^{TM} serum-free medium supplemented with 2 mM L-Glutamine, 100 unit/ml penicillin and 100 µg/ml streptomycin. HUVEC cells were trypsinized and resuspended in EGM-2 medium (-) BBE. The cells were plated at a concentration of 2,000 HDF cells/well or 1,000 HUVEC cells/well in a 96-well plate and allowed to adhere for 16 hours at 37 °C, 5% CO$_2$. At the end of the 16-hour incubation, 100 µL of working medium containing bFGF or the tested compounds were replaced in each well. After an incubation of 72 hours at 37 °C, 5% CO$_2$, CellTiter-Blue® assay was carried out to evaluate cell proliferation. All experimental groups were normalized to the control group, which received only blank medium. Each group was done with six replicates.

BaF3-FR1C cells were collected and washed two times with cultured medium lacking IL-3. The cells were plated at the density of 20,000 cells/well/50 µL in a 96-well plate in the working medium. The samples were prepared in the working medium to contain the tested compounds at double the final concentrations. Subsequently, 50 µL of each sample was added into each corresponding well. After incubation for 42 hours at 37 °C, 5% CO$_2$, CellTiter-Blue® assay was carried out to evaluate the extent of cell growth. All of the groups were normalized to

130

the control group, which had only medium. Each group was performed with four replicates.

Migration assays. HUVECs were grown until reaching 90-95% confluency in 24-well-plates. The cell monolayers were washed once with PBS, then starved for 24 hours with EGM-2 medium (-) BBE (-) rhEGF at 37 °C, 5% CO_2. At the end of the starving period, the medium was replaced with PBS; a scratch in the center of each well was made using a standard P1000 pipette tip. A marker line perpendicular to the scratch was drawn on the bottom of the other side of each well. PBS was aspirated and the wells were washed once more time with PBS to remove cell debris. The cell monolayers were allowed to incubate with blank medium or samples containing either 10 ng/mL of bFGF or 10 ng/mL of bFGF-p(SS-*co*-PEGMA-*b*-VS) (400 µL) in the starving medium at 37 °C, 5% CO_2. Immediately after treatment (T = 0), two pictures of the scratch/well (one above and one below the marker) were taken using 5x objective on the Axiovert 200 microscope equipped with an AxioCam MRm camera, n = 4 - 6. At the end of 18-hour incubation (T = 18), pictures of the scratches were taken again in the same manner as at T = 0. Then the wells were subjected to CellTiter-Blue® assay to quantify the extent of cell growth. The NIH ImageJ software was used to analyze the pictures: two parallel lines were drawn to outline each scratch, then the distance between them was measured using "Measure Length" option.   Percent   migration   was   calculated   using   the   formula: $100\% - (distance\ T = 18/distance\ T = 0) \times 100$. The experiment was repeated three times, all of the experiments were blinded.

Statistical analysis. The data was presented as the average and the STDEV or SEM where SEM = STDEV/$(n-1)^{1/2}$ and n = the number of independent repeats.   Individual comparisons were made with Student's t-test. All tests were two-tailed, unpaired and $p < 0.05$ was considered significant.

4.3. Results

4.3.1. Screening for 2nd-generation heparin-mimicking polymer

Since the 1st-generation heparin-mimicking polymer, p(SS-*co*-PEGMA), was not able to facilitate the dimerization of FGFRs in the presence of bFGF molecules,[20] we conducted the screening studies to identify another heparin-mimicking polymer with this specific property. Five polysulfonated polymers (Figure 4.1a) were either prepared via free radical polymerization or commercially bought. BaF3-FR1C cells, which express FGFR1s but lack HS, were used for *in vitro* screening (Figure 4.1b, c, d).[27] Heparin was used as the positive control; in the presence of bFGF, heparin facilitates the dimerization of FGFRs leading to receptor phosphorylation and subsequent cell proliferation.[25] Such activation effect was screened for in the polysulfonated polymers. However, some polysulfonated polymers have been reported to inhibit cell proliferation at high concentrations, probably due to competition with the high-affinity receptors for binding to bFGF.[18,19] Such inhibition effect was also carefully evaluated.

a
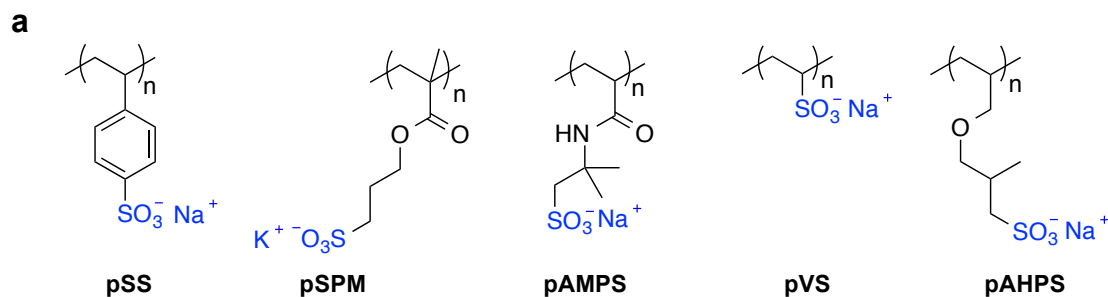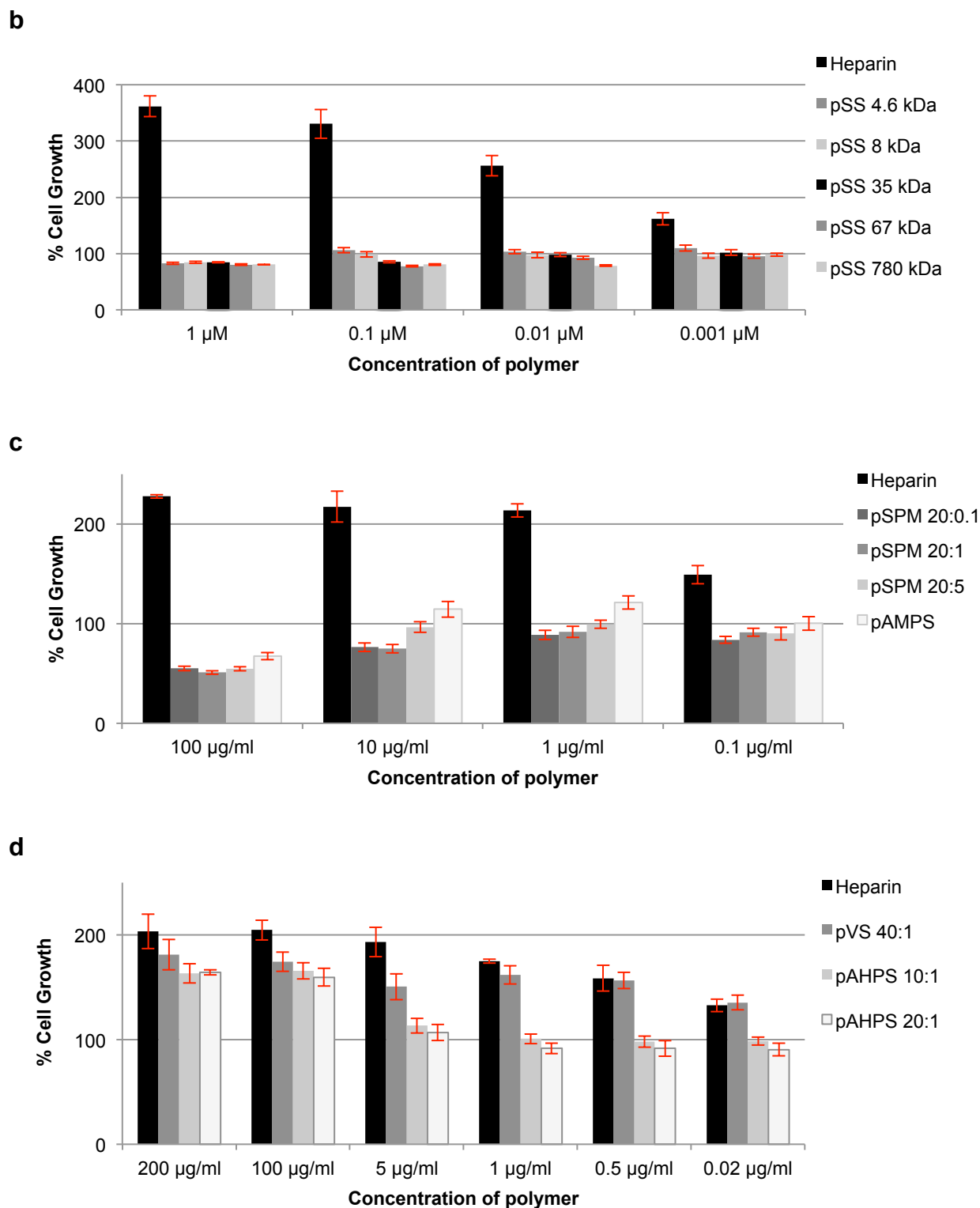
Figure 4.1. Screening studies for a 2nd-generation heparin-mimicking polymer. a) Chemical structures of the sulfonated polymers used in the screening studies. Proliferation studies of

BaF3-FR1C cells in the presence of 1 ng/mL bFGF and various concentrations of pSS (b), pSPM or pAMPS (c), pVS or pAHPS polymers (d). Except for pSS polymers, the set of numbers following each polymer's abbreviation indicates the monomer:initiator molar ratio in the synthesis. Incubation of 20,000 cells/well in 96-well plate with each of the samples was carried out for 48 hours. CellTiter®-Blue assay was performed to quantify the extent of cell growth. Samples with heparin were used as positive control groups. Data was normalized to the blank medium group, which was set at 100%. Each sample had four replicates. Error bars represent STDEV.

As shown in Figure 4.1, pSS and pSPM inhibited cell proliferation at high concentrations. 100 μg/mL of pSPM decreased cell proliferation to approximately 50%. pAMPS was also an inhibitor at high concentration tested which was consistent with literature.[19] pVS and pAHPS were strong activators at high concentrations, but the activating effect of pAHPS decreased quickly as the concentration decreased. However, pVS displayed very similar profile to heparin at all of the centration tested; at 0.5 and 0.02 μg/mL, the percent cell growth was not significantly different in the presence of either heparin or the polymer. This result is important because reported heparin mimics always show decreased activity compared to heparin in various assays. Therefore, pVS was chosen as the 2nd-generation heparin-mimicking polymer for subsequent studies. The results were summarized in Table 4.1.

Table 4.1. Summary from the screening studies.

Polymer screened	Inhibitor	Activator
pSS	Slight at high concentrations	No
pSPM	Strong at high concentrations	No
pAMPS	Moderate at high concentrations	at Low concentrations
pAHPS	No	at High concentrations
pVS	No	at All concentrations

In the screening studies, only one molecular weight pVS was prepared and tested; therefore, to understand the effect of the polymer size on the cell proliferation, various sizes of pVS were prepared via RAFT polymerization. To our knowledge, RAFT polymerization of unprotected VS monomer has never been reported. Since VS monomer belongs to a class of "less activated" monomers similar to vinyl acetate monomer, a dithiocarbonate- or xanthate- functionalized CTA was synthesized to better facilitate RAFT polymerization of this monomer (Scheme 4.1).[29]

Scheme 4.1. Synthesis of different sizes of pVS.
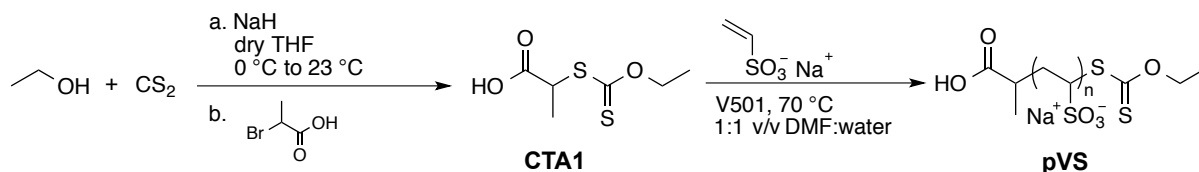
Figure 4.2a-c shows the characterization of **CTA1**. Five pVS polymers with molecular weights ranging from 6.6 kDa to 80.3 kDa were synthesized. The molecular weights of the polymers were calculated from their ^{1}H NMR spectra using the integral value of the CTA's peak at 1.45-1.2 ppm (CH**CH₃**) and the integral value of the polymer backbone at 4.2-1.45 ppm. Figure 4.2.d-f shows the representative characterization of **pVS 6.6 kDa**. The integration of the peak OCH₂**CH₃** at 1.45 ppm was less than 3, which indicated the hydrolysis of the xanthate end group. The broad peaks at 6.0 and 5.5 ppm were thought to be the internal olefins within the polymer backbone. Jiang and co-workers studied the thermal degradation of pVS and showed that the degradation involved the cleavage of the carbon sulfur bonds to give radicals along the polymer chain that coupled to form internal alkenes.[30] The UV-Vis spectrum of **pVS 6.6 kDa** had a maximum absorbance at 287 nm, which was the known absorbance of the xanthate functional group,[31] and was also observed in the UV-Vis spectrum of **CTA1** (Figure 4.2f).

a
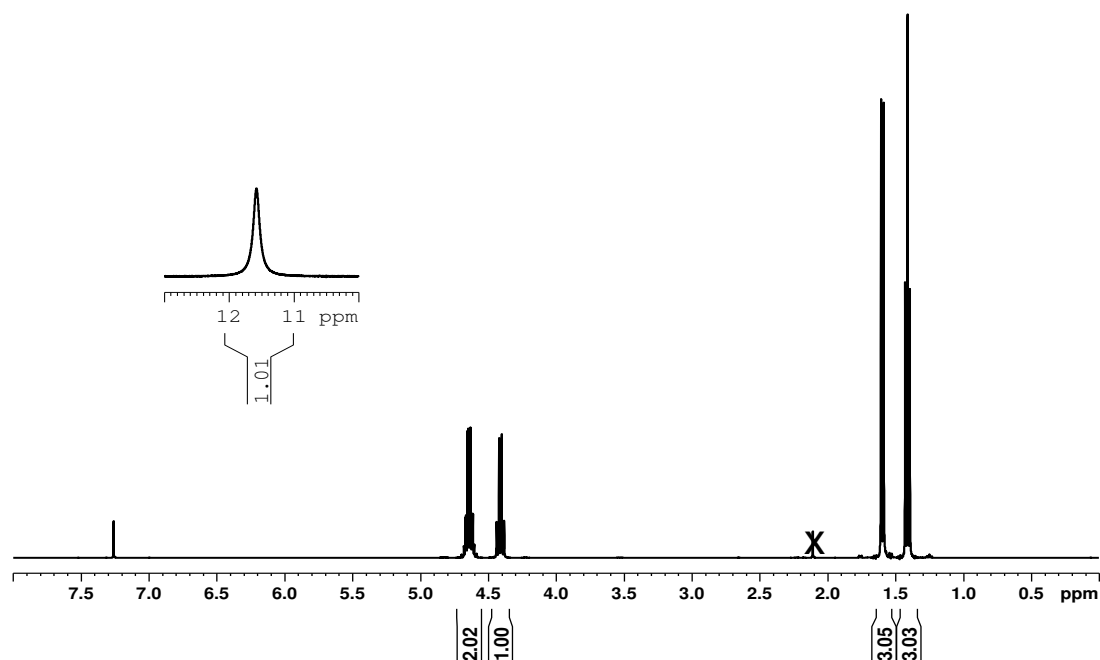
b
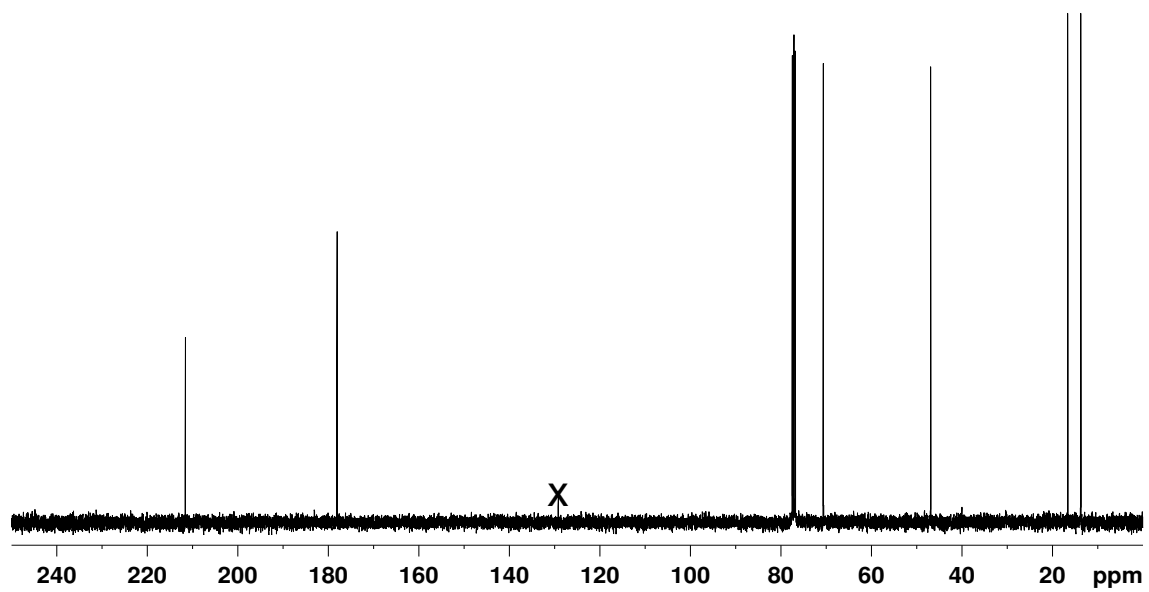
c
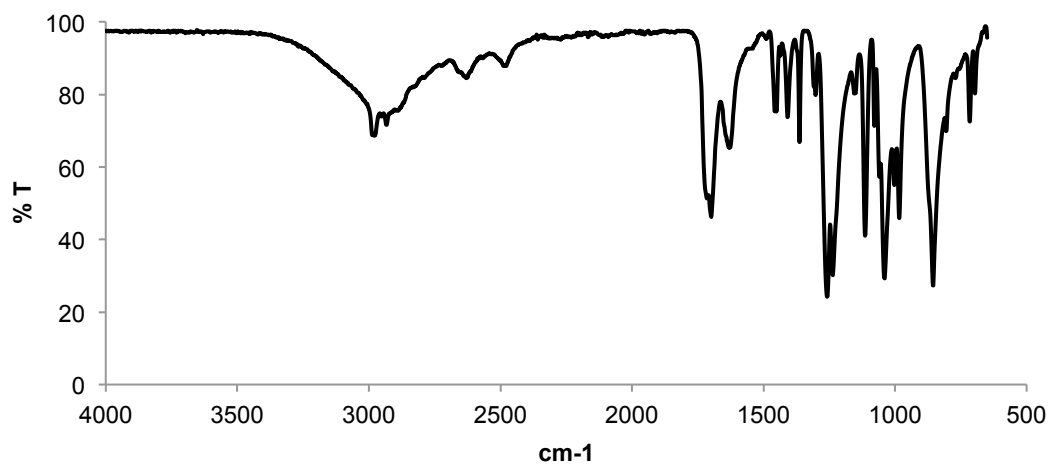
d
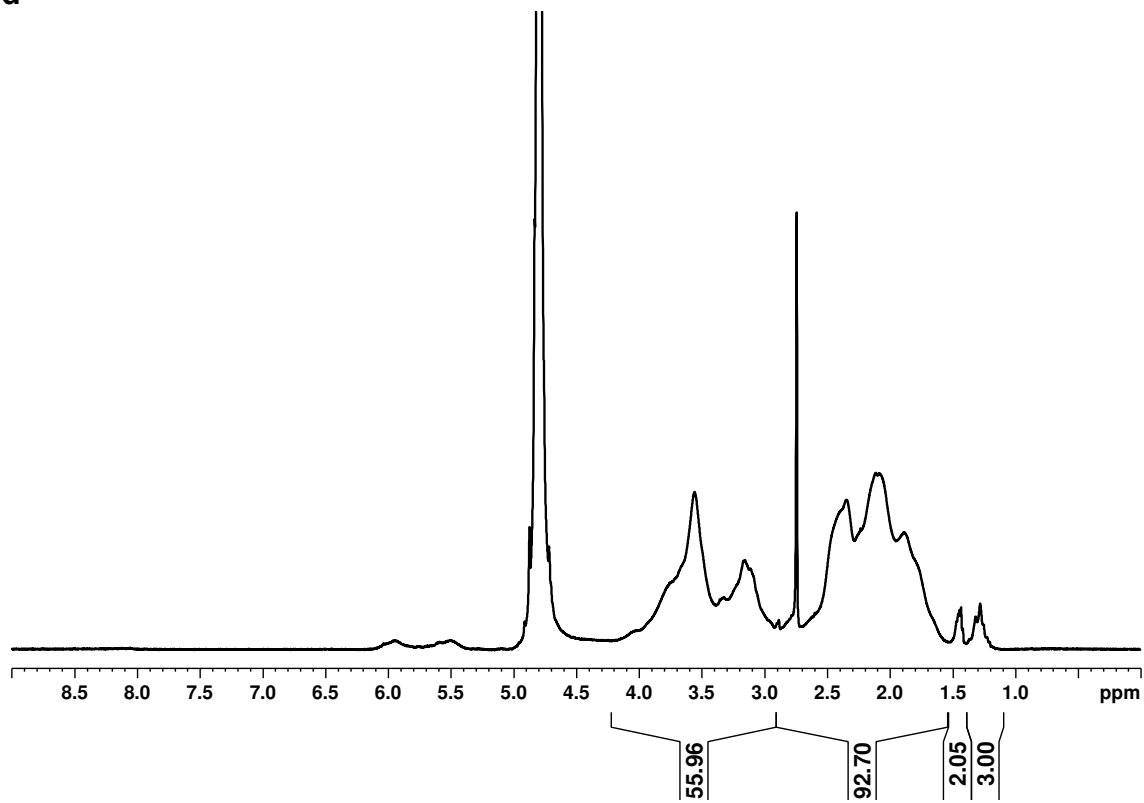
e
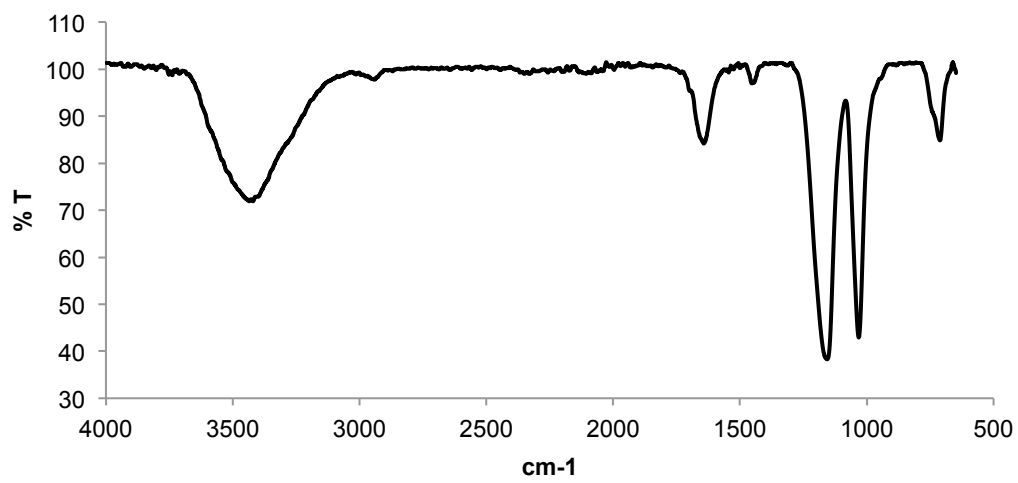
f
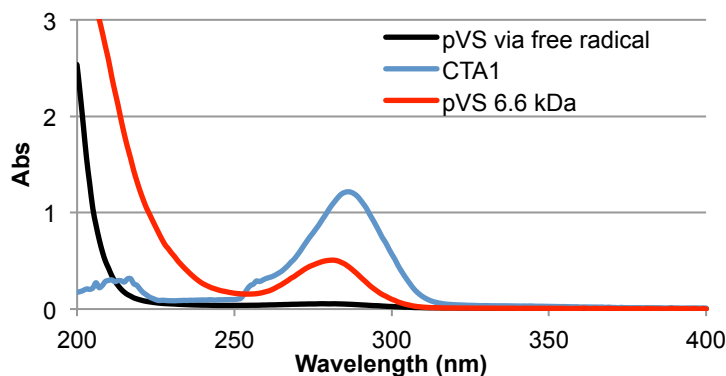
Figure 4.2. Characterization of **CTA1** and **pVS 6.6 kDa**. ^{1}H NMR spectrum in CDCl$_3$ (a), ^{13}C NMR spectrum in CDCl$_3$ (b), and FTIR spectrum (c) of **CTA1**. ^{1}H NMR spectrum in D$_2$O (d), FTIR spectrum (e), and UV-Vis spectrum of **pVS 6.6 kDa** synthesized via RAFT polymerization, compared to the UV-Vis spectra of pVS prepared via free radical polymerization and **CTA1** in MilliQ-water (f).

The pVS polymers were tested on BaF3-FR1C cells in the presence of 1 ng/mL of bFGF to evaluate the extent of stimulated cell growth (Figure 4.3a). The stimulation effect of all the pVS polymers was concentration dependent. The effect was similar to each other and to heparin when tested from 100 μg/mL to 0.001 μg/mL. The cytotoxicity of pVS polymer was also evaluated. Figure 4.3b shows that **pVS 80.3 kDa** was not toxic to HDF cells up to at least 1 mg/mL.
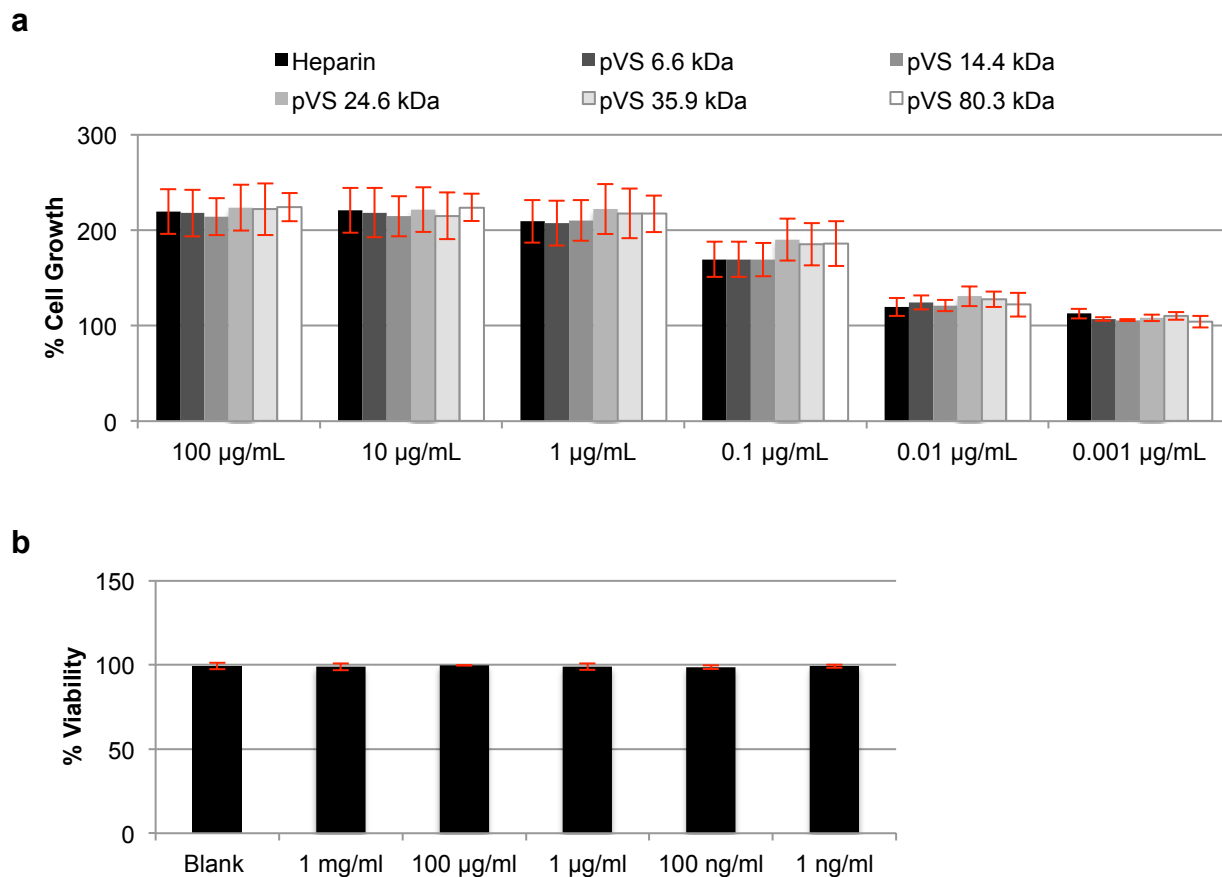
Figure 4.3. Proliferation studies of different sizes of pVS polymers on BaF3-FR1C cells and cytotoxicity studies on HDF cells. a) Proliferation studies of BaF3-FR1C cells in the presence of 1 ng/mL bFGF and various concentrations of heparin, **pVS 6.6 kDa, 14.4 kDa, 24.6 kDa, 35.9 kDa, and 80.3 kDa**. Incubation of 20,000 cells/well in 96-well plate with each of the samples was carried out for 48 hours. CellTiter®-Blue assay was performed to quantify the extent of cell growth. Data was normalized to the blank medium group, which was set at 100%. Each sample had four replicates and the experiment was repeated three times. Error bars represent SEM. b) Cytotoxicity studies of **pVS 80.3 kDa** on HDF cells. Incubation of 5,000 HDF cells/well in 48-well plate with various concentrations of the polymer was carried out for 24 hours. Each well was washed twice with D-PBS and subsequently incubated with 1 mM calcein AM and 4 mM ethidium homodimer-1 for 20 minutes. The percentage of live cells was calculated by dividing

140

the number of live cells by the total number of live and dead cells. The experiment was repeated three times. Error bars represent SEM.

4.3.2. Synthesis of the 2nd-generation heparin-mimicking polymer conjugate and biological studies

Since pVS polymer could facilitate binding of bFGF to its high-affinity receptors similar to heparan sulfate, we hypothesized that the covalent conjugate between bFGF and pVS polymer could result in a hybrid that is more active than its native protein. In order to prepare such conjugate, a cysteine-reactive pyridyl disulfide (PDS)-functionalized CTA was synthesized (Scheme 4.2). A neopentyl alcohol was used to synthesize the carboxylic acid xanthate-functionalized **CTA2** to reduce the rate of hydrolysis of the xanthate by increasing the hydrophobicity compared to the ethyl derivative in **CTA1**. Coupling of **CTA2** to a PDS-functionalized alcohol resulted in **CTA3**. Figure 4.4 shows the characterization of **CTA2** and **CTA3**.

Scheme 4.2. Synthesis of **PDS-pVS** and **bFGF-pVS**.
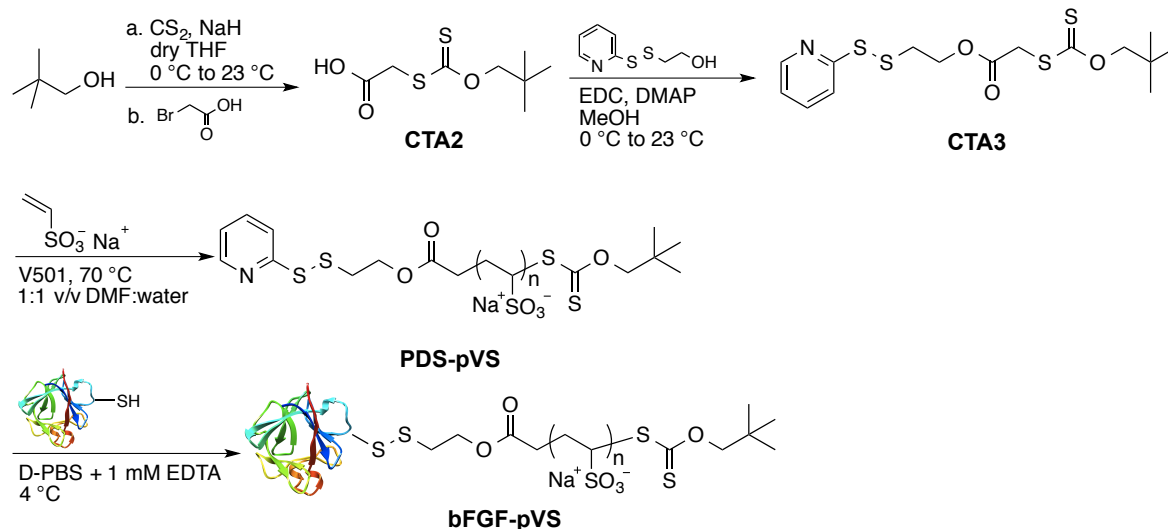
CTA3 was used in the RAFT polymerization of VS monomer to produce three **PDS-pVS**

7.6 kDa, **10.2 kDa**, and **16.3 kDa**. Figure 4.5 shows the characterization of a representative

PDS-pVS 10.2 kDa. In the ^{1}H NMR, the PDS protons were used as calibrants and the molecular

weights of the polymers were calculated using the polymer backbone protons at 4.2-2.9 ppm.

The integration of the OCH$_2$(**CH$_3$**)$_3$ at 1.2 ppm was about 9 which shows that the hydrolysis of

the xanthate end group was avoided. The conjugates between the polymers and bFGF via

disulfide exchanged were prepared similarly to previous report. Figure 4.6 shows the

representative western blot of the Native PAGE of **bFGF-pVS7.6k**. Since pVS 7.6 kDa is small

and highly negatively charged, its conjugate to bFGF appeared as a smear closer to the cathode

of the PAGE.

c

d

e

f
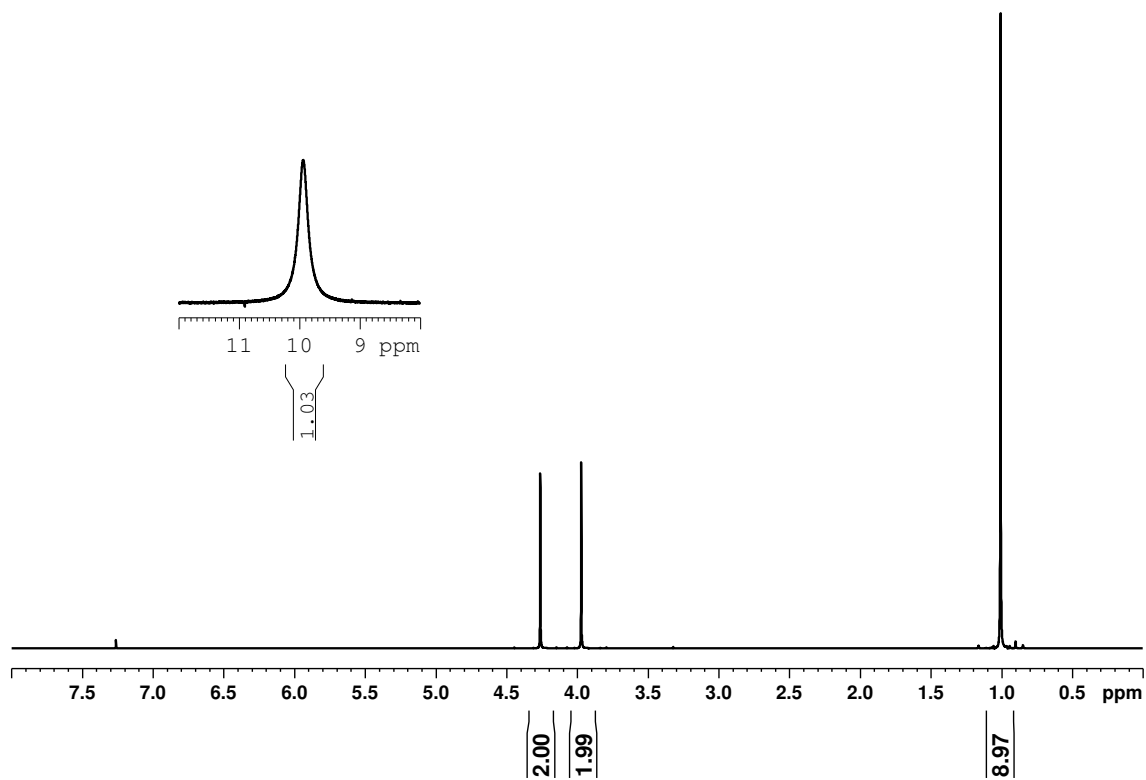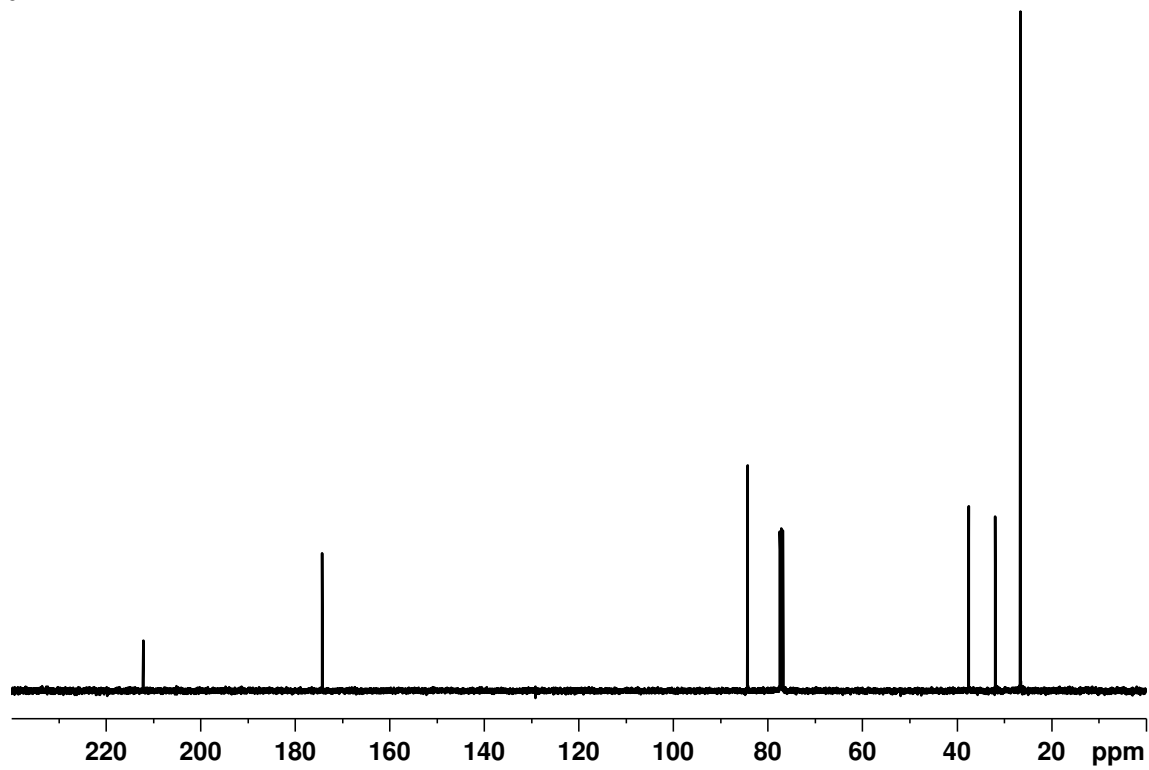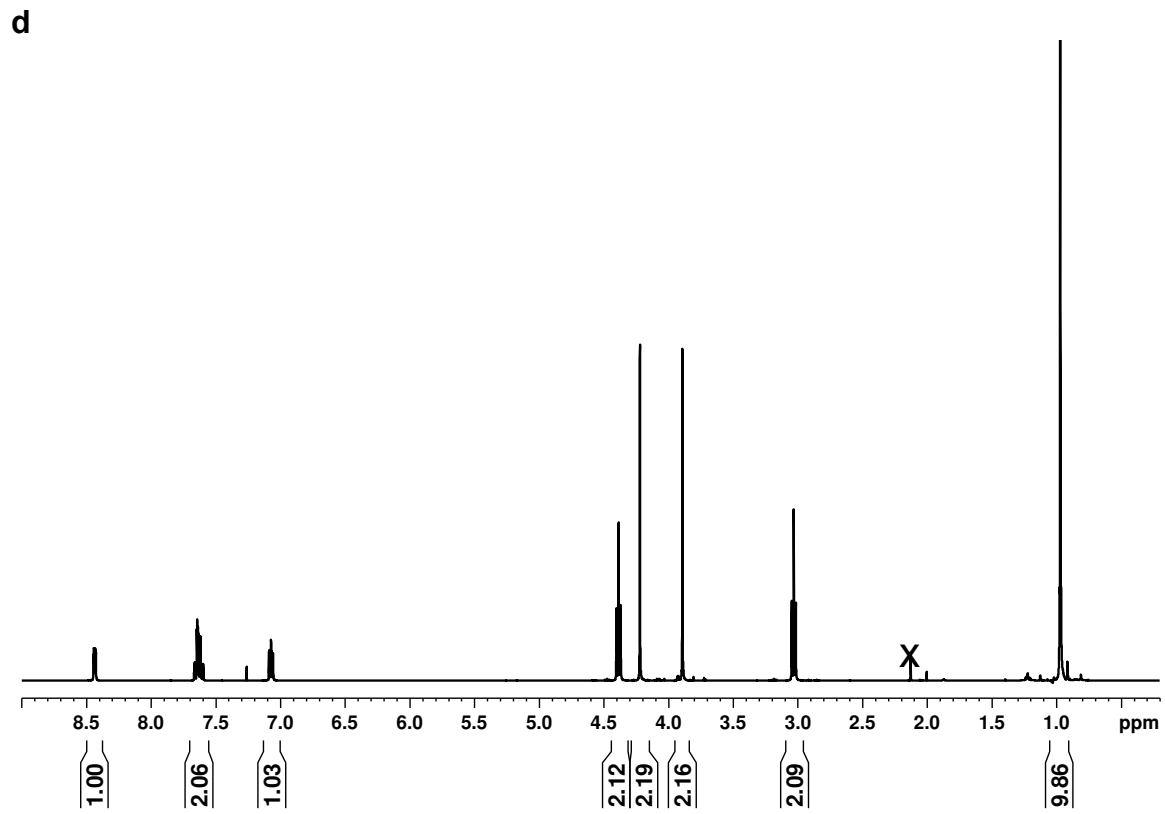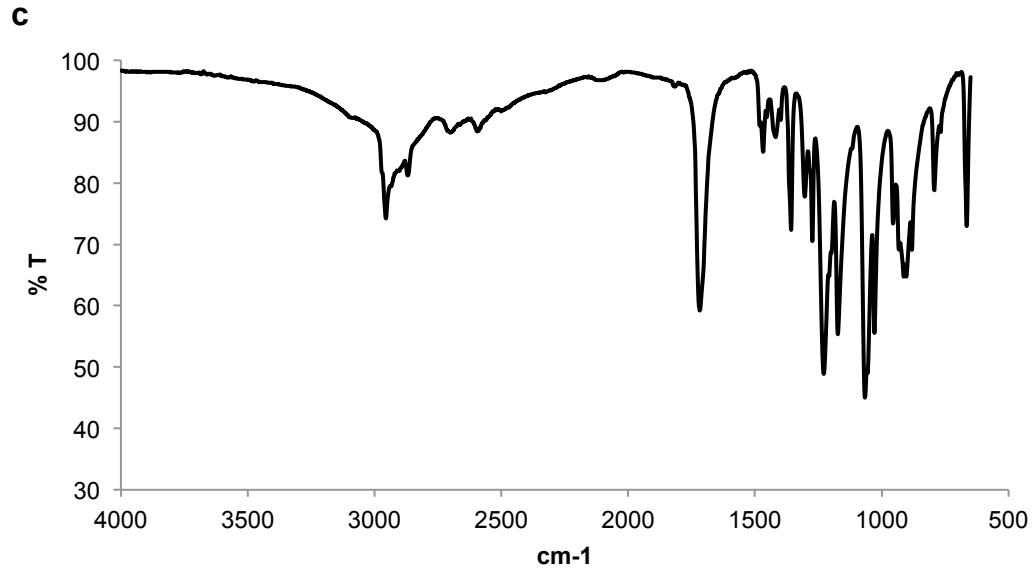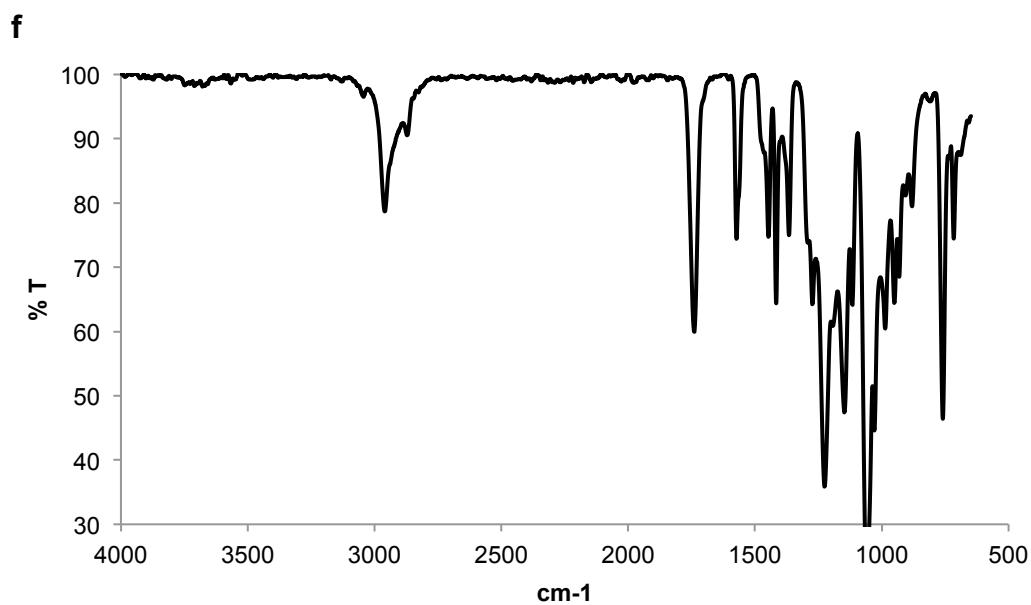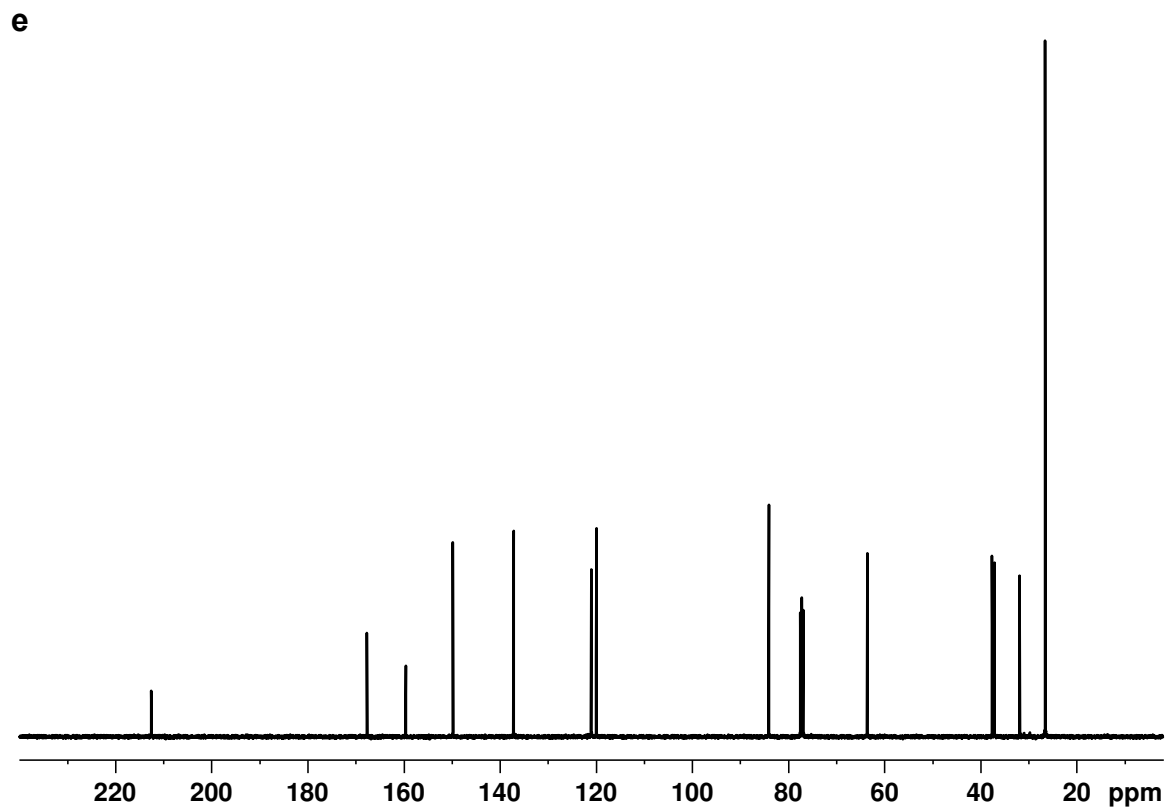
Figure 4.4. Characterization of **CTA2** and **CTA3**. ^{1}H NMR spectrum in CDCl$_3$ (a), ^{13}C NMR

spectrum in CDCl$_3$ (b), and FTIR spectrum (c) of **CTA2**. ^{1}H NMR spectrum in CDCl$_3$ (d), ^{13}C

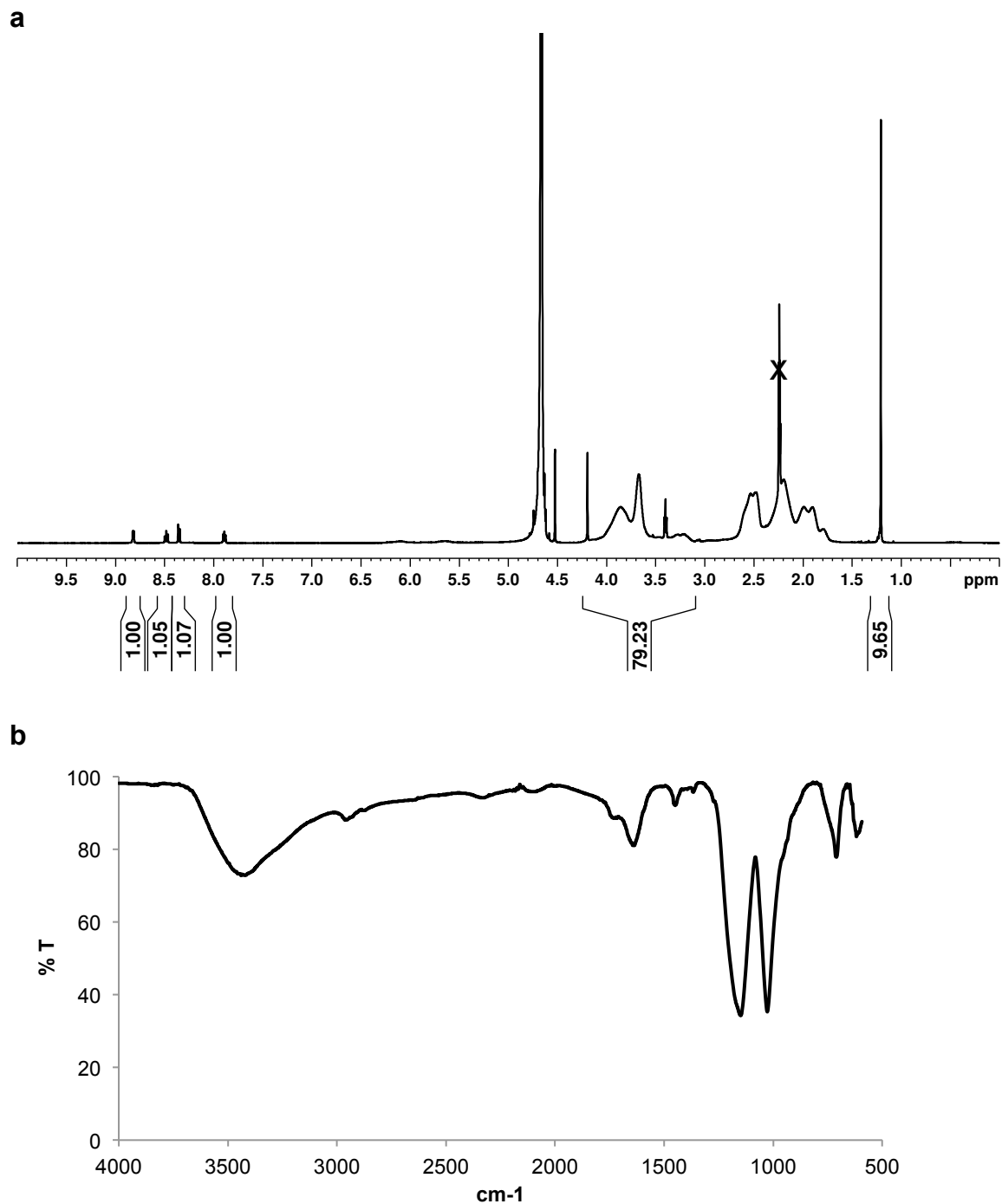NMR spectrum in CDCl$_3$ (e), and FTIR spectrum (f) of **CTA3**.

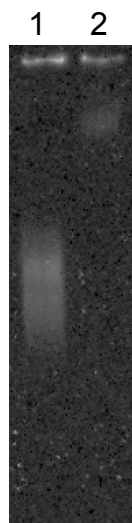**Figure 4.5.** Characterization of PDS-pVS. ^{1}H NMR spectrum in D$_2$O (a) and FTIR spectrum (b) of **PDS-pVS 10.2 kDa**.

Figure 4.6. Western blot of Native PAGE of **bFGF-pVS7.6k** (lane 1) and control bFGF (lane 2).

The bFGF-pVS conjugates were examined on BaF3-FR1C cells for the extent of stimulated cell growth (Figure 4.7a). While bFGF-p(SS-*co*-PEGMA) conjugate induced cell proliferation to $166 \pm 10\%$ compared to bFGF ($128 \pm 5\%$) which was consistent with previous finding,[20] cell proliferation was much lower in the presence of bFGF-pVS conjugates. The percent cell growth in the presence of **bFGF-pVS7.6k** ($108 \pm 2\%$) was statistically lower than that in the presence of bFGF. The percent cell growth in the presence of **bFGF-pVS10.2k** and **bFGF-pVS16.3k** were $116 \pm 2\%$ and $133 \pm 4\%$, respectively. And there appeared to be a size-dependent effect from the bFGF-pVS conjugates. To verify the pVS polymers used for this study were not different than the ones synthesized using **CTA1**, **pVS 7.6 kDa**, **10.2 kDa**, and **16.3 kDa** were tested on BaF3-FR1C cells in the presence of unconjugated bFGF. The percent cell growths were over 300% similarly to when heparin was used; no size-dependent phenomenon was observed (Figure 4.7b). This data suggested that the pVS polymers were not able to facilitate the dimerization of FGFRs in the conjugate forms. When the pVS conjugates

were tested on HDF cells, the percent cell growths were similar to what was observed in the case

of bFGF and bFGF-p(SS-*co*-PEGMA) (Figure 4.8). HDF cells express HS that is responsible for

facilitating binding of bFGF to its receptors and receptor dimerization. Therefore, this data

suggested that the conjugated pVS polymers did not block the heparin-binding site on bFGF.
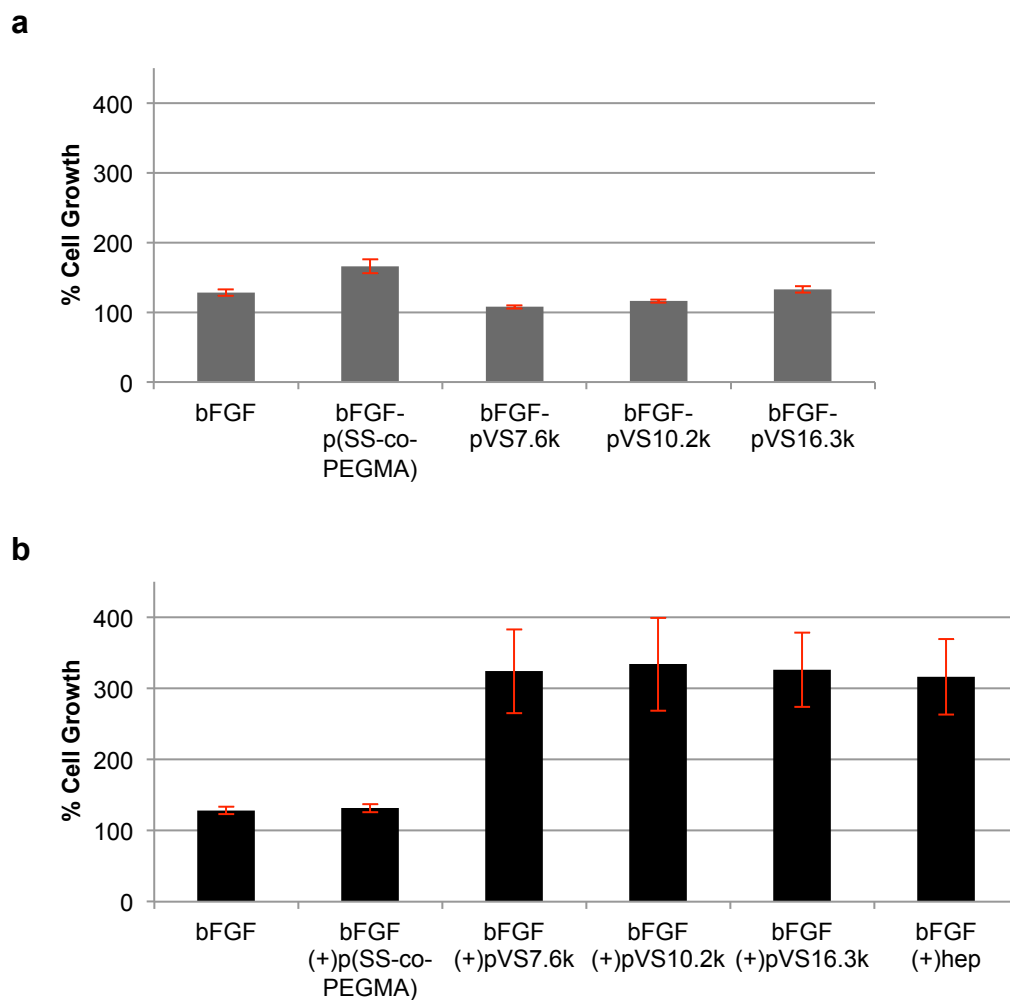
a

b

Figure 4.7. Proliferation studies of **PDS-pVS** polymers and **bFGF-pVS** conjugates on BaF3-

FR1C cells. a) Proliferation studies of BaF3-FR1C cells in the presence of 1 ng/mL of either

bFGF, bFGF-p(SS-*co*-PEGMA), **bFGF-pVS7.6k**, **bFGF-pVS10.2k**, or **bFGF-pVS16.3k**. b)

Proliferation studies of BaF3-FR1C cells in the presence of 1 ng/mL of bFGF with our without 1

µg/mL of either p(SS-*co*-PEGMA), **PDS-pVS7.6k**, **PDS-pVS10.2k**, or **PDS-pVS16.3k**. Incubation of 20,000 cells/well in 96-well plate with each of the samples was carried out for 48 hours. CellTiter®-Blue assay was performed to quantify the extent of cell growth. Data was normalized to the blank medium group, which was set at 100%. Each sample had four replicates and the experiment was repeated three times. Error bars represent SEM.
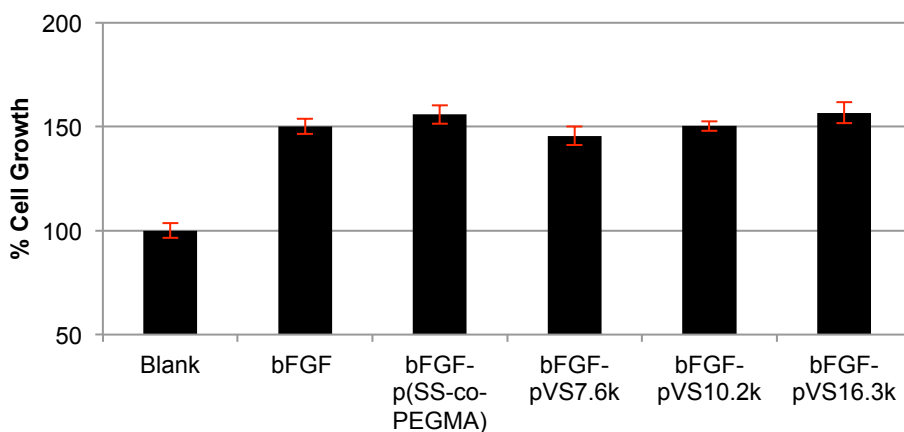

Figure 4.8. Proliferation studies of **bFGF-pVS** conjugates on HDF cells. Proliferation studies of HDF cells in the presence of 1 ng/mL of either bFGF, bFGF-p(SS-*co*-PEGMA), **bFGF-pVS7.6k**, **bFGF-pVS10.2k**, or **bFGF-pVS16.3k**. Incubation of 2,000 cells/well in 96-well plate with each of the samples was carried out for 72 hours. CellTiter®-Blue assay was performed to quantify the extent of cell growth. Data was normalized to the blank medium group, which was set at 100%. Each sample had six replicates. Error bars represent STDEV.

To elucidate why a strong heparin-mimicking polymer such as pVS failed to mimic the biological role of heparin only in the conjugate form, we conducted the following experiments. First, since the bioactivity of the bFGF-pVS conjugates were reduced on BaF3-FR1C cells, we wanted to ensure that the conjugates did not degrade. When excess corresponding pVS polymer was added to each of the bFGF-pVS conjugate, the percent BaF3-FR1C cell growth increased tremendously to about 300% (Figure 4.9). This confirmed that the bFGF-pVS conjugates were still bioactive and could be turned on using excess heparin-mimicking polymer. The data also suggested that the conjugated pVS polymers did not inhibit binding of bFGF to FGFR.
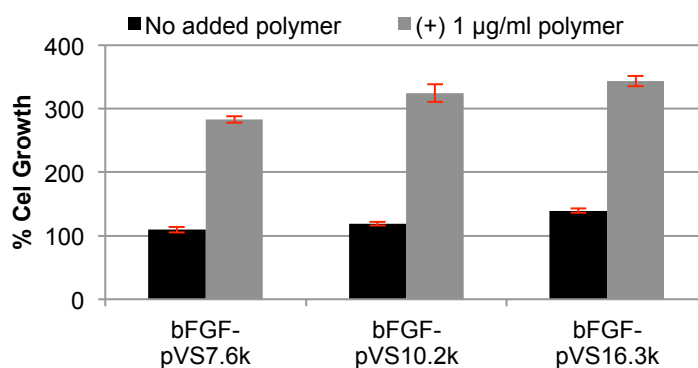

Figure 4.9. Proliferation studies of bFGF-pVS conjugates in the absence or presence of excess polymer on BaF3-FR1C cells. Incubation of 20,000 cells/well in 96-well plate with 1 ng/mL of either **bFGF-pVS7.6k**, **bFGF-pVS10.2k**, or **bFGF-pVS16.3k** alone (black bars) or with 1 μg/mL of the respective polymer (gray bars) was carried out for 48 hours. CellTiter®-Blue assay was performed to quantify the extent of cell growth. Data was normalized to the blank medium group, which was set at 100%. Each sample had four replicates. Error bars represent STDEV.

Second, it has been shown that HS can internalize bFGF into the cell cytoplasm independently of FGFR.[32,33] When this mechanism of endocytosis occurs, receptor dimerization and phosphorylation events are bypassed, therefore no cell proliferation is observed. In order to study whether the 2nd-generation heparin-mimicking polymer could mediate the internalization of bFGF in such a way, we synthesized a red fluorescent 2nd-generation heparin-mimicking polymer for cellular uptake study. VS monomer was copolymerized with Rhodamine B-based methacrylate monomer to produce **p(VS-*co*-RhoB)** (Figure 4.10a). CHO cells were used for this cellular uptake study because they express minimal amount of FGFRs.[33] When CHO cells were treated with only **p(VS-*co*-RhoB)**, no red signals was observed inside the cells (Figure 4.10d). But when the cells were treated with the polymer and bFGF, strong red signals were observed inside the cell cytoplasm (Figure 4.10e), which indicated the **p(VS-*co*-RhoB)** bound with bFGF and pulled the complex inside the cells. As a control, the CHO cells were treated with p(SS-*co*-PEGMA-*co*-RhoB) in the absence or presence of bFGF (Figure 4.10b and c, respectively). Only in the presence of bFGF, the red signals were observed but less pronounced than in the case of **p(VS-*co*-RhoB)**. This finding is consistent with our previous results showing that the 1st-generation heparin-mimicking polymer was much less like heparin than the 2nd-generation heparin-mimicking polymer. Since the unconjugated pVS polymer could internalize with bFGF well, it is speculated that in the conjugate form, pVS could internalize the hybrid even faster leaving it unable to interact with the FGFRs, therefore no stimulated cell proliferation was observed.
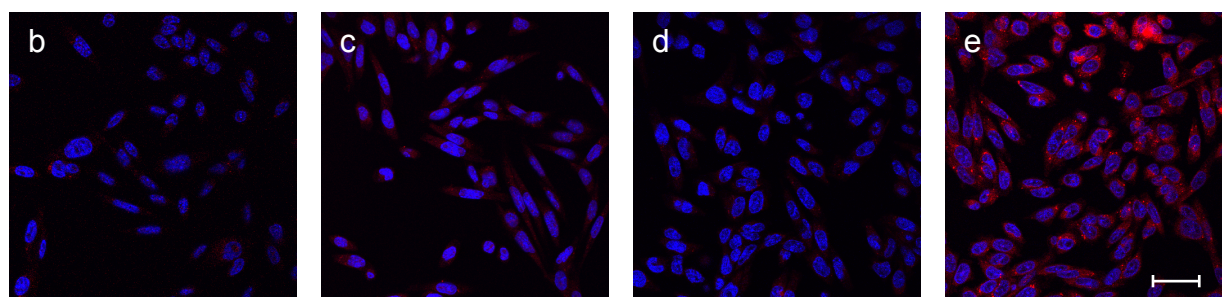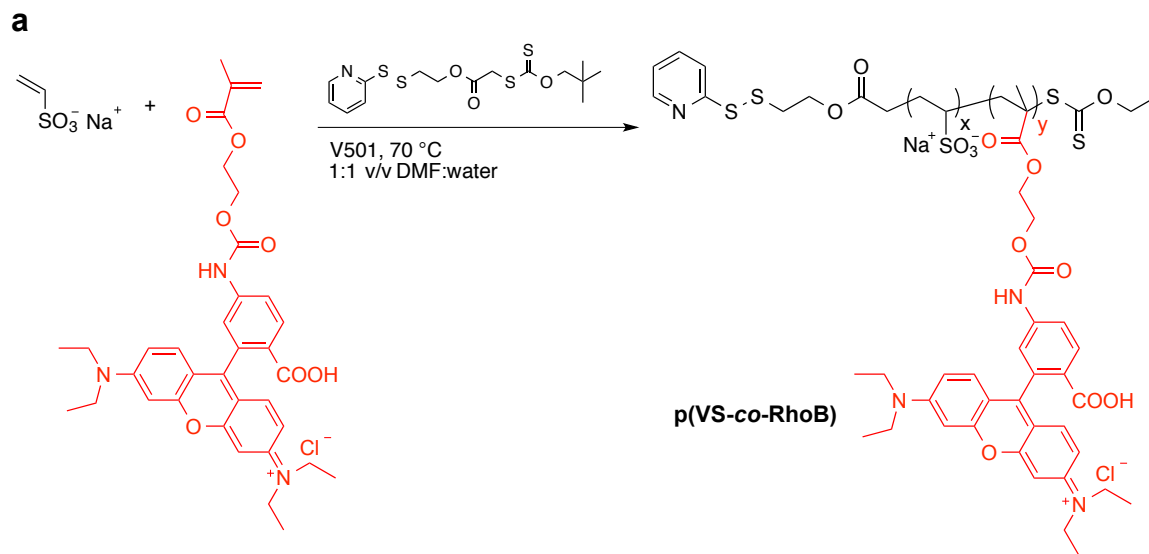
Figure 4.10. Cell uptake studies on CHO cells. a) Synthesis scheme of **p(VS-*co*-RhoB)**. b-e) Images of CHO cells treated with 25 μg/mL of either p(SS-*co*-PEGMA-*co*-RhoB) (b) or **p(VS-*co*-RhoB)** alone (d), or in the presence of 0.1 μg/mL of bFGF (c and e, respectively). Images were captured under two channels: DAPI for nuclei (blue), Rhodamine B for (pSS-*co*-PEGMA-*co*-RhoB) and p(VS-*co*-RhoB) (red). Scale bar is 60 μm.

4.3.3. Synthesis of the 3rd-generation heparin-mimicking polymer conjugate and biological studies

Even though the 2nd-generation heparin-mimicking polymer was a strong activator, its biological effects were undesirable after conjugation to bFGF. We also observed that the 1st-generation polymer could not activate bFGF in HS-deficient cells, but when heparin was added, the conjugate was more active than when heparin was added to native bFGF (see Chapter 3). Therefore, since the 2nd-generation polymer is an excellent heparin mimic, we hypothesized that a block copolymer of pVS and p(SS-co-PEGMA) might activate bFGF in the conjugate form.
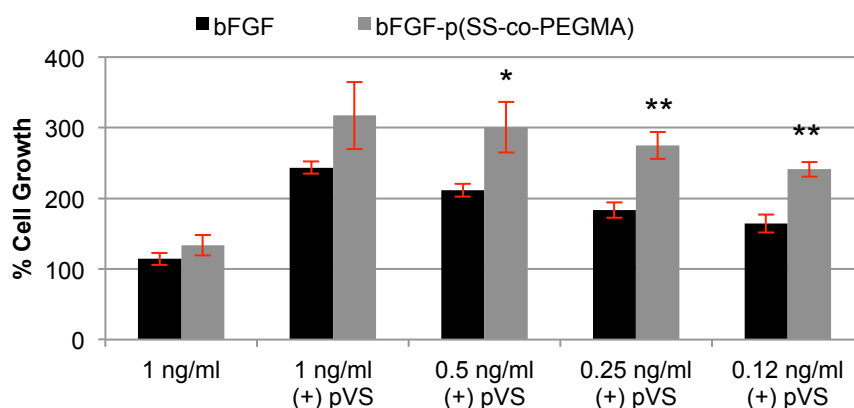

Figure 4.11. Proliferation studies of bFGF and bFGF-p(SS-co-PEGMA) in the presence of pVS on BaF3-FR1C cells. Incubation of 20,000 cells/well in 96-well plate with various concentrations of either bFGF (blank bars) or bFGF-p(SS-co-PEGMA) (gray bars) in the absence or presence of 1 μg/mL of **PDS-pVS7.6kDa** was carried out for 48 hours. CellTiter®-Blue assay was performed to quantify the extent of cell growth. Data was normalized to the blank medium group, which was set at 100%. Each sample had four replicates and the experiment was repeated four times. Error bars represent SEM. Statistical analysis was done using Student's t-

test. * $p < 0.05$, ** $p < 0.01$ for the bFGF-p(SS-*co*-PEGMA) group compared to the bFGF group at the same concentration test.

To test our hypothesis, **pVS 7.6 kDa** was combined with the 1st-genenration heparin-mimicking polymer, bFGF-p(SS-*co*-PEGMA), which was not a super-active hybrid, and tested on BaF3-FR1C cells. Figure 4.11 shows that when 1 μg/mL of pVS was used in combination with bFGF-p(SS-*co*-PEGMA), the percent cell growth was higher than when the polymer was used in combination with bFGF. For example, at 0.25 ng/mL of bFGF or bFGF-p(SS-*co*-PEGMA), pVS stimulated cell growth to $183 \pm 11\%$ and $274 \pm 19\%$, respectively ($p = 0.003$). This finding is consistent with our previous finding that adding heparin to the 1st-genenration heparin-mimicking polymer conjugate increased BaF3-FR1C cell proliferation much more than when added to native bFGF (see Chapter 3).

Scheme 4.3. Synthesis of **PDS-p(SS-*co*-PEGMA-*b*-VS)** and **bFGF-p(SS-*co*-PEGMA-*b*-VS)**.
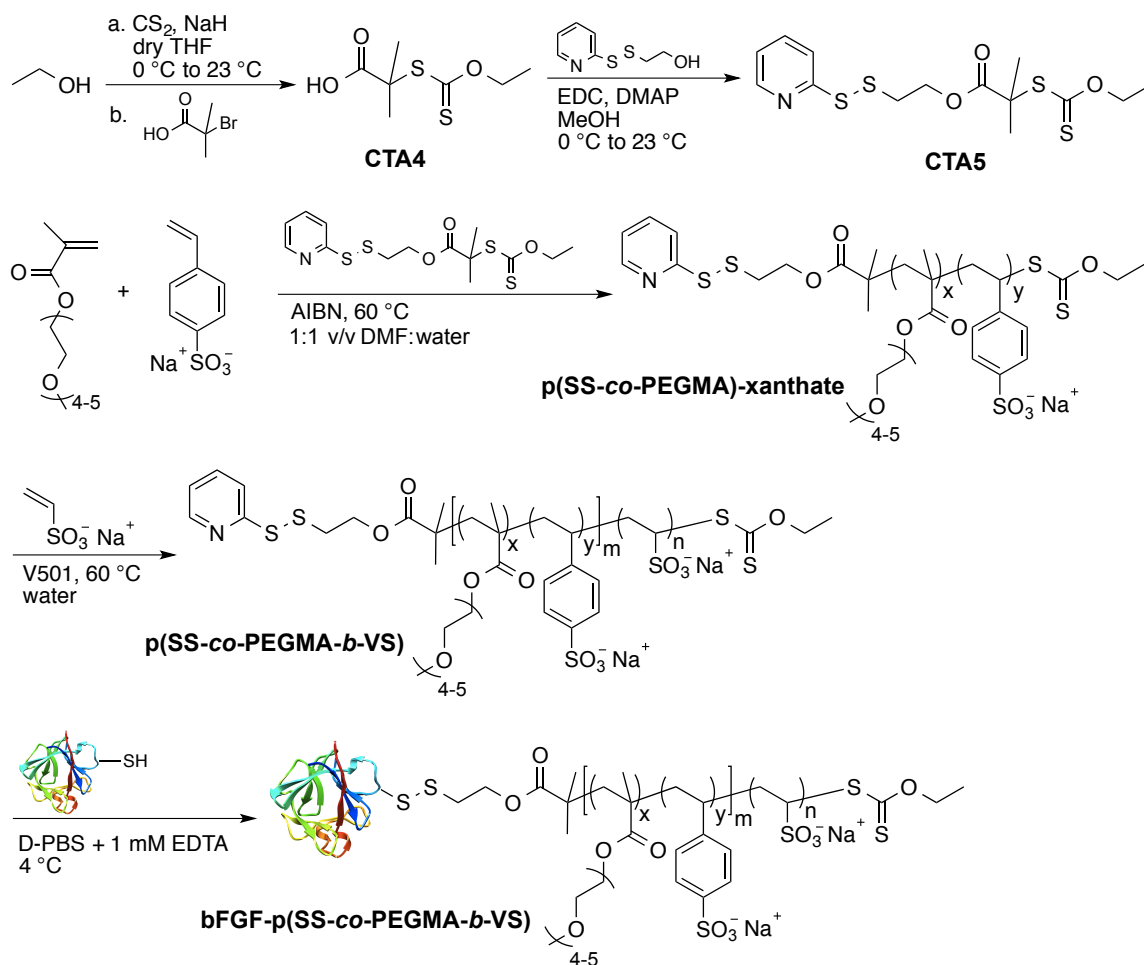

The 3rd-generation heparin-mimicking polymer, therefore, was synthesized as a fusion between the 1st-generation and 2nd-generation heparin-mimicking polymer. In order to synthesize the fusion polymer, we first synthesized a macro-CTA, **p(SS-*co*-PEGMA)-xanthate** (Scheme 4.4). Since SS and PEGMA monomer are "more-activated" monomers, xanthate-type CTAs are considered slow-acting CTAs, we synthesized **CTA4** bearing a di-methyl substitute at the fragmentation site to better match the rate of addition of the monomers and the rate of fragmentation of the CTA or the growing polymer chain. **CTA4** was then coupled to a PDS-

functionalized alcohol to make **CTA5** (Scheme 4.4). Figure 4.12 shows the characterization of

CTA4 and **CTA5**. RAFT polymerization of SS and PEGMA monomer in the presence of **CTA5**

produced a 33.0 kDa **p(SS-*co*-PEGMA)-xanthate** by ^{1}H NMR (Figure 4.13a and b). The PDI

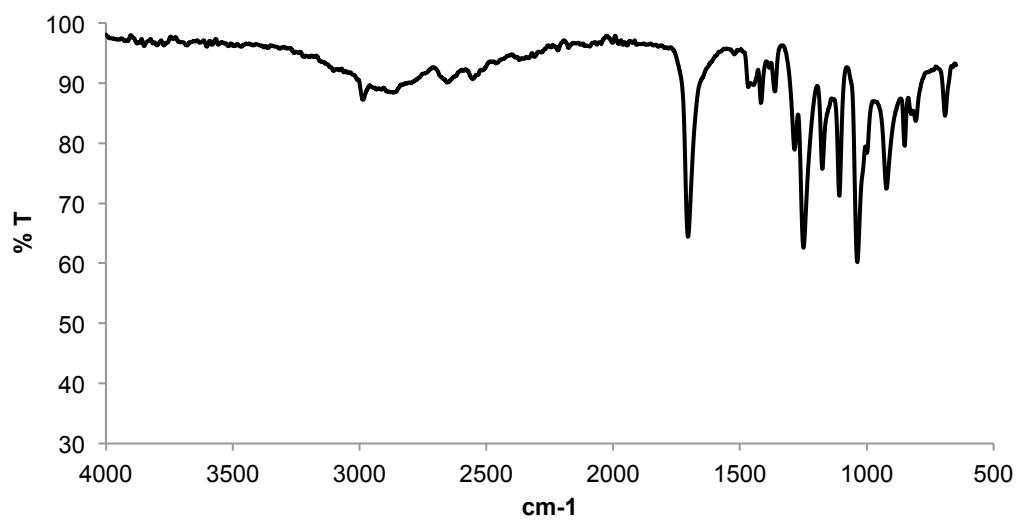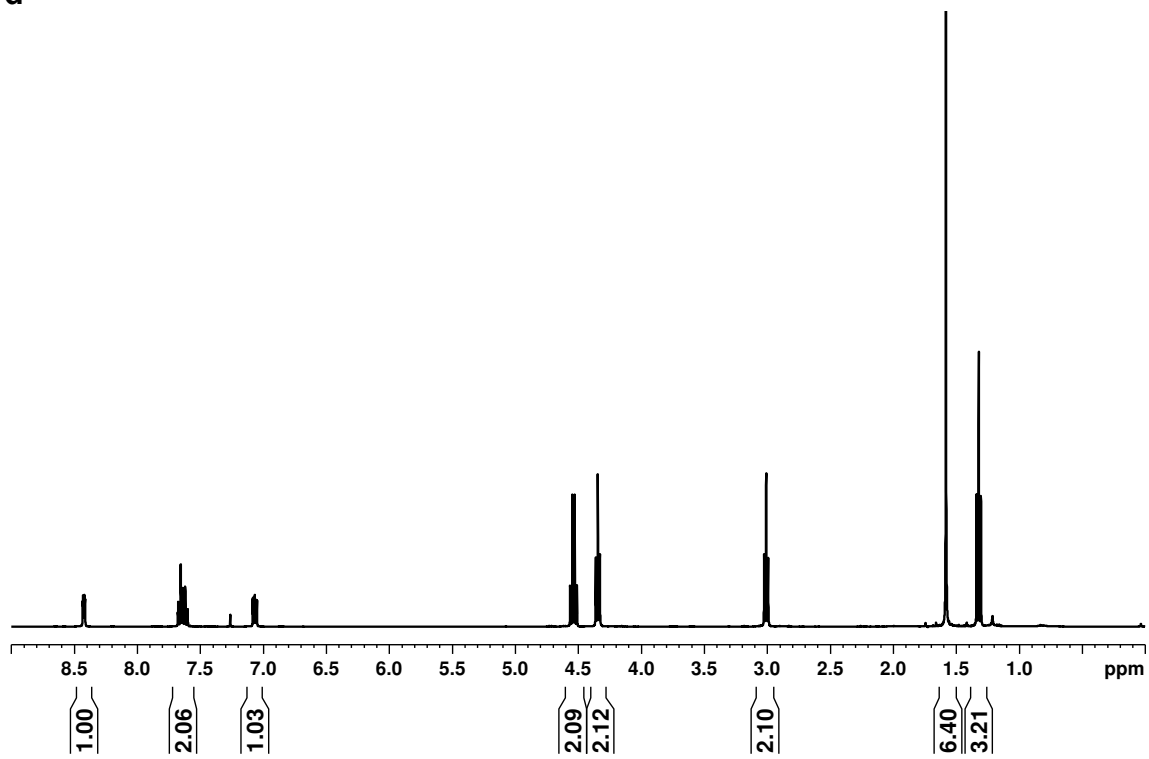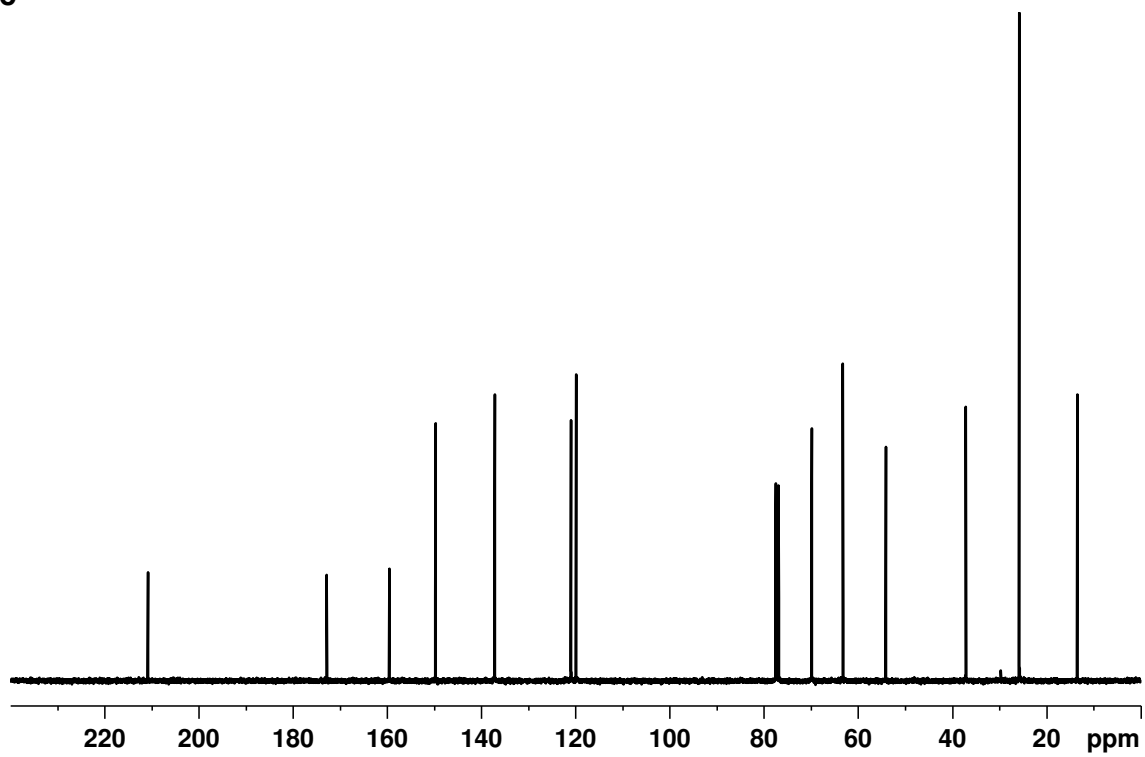of the polymer was broad (1.56) which was expected (Figure 4.13e).

a

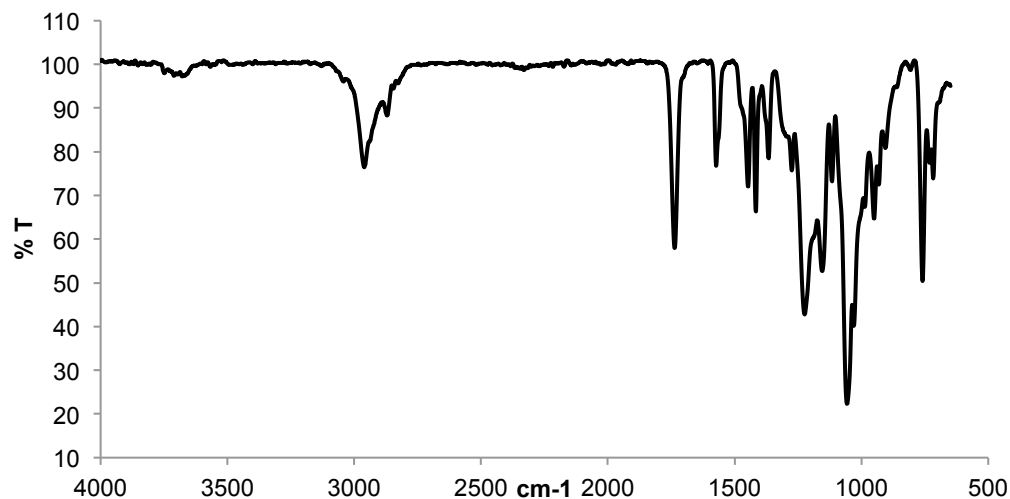**b**

c

d

e

158
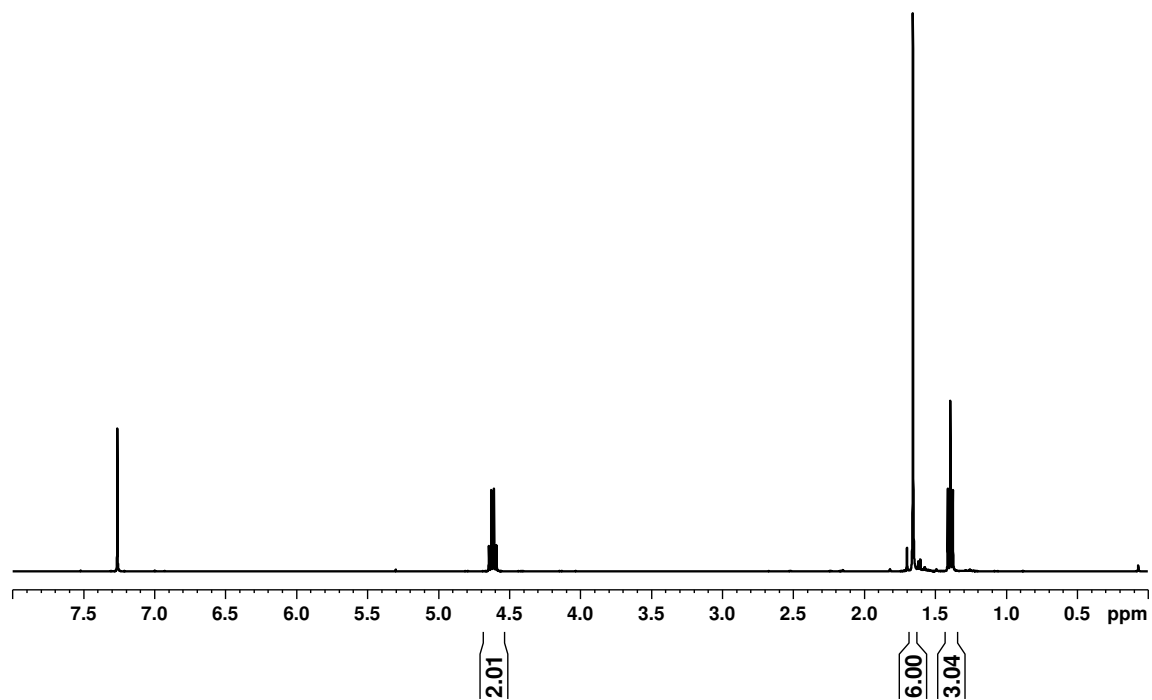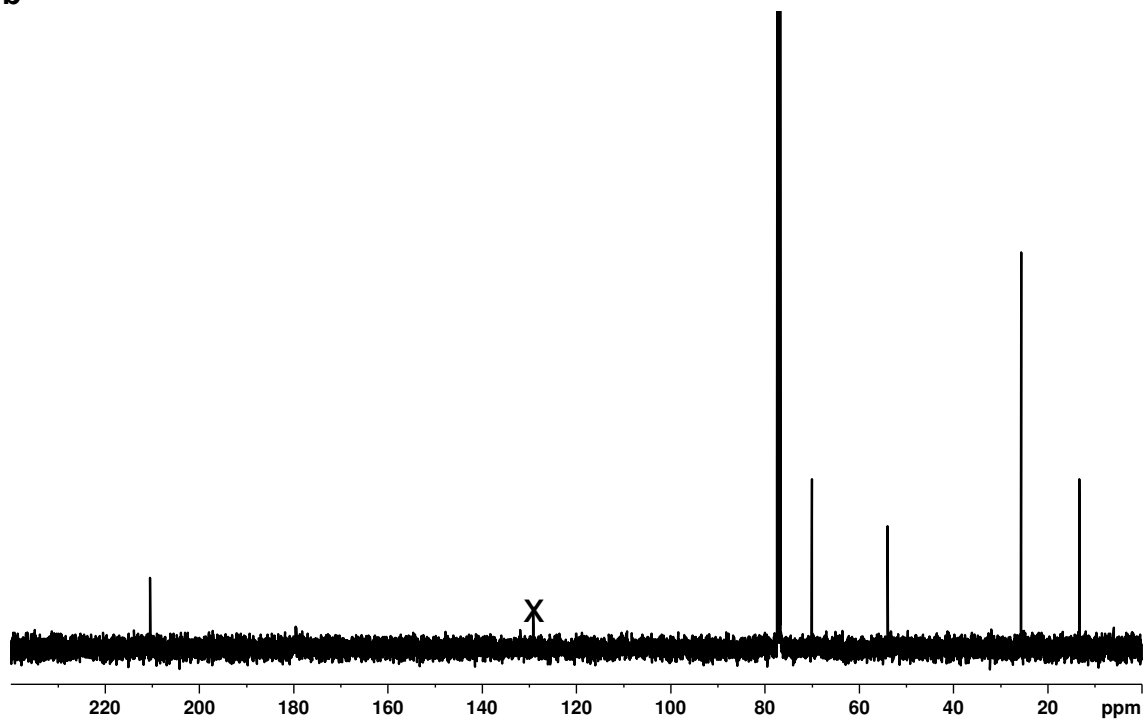
f

Figure 4.12. Characterization **CTA4** and **CTA5**. ^{1}H NMR spectrum in CDCl₃ (a), ^{13}C NMR

spectrum in CDCl₃ (b), and FTIR spectrum (c) of **CTA4**. ^{1}H NMR spectrum in CDCl₃ (d), [13]C

NMR spectrum in CDCl₃ (e), and FTIR spectrum (f) of **CTA5**.\

RAFT polymerization of VS monomer using **p(SS-*co*-PEGMA)-xanthate** as the macro-

CTA produced a 57.2 kDa **p(SS-*co*-PEGMA-*b*-VS)** polymer (by ^{1}H NMR) with the PDI of 1.46.

Figure 4.13c shows the ^{1}H NMR of the polymer. The obvious evidence for the incorporation of

pVS could be seen in the 2.7-0 ppm chemical shift; the peak pattern was different in the final

polymer's NMR compared to the macro-CTA's NMR. The molecular weight of the final

polymer was calculated by first setting the integration of the sulfonate styrene's proton at 8.0-6.0

ppm to what observed in the macro-CTA's NMR. Then, the difference in the chemical shift at

4.2-2.7 ppm region contributed to the integration of one equivalent proton of pVS's backbone

protons. The molecular weight of the final polymer contributed from the pVS block was

calculated by multiplying the molecular weight of the monomer to the number of repeating units

which was 24.2 kDa. This analysis also revealed a loss in the PDS end group of about 34%, probably due to the hydrolysis of the ester linkage in the polymer backbone throughout the 2nd polymerization process and extensive purification in water. GPC analysis showed a slight shift in M_n of polymer from 25.6 kDa to 31.6 kDa (Figure 4.13e).

a

b

c

d

e

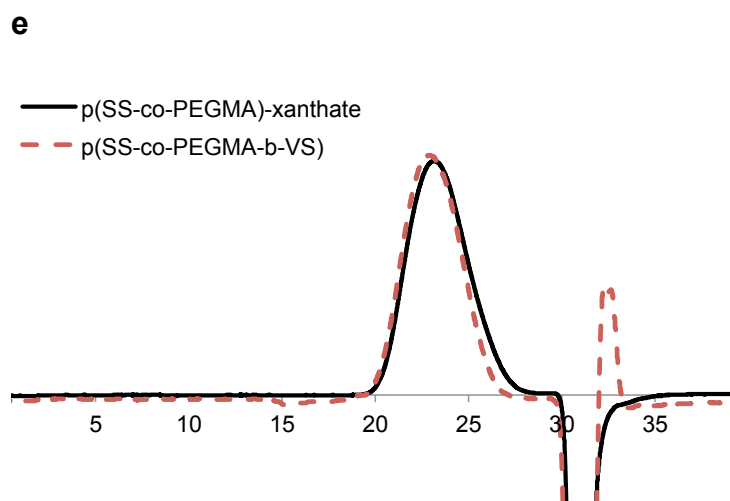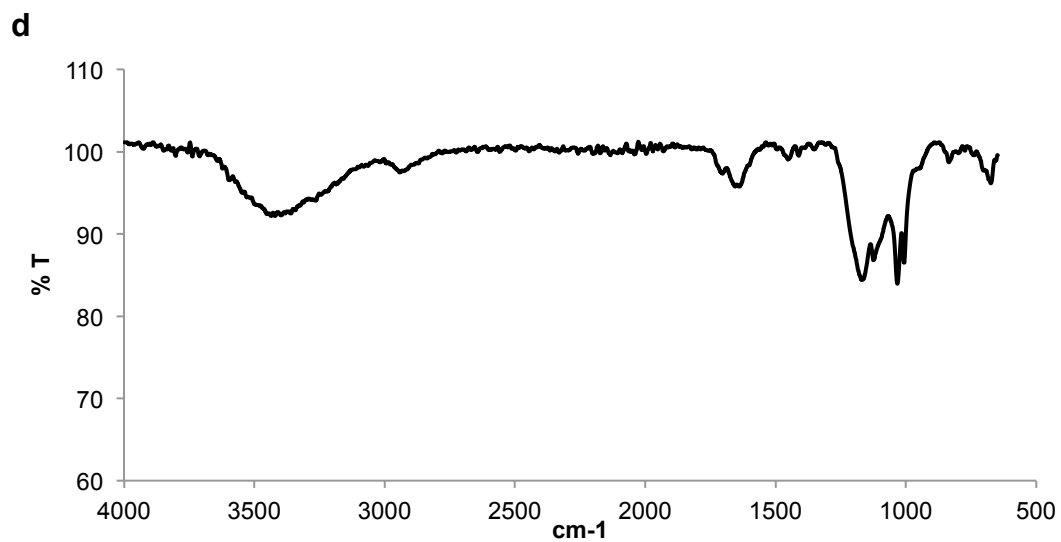— p(SS-co-PEGMA)-xanthate
- - p(SS-co-PEGMA-b-VS)
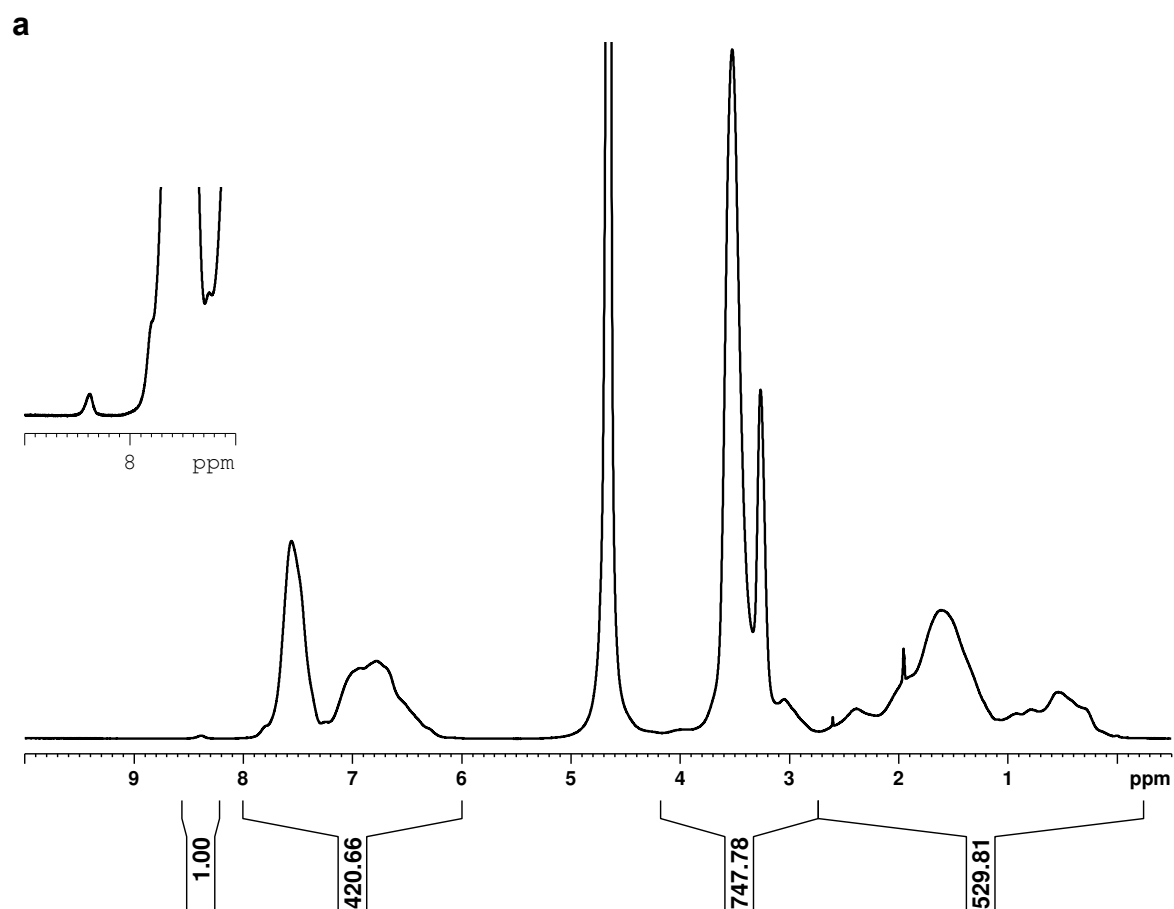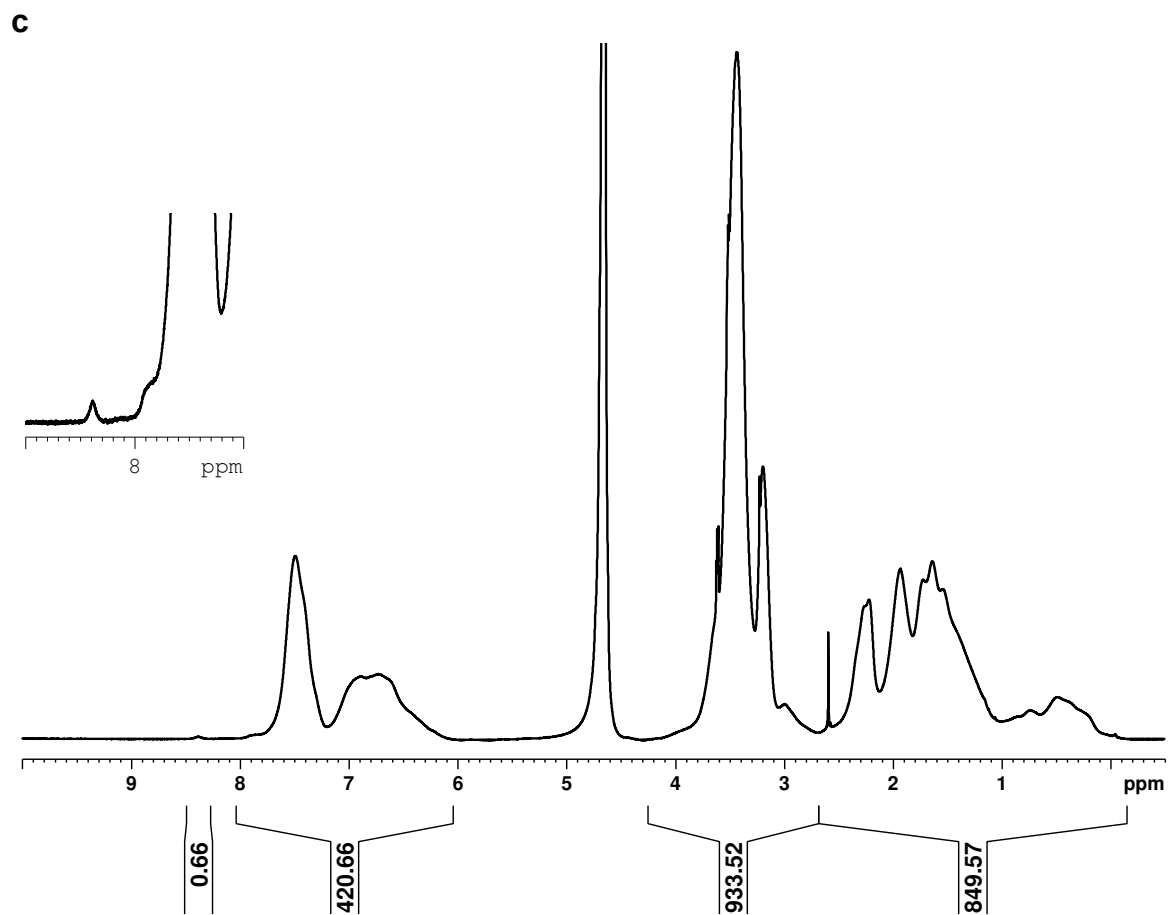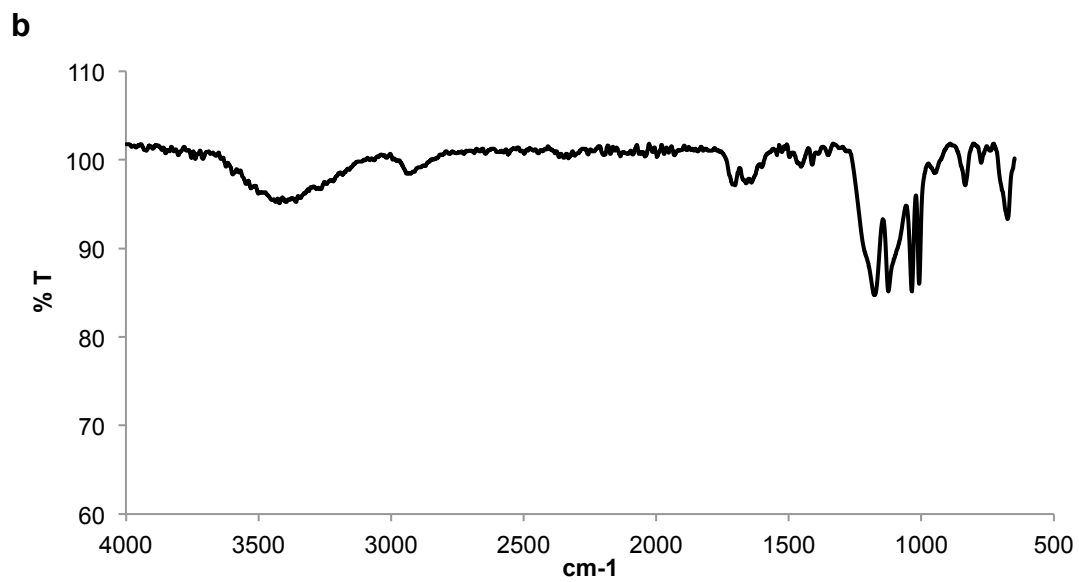
Figure 4.13. Characterization of **p(SS-*co*-PEGMA)-xanthate** and **p(SS-*co*-PEGMA-*b*-VS)**. ^{1}H NMR spectrum in D_2O (a) and FTIR spectrum (b) of **p(SS-*co*-PEGMA)-xanthate**. ^{1}H NMR spectrum in D_2O (c) and FTIR spectrum (d) of **p(SS-*co*-PEGMA-*b*-VS)**. GPC traces of **p(SS-*co*-PEGMA)-xanthate** and **p(SS-*co*-PEGMA-*b*-VS)** (e).

In our in-house-developed FGFR-binding assay, the three generations of heparin-mimicking polymers were compared side-by-side for their ability to facilitate binding of bFGF to FGFR (Figure 4.14). Recombinant human FGFR1α(IIIc) was coated a 96-well-plate and used to capture bFGF. Heparin is known to enhance binding of bFGF to FGFR[23] and was used as the positive control. As already learned from proliferation studies, the 2nd-generation polymer was much better than the 1st-generation polymer in enhancing the interaction between bFGF and its receptors. The effect of the 2nd-generation heparin-mimicking polymer (0.82 ± 0.06) in this ELISA assay was actually stronger than that of heparin (0.63 ± 0.05, $p = 0.01$), which confirmed the heparin-like behavior of pVS. Also in agreement with our hypothesis, the 3rd-generation polymer exerted binding affinity that was higher than the 1st-generation polymer but lower than the 2nd-generation polymer.
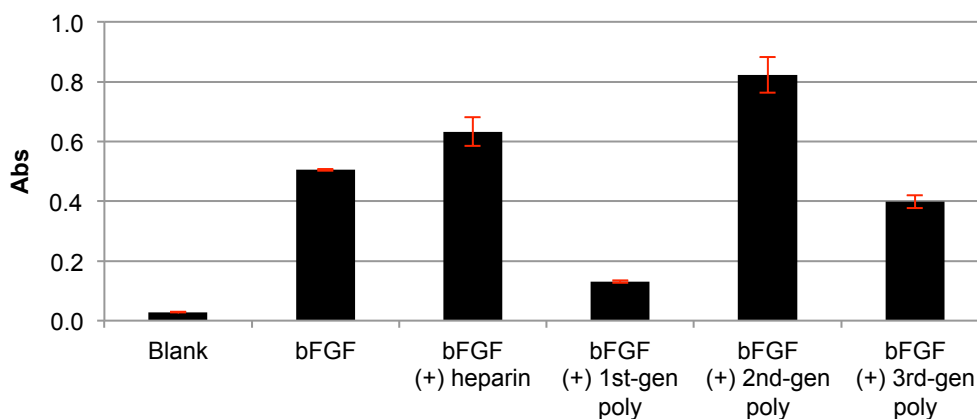

Figure 4.14. ELISA-based FGFR-binding assay. FGFR1α(IIIc) was coated a 96-well-plate. The wells were treated with various formulations: blank buffer, 1 ng/mL of bFGF with or without 1 µg/mL of heparin or the heparin-mimicking polymers. The procedure is detailed in the Methods

section. The graphed absorbance was the difference between the signals at $\lambda = 450$ nm and the background signals at $\lambda = 630$ nm.

The 3rd-generation heparin-mimicking polymer conjugate, **bFGF-p(SS-*co*-PEGMA-*b*-VS)**, was synthesized similarly to 1st- and 2nd-generation conjugates (Scheme 4.4). Figure 4.15 shows the western blot of the Native PAGE of the conjugate. Since the polymer has a large molecular weight and is highly negatively charged, the conjugate with bFGF appeared as a smear closer to the top of the PAGE.

Figure 4.15. Western blot of Native PAGE of native bFGF (lane 1) and **bFGF-p(SS-*co*-PEGMA-*b*-VS)** (lane 2).

To investigate whether the 3rd-generation heparin-mimicking polymer conjugate could result in a more bioactive hybrid than the native protein, we first tested the conjugate on BaF3-FR1C cells. As shown in Figure 4.16, the 3rd-geneneration conjugate, at 5 ng/mL, stimulated more cell growth than native bFGF, 1st- and 2nd-generation conjugates ($319 \pm 24\%$, $178 \pm 18\%$, $232 \pm 24\%$ and $146 \pm 13\%$ respectively). The **bFGF-pVS7.6k** was used as the 2nd-generatin conjugate. When 1 μg/mL of heparin was added to each of the group, the percent cell growths of all the groups were not different than one another. Yet, in the presence of heparin, the percent cell growth of all of the groups increased tremendously compared to the absence of heparin, except for the 3rd-generation conjugate (percent cell growth = $319 \pm 24\%$ and $353 \pm 12\%$ before and after adding heparin, respectively). This data suggested that the 3rd-generation conjugate successfully activated all of the receptors; therefore adding excess heparin had no contributing effect.
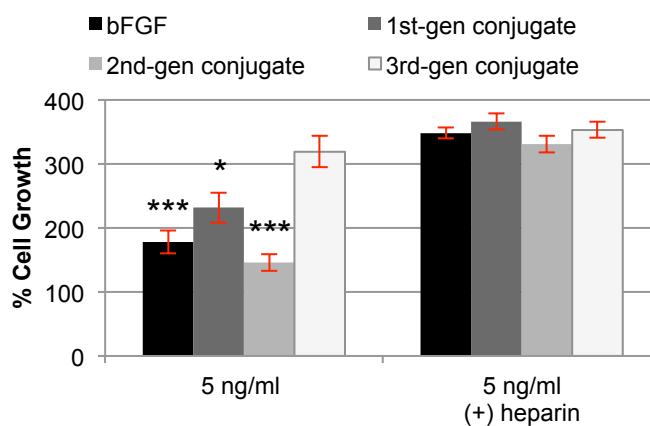

Figure 4.16. Proliferation studies of the heparin-mimicking polymer conjugates on BaF3-FR1C cells. Incubation of 20,000 cells/well in 96-well plate with 5 ng/mL of either bFGF or the heparin-mimicking polymer conjugates in the absence or presence of 1 μg/mL of heparin was carried out for 48 hours. CellTiter®-Blue assay was performed to quantify the extent of cell

growth. Data was normalized to the blank medium group, which was set at 100%. Each sample had four replicates and the experiment was repeated three-six times. Error bars represent SEM. Statistical analysis was done using Student's t-test. * $p < 0.05$, *** $p < 0.001$ for each of the denoted group compared to the 3rd-generation conjugate.

The same stimulation effect was not observed on HDF cells. When 1 ng/mL or 0.5 ng/mL of bFGF or the conjugate was tested on HDF cells, the percent cell growth was the same for all of the groups (Figure 4.17). In the presence of 5 ng/mL of the 3rd-generation conjugate, the percent cell growth dropped to 111 ± 13%, and was statistically lower than that in the presence of bFGF and the other conjugates. More experiments will need to be undertaken to explain this phenomenon.
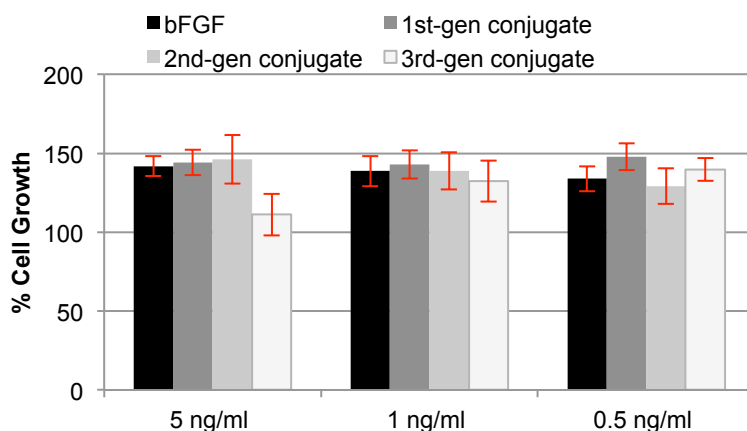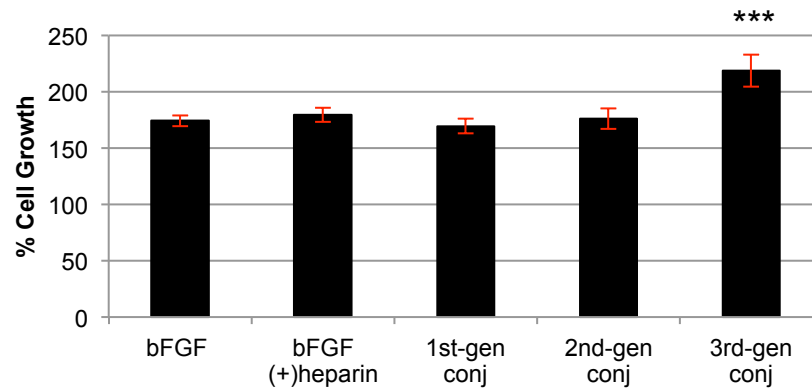

Figure 4.17. Proliferation studies of the heparin-mimicking polymer conjugates on HDF cells. Incubation of 2,000 cells/well in 96-well plate with various concentrations of either bFGF or the heparin-mimicking polymer conjugates were carried out for 72 hours. CellTiter®-Blue assay was performed to quantify the extent of cell growth. Data was normalized to the blank medium
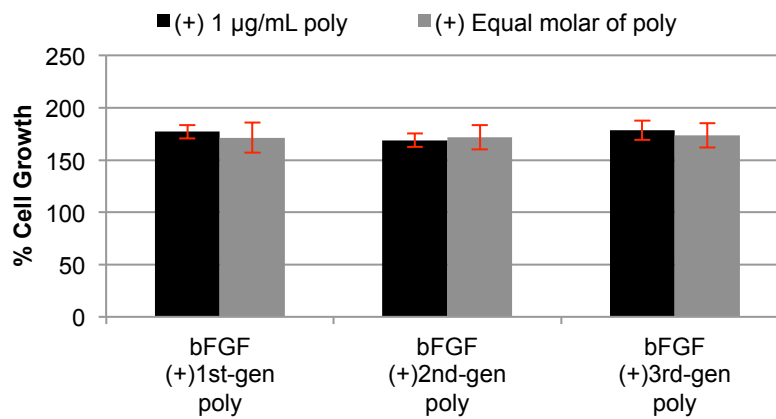
group, which was set at 100%. Each sample had six replicates and the experiment was repeated three times. Error bars represent SEM.

bFGF stimulates proliferation of many different cell types beside HDF cells such as HUVECs.[34,35] When HUVECs were incubated with the 3rd-generation conjugate, we discovered that the cells responded well to the conjugate (Figure 4.18a). The percent cell growth in the presence of 5 ng/mL of the 3rd-generation conjugate was $219 \pm 6\%$, which was much higher than in the presence of bFGF ($174 \pm 5\%$), bFGF with heparin ($180 \pm 7\%$), the 1st-generation conjugate ($170 \pm 4\%$), or the 2nd-generation conjugate ($176 \pm 6\%$) ($p < 0.005$ for all the groups). When each of the polymers, either in excess or at equal molar equivalent to bFGF, was used in combination with bFGF, the percent cell growths were not different than when bFGF was used alone (Figure 4.18b). This data proves that the covalent conjugate between bFGF and the 3rd-generation heparin-mimicking polymer was responsible for the conjugate's enhanced bioactivity meaning that the polymer needed to be in close proximity to the bFGF to observe the effect. Incubating the polymers alone with HUVEC cells did not show any effect on cell proliferation, while heparin inhibited HUVEC proliferation, which was consistent with literature report (Figure 4.18c).[34]
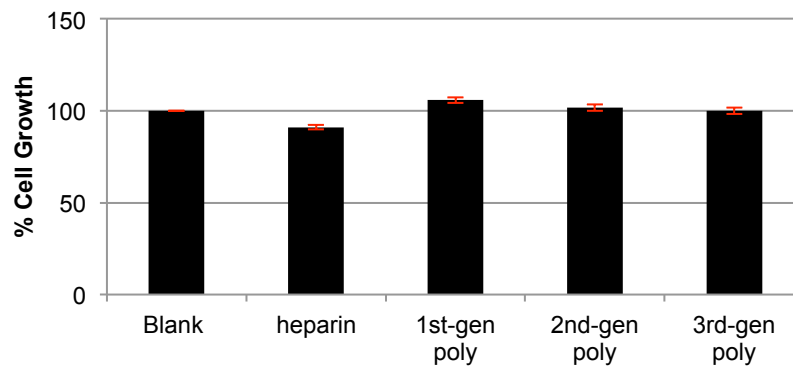
Figure 4.18. Proliferation studies of the heparin-mimicking polymers and the conjugates on HUVEC cells. 1,000 cells/well in 96-well plate was treated with 5 ng/mL of bFGF or the heparin-mimicking polymer conjugates (a), 5 ng/mL of bFGF with either 1 μg/mL (black bar) or

equal molar (gray bars) of the heparin-mimicking polymers (b), or 1 μg/mL of heparin or the heparin-mimicking polymers in the absence of bFGF (c). CellTiter®-Blue assay was performed to quantify the extent of cell growth. Data was normalized to the blank medium group, which was set at 100%. Each sample had six replicates and the experiment was repeated three-seven times. Error bars represent SEM. Statistical analysis was done using Student's t-test. *** p < 0.001 for all of the groups compared to the 3rd-gen conjugate.

bFGF also induces migration of HUVECs.[36,37] To examine whether the 3rd-generation conjugate can influence migration of HUVECs better than the native protein, we conducted the scratch assays. The experiment was repeated three times, all of which were blinded studies. Figure 4.19a shows the results of the scratch/migration assays. The 3rd-generation conjugate induced migration of HUVECs better than bFGF (83 ± 6% and 54 ± 4%, respectively, p = 0.008). Figure 4.19c shows some representative images of the samples taken at T = 0 hr and T = 18 hr. To ensure the effect of migration observed was not attributed from the ability of the conjugate to induce HUVEC proliferation, we quantified cell proliferation post 18-hour incubation period. The percent cell growth induced by the 3rd-generation conjugate was not different than by native bFGF (Figure 4.19b). This was expected since the cells were grown close to confluency prior to introduction of the scratches and the incubation time of the assay was only for 18 hours. The same phenomenon was also observed elsewhere.[38]
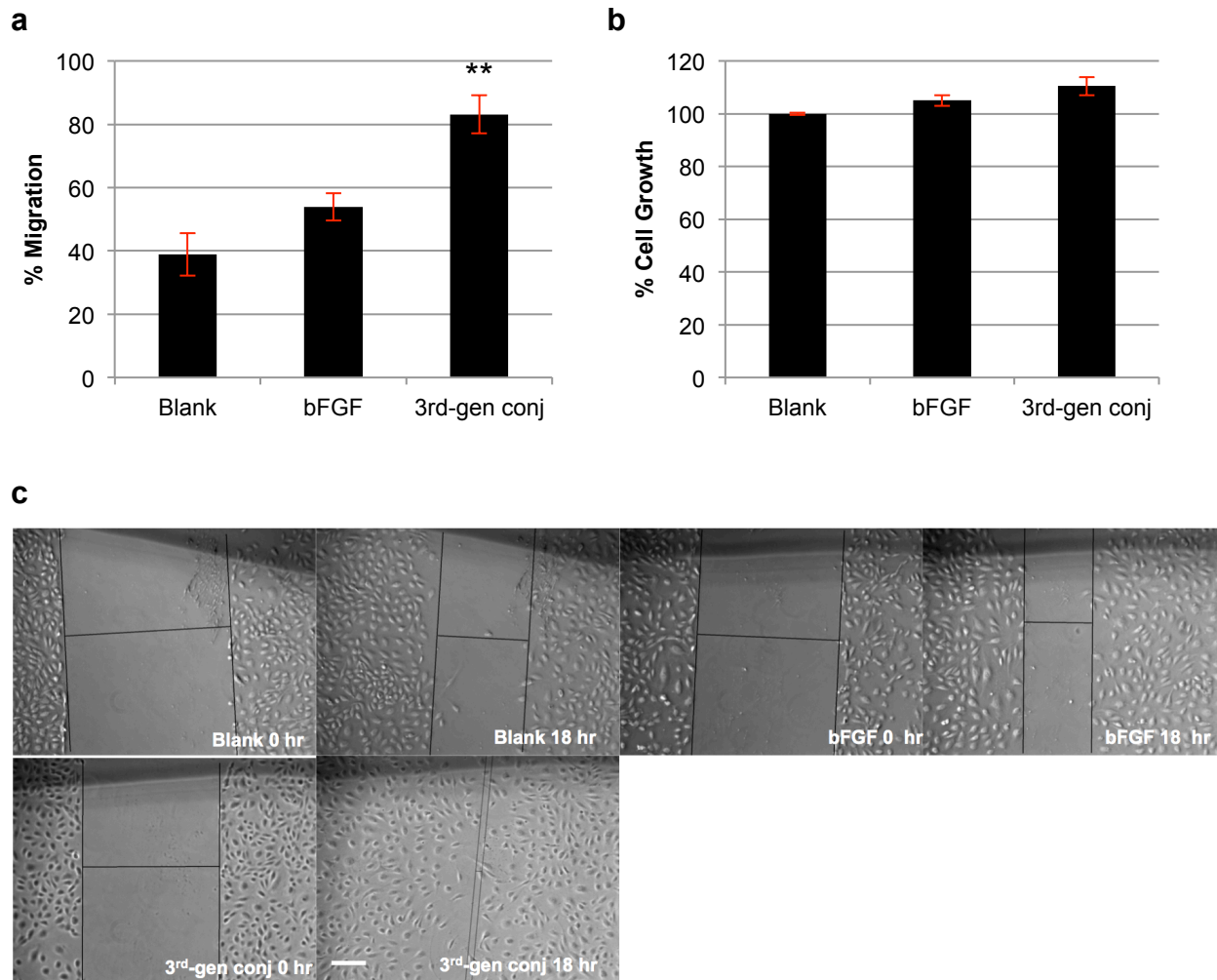
Figure 4.19. Migration assay with HUVECs. See the Methods section for details of the assay. a) Percent migration of HUVECs after 18 hours incubating with either blank medium, 10 ng/mL of bFGF, or 10 ng/mL of bFGF-p(SS-*co*-PEGMA-*b*-VS). Percent migration was calculated using the formula: $100\% - (distance\ T = 18/distance\ T = 0) \times 100$. Each sample had four-six replicates and the experiment was repeated three times, all of which were blinded. Error bars represent SEM. b) CellTiter®-Blue assay of all the experimental groups to quantify the extent of cell growth post 18-hour incubation period. Data was normalized to the blank medium group, which was set at 100%. c) Representative images of each group taken at T = 0 hr and T =

18 hr. Scale bar is 50 μm. Statistical analysis was done using Student's t-test. ** $p < 0.01$ for each of the group compared to the 3rd-generation conjugate.

4.4. Discussion

Basic FGF is an original member of a family of 21 structure-related heparin-binding growth factors. Its biological functions are diverse and have been shown to be crucial in embryonic development,[39] angiogenesis,[40] tissue regeneration,[41] bone regeneration,[42] development and maintenance of the nervous system,[43] stem cell self-renewal[44] and wound healing.[45] *In vitro*, bFGF is a potent mitogen to different cell types including endothelial cells such as HUVECs and fibroblast cells such as HDF cells.[46,47] *In vivo*, bFGF is a potent inducer of angiogenesis and responsible for the development and differentiation of many organs.[48,49] In the context of angiogenesis, a process describing the formation of new capillaries from pre-existing blood vessels, bFGF is one of the most potent proangiogenic factors.[48] In physiological angiogenesis such as embryonic development and wound healing, bFGF induces endothelial cells to proliferate, migrate and differentiate.[35,50]

In this chapter, we described the development of a novel 3rd-generation heparin-mimicking polymer, p(SS-*co*-PEGMA-*b*-VS). Conjugation to bFGF resulted in a super-bioactive hybrid. To our knowledge, although protein conjugates with the same activity were reported,[51] a protein-polymer conjugate with higher bioactivity than the native protein has never been reported. The bFGF-heparin-mimicking polymer conjugate, bFGF-p(SS-*co*-PEGMA-*b*-VS), induced substantial cell proliferation and fast cell migration when tested on HUVECs compared to native bFGF or bFGF with the polymer as an additive. bFGF induces proliferation of HUVEC cells by initiating the dimerization and phosphorylation of FGFR1; HS or heparin is also required in these mechanisms.[52] We showed that bFGF-p(SS-*co*-PEGMA-*b*-VS) was very

171

potent in inducing proliferation of HS-deficient cells. The designed heparin-mimicking polymer was able to replace the biological role of heparin in facilitating binding of bFGF to FGFR and receptor dimerization.

During the development of p(SS-*co*-PEGMA-*b*-VS), we discovered pVS as a potential 2nd-generation heparin-mimicking polymer. The polymer was as efficient as heparin in facilitating binding of bFGF to FGFR1 and in inducing BaF3-FR1C cell proliferation. However, after conjugation to bFGF, pVS lost its efficacy potentially due to the ability of the polymer to internalize bFGF independently of its high-affinity receptors. pVS has been explored before as an antithrombogenic agent,[53,54] HIV-inhibitor,[55] coatings for antibacterial surfaces,[56] and as polyelectrolytes for antibody and protein purification processes,[57-59] but never before as a low-affinity receptor for bFGF like HS proteoglycan. Even though bFGF-pVS conjugate has reduced bioactivity, non-covalent pVS has tremendous potential to be used as a co-myogenic agent to bFGF with equivalent activity to heparin.

Fusion of pVS to the 1st-generation heparin-mimicking polymer, p(SS-*co*-PEGMA), was deleterious as seen in the FGFR-binding assay, but the conjugate of the resulting polymer to bFGF had higher bioactivity than the 1st-, 2nd-generation conjugates and the native protein. Previously, we showed that the 1st-generation heparin-mimicking polymer could stabilize bFGF in the conjugate form.[20] With the 3rd-generation heparin-mimicking polymer, we expected that bFGF conjugate will have the same stability effect while having enhanced bioactivity, although this still needs to be tested.

Despite the potential therapeutic values of bFGF mentioned before, bFGF has not been approved for clinical usage in the USA, possibly because of its inherent instability.[60] PEG is

commonly used to conjugate to biomolecules for increased stabilization.[61,62] However, since the mechanism of actions of bFGF has been so well-elucidated, we took this advantage to design and synthesize a biomimic, multi-functional polymer that better accommodates the protein's structure and functions. The bFGF-p(SS-*co*-PEGMA-*b*-VS) has potential in accelerating angiogenesis, which is useful in a variety of applications including tissue engineering.

4.5. Conclusions

In this chapter, we described the development of two heparin-mimicking polymers, pVS and p(SS-*co*-PEGMA-*b*-VS) that are capable of replacing the biological role of HS and heparin. The polymers were synthesized via RAFT polymerization and their covalent conjugates to bFGF were prepared via disulfide exchange. pVS had the most heparin-like behavior when used in conjunction with bFGF, but its conjugate to bFGF failed to facilitate dimerization and phosphorylation of FGFR. bFGF-p(SS-*co*-PEGMA-*b*-VS) conjugate was more potent than bFGF in aiding FGFR dimerization leading to cell proliferation in HS-deficient cells. This novel bFGF-heparin-mimicking polymer conjugate stimulated proliferation and migration of HUVEC cells better than the native protein and could have great potential in accelerating physiological angiogenesis process such as in wound healing. We anticipate that this strategy of using biomimic polymers for conjugation can benefit the field of therapeutic proteins tremendously.

4.6. References

1) Ratner, B. D.; Bryant, S. J. *Annu. Rev. Biomed. Eng.* **2004**, *6*, 41.

2) Anderson, J. M. *Ann. Rev. Mater. Res.* **2001**, *31*, 81.

3) Drotleff, S.; Lungwitz, U.; Breunig, M.; Dennis, A.; Blunk, T.; Tessmar, J.; Gopferich, A. *Eur. J. Pharm. Biopharm.* **2004**, *58*, 385.

4) Ma, P. X. *Adv. Drug Deliv. Rev.* **2008**, *60*, 184.

5) Yoo, J. W.; Irvine, D. J.; Discher, D. E.; Mitragotri, S. *Nat. Rev. Drug Discov.* **2011**, *10*, 521.

6) Ladmiral, V.; Melia, E.; Haddleton, D. M. *Eur. Polym. J.* **2004**, *40*, 431.

7) Kogan, G.; Soltes, L.; Stern, R.; Gemeiner, P. *Biotechnol. Lett* **2007**, *29*, 17.

8) Sasisekharan, R.; Venkataraman, G. *Curr. Opin. Chem. Biol.* **2000**, *4*, 626.

9) Mauzac, M.; Aubert, N.; Jozefonvicz, J. *Biomaterials* **1982**, *3*, 221.

10) Mauzac, M.; Jozefonvicz, J. *Biomaterials* **1984**, *5*, 301.

11) Capila, I.; Linhardt, R. J. *Angew. Chem. Int. Ed.* **2002**, *41*, 391.

12) Logeart-Avramoglou, D.; Jozefonvicz, J. *J. Biomed. Mater. Res.* **1999**, *48*, 578.

13) Benezra, M.; Ishai-Michaeli, R.; Ben-Sasson, S. A.; Vlodavsky, I. *J. Cell. Physiol.* **2002**, *192*, 276.

14) Regan, J. R.; Bruno, J. G.; Chang, M. N.; Sabatino, R.; Dalisa, R.; Bensasson, S. A.; Eilat, D. *J. Bioact. Compatible Polym.* **1993**, *8*, 317.

15) Guan, R.; Sun, X. L.; Hou, S. J.; Wu, P. Y.; Chaikof, E. L. *Bioconjugate Chem.* **2004**, *15*, 145.

16) Sun, X. L.; Grande, D.; Baskaran, S.; Hanson, S. R.; Chaikof, E. L. *Biomacromolecules* **2002**, *3*, 1065.

17) Christman, K. L.; Vazquez-Dorbatt, V.; Schopf, E.; Kolodziej, C. M.; Li, R. C.; Broyer, R. M.; Chen, Y.; Maynard, H. D. *J. Am. Chem. Soc.* **2008**, *130*, 16585.

18) Liekens, S.; Leali, D.; Neyts, J.; Esnouf, R.; Rusnati, M.; Dell'Era, P.; Maudgal, P. C.; De Clercq, E.; Presta, M. *Mol. Pharmacol.* **1999**, *56*, 204.

19) Liekens, S.; Neyts, J.; Degreve, B.; DeClercq, E. *Oncol. Res.* **1997**, *9*, 173.

20) Nguyen, T. H.; Kim, S. H.; Decker, C. G.; Wong, D. Y.; Loo, J. A.; Maynard, H. D. *Nature Chem.* **2013**, 5, 221.

21) Kolodziej, C. M.; Kim, S. H.; Broyer, R. M.; Saxer, S. S.; Decker, C. G.; Maynard, H. D. *J. Am. Chem. Soc.* **2012**, *134*, 247.

22) Gospodarowicz, D.; Cheng, J. *J. Cell Physiol.* **1986**, 475.

23) Yayon, A.; Klagsbrun, M.; Esko, J. D.; Leder, P.; Ornitz, D. M. *Cell* **1991**, *64*, 841.

24) Plotnikov, A. N.; Schlessinger, J.; Hubbard, S. R.; Mohammadi, M. *Cell* **1999**, *98*, 641.

25) Schlessinger, J.; Plotnikov, A. N.; Ibrahimi, O. A.; Eliseenkova, A. V.; Yeh, B. K.; Yayon, A.; Linhardt, R. J.; Mohammadi, M. *Mol. Cell* **2000**, *6*, 743.

26) Chen, R.; John, J.; Lavrentieva, A.; Muller, S.; Tomala, M.; Zhao, Y. X.; Zweigerdt, R.; Beutel, S.; Hitzmann, B.; Kasper, C.; Martin, U.; Rinas, U.; Stahl, F.; Scheper, T. *Eng. Life Sci.* **2012**, *12*, 29.

27) Ornitz, D. M.; Leder, P. *J. Biol. Chem.* **1992**, *267*, 16305.

28) Murthy, N.; Campbell, J.; Fausto, N.; Hoffman, A. S.; Stayton, P. S. *Bioconjugate Chem.* **2003**, *14*, 412.

29) Destarac, M.; Blidi, I.; Coutelier, O.; Guinaudeau, A.; Mazieres, S.; Van Gramberen, E.; Wilson, J. *Acs. Sym. Ser.* **2012**, *1100*, 259.

30) Jiang, D. D.; Yao, Q.; McKinney, M. A.; Wilkie, C. A. *Polym. Degrad. Stab.* **1999**, *63*, 423.

31) Johnson, R. S.; Finnegan, P. S.; Wheeler, D. R.; Dirk, S. M. *Chem. Commun.* **2011**, *47*, 3936.

32) Reiland, J.; Rapraeger, A. C. *J. Cell Sci.* **1993**, *105 (Pt 4)*, 1085.

33) Roghani, M.; Moscatelli, D. *J. Biol. Chem.* **1992**, *267*, 22156.

34) Giraux, J. L.; Matou, S.; Bros, A.; Tapon-Bretaudiere, J.; Letourneur, D.; Fischer, A. M. *Eur. J. Cell Biol.* **1998**, *77*, 352.

35) Yoshida, A.; Anand-Apte, B.; Zetter, B. R. *Growth Factors* **1996**, *13*, 57.

36) van Horssen, R.; Galjart, N.; Rens, J. A.; Eggermont, A. M.; ten Hagen, T. L. *J. Cell. Biochem.* **2006**, *99*, 1536.

37) Wu, J. C.; Yan, H. C.; Chen, W. T.; Chen, W. H.; Wang, C. J.; Chi, Y. C.; Kao, W. Y. *Exp. Cell Res.* **2008**, *314*, 421.

38) Pintucci, G.; Moscatelli, D.; Saponara, F.; Biernacki, P. R.; Baumann, F. G.; Bizekis, C.; Galloway, A. C.; Basilico, C.; Mignatti, P. *FASEB J.* **2002**, *16*, 598.

39) Slack, J. M. W.; Darlington, B. G.; Heath, J. K.; Godsave, S. F. *Nature* **1987**, *326*, 197.

40) Cross, M. J.; Claesson-Welsh, L. *Trends Pharmacol. Sci.* **2001**, *22*, 201.

41) Kawai, K.; Suzuki, S.; Tabata, Y.; Ikada, Y.; Nishimura, Y. *Biomaterials* **2000**, *21*, 489.

42) Canalis, E.; Centrella, M.; McCarthy, T. *J. Clin. Invest.* **1988**, *81*, 1572.

43) Timmer, M.; Cesnulevicius, K.; Winkler, C.; Kolb, J.; Lipokatic-Takacs, E.; Jungnickel, J.; Grothe, C. *J. Neurosci.* **2007**, *27*, 459.

44) Levenstein, M. E.; Ludwig, T. E.; Xu, R. H.; Llanas, R. A.; VanDenHeuvel-Kramer, K.; Manning, D.; Thomson, J. A. *Stem Cells* **2006**, *24*, 568.

45) Barrientos, S.; Stojadinovic, O.; Golinko, M. S.; Brem, H.; Tomic-Canic, M. *Wound Repair Regen.* **2008**, *16*, 585.

46) Munoz-Chapuli, R.; Quesada, A. R.; Angel Medina, M. *Cell. Mol. Life Sci.* **2004**, *61*, 2224.

47) Shipley, G. D.; Keeble, W. W.; Hendrickson, J. E.; Coffey, R. J.; Pittelkow, M. R. *J. Cell Physiol.* **1989**, *138*, 511.

48) Bikfalvi, A.; Klein, S.; Pintucci, G.; Rifkin, D. B. *Endocr. Rev.* **1997**, *18*, 26.

49) Seghezzi, G.; Patel, S.; Ren, C. J.; Gualandris, A.; Pintucci, G.; Robbins, E. S.; Shapiro, R. L.; Galloway, A. C.; Rifkin, D. B.; Mignatti, P. *J. Cell Biol.* **1998**, *141*, 1659.

50) Naik, M. U.; Vuppalanchi, D.; Naik, U. P. *Arterioscler. Thromb. Vasc. Biol.* **2003**, *23*, 2165.

51) Kochendoerfer, G. G.; Chen, S. Y.; Mao, F.; Cressman, S.; Traviglia, S.; Shao, H. Y.; Hunter, C. L.; Low, D. W.; Cagle, E. N.; Carnevali, M.; Gueriguian, V.; Keogh, P. J.; Porter, H.; Stratton, S. M.; Wiedeke, M. C.; Wilken, J.; Tang, J.; Levy, J. J.; Miranda, L. P.; Crnogorac, M. M.; Kalbag, S.; Botti, P.; Schindler-Horvat, J.; Savatski, L.; Adamson, J. W.; Kung, A.; Kent, S. B. H.; Bradburne, J. A. *Science* **2003**, *299*, 884.

52) Mader, J. S.; Smyth, D.; Marshall, J.; Hoskin, D. W. *Am. J. Pathol.* **2006**, *169*, 1753.

53) Ito, Y.; Iguchi, Y.; Kashiwagi, T.; Imanishi, Y. *J. Biomed. Mater. Res.* **1991**, *25*, 1347.

54) Ito, Y.; Liu, L.; Imanishi, Y. *J. Biomed. Mater. Res.* **1991**, *25*, 99.

55) Mohan, P.; Schols, D.; Baba, M.; De Clercq, E. *Antiviral Res.* **1992**, *18*, 139.

56) Vasilev, K.; Sah, V. R.; Goreham, R. V.; Ndi, C.; Short, R. D.; Griesser, H. J. *Nanotechnology* **2010**, *21*, 215102.

57) Braia, M.; Ferrero, M.; Rocha, M. V.; Loureiro, D.; Tubio, G.; Romanini, D. *Protein Expr. Purif.* **2013**, *91*, 91.

58) Braia, M.; Porfiri, M. C.; Farruggia, B.; Pico, G.; Romanini, D. *J. Chromatogr. B Analyt. Technol. Biomed. Life Sci.* **2008**, *873*, 139.

59) McDonald, P.; Victa, C.; Carter-Franklin, J. N.; Fahrner, R. *Biotechnol. Bioeng.* **2009**, *102*, 1141.

60) Richard, J. L.; Bringer, J.; Parerrichard, C.; Rodier, M.; Daures, J. P.; Jacob, C.; Clouet, S.; Comtebardonnet, M.; Vannereau, D. *Diabetes Care* **1995**, *18*, 64.

61) Abuchowski, A.; Vanes, T.; Palczuk, N. C.; Davis, F. F. *J. Biol. Chem.* **1977**, *252*, 3578.

62) Duncan, R. *Nat. Rev. Drug Discov.* **2003**, *2*, 347.